VARIATIONS IN MASS TRANSFER

WITH DISPERSED BUBBLES

VARIATIONS IN MASS TRANSFER

WITH DISPERSED BUBBLES

By

ARTHUR WARREN WILSON, B. Eng.

A Thesis

Submitted to the Faculty of Graduate Studies

in Partial Fulfilment of the Requirements

for the Degree

Master of Engineering

McMaster University

October 1967

MASTER OF ENGINEERING (1967) McMASTER UNIVERSITY
(Civil Engineering) Hamilton, Ontario.

TITLE: Variation in Mass Transfer with Dispersed Bubbles.

AUTHOR: Arthur Warren Wilson, B. Eng. (McMaster University)

SUPERVISOR: Dr. K. L. Murphy

NUMBER OF PAGES: ix, 123

SCOPE AND CONTENTS:

Using a single bubble suspended in a liquid flow regime, the effects of velocity, bubble size, and surfactant levels on the gas transfer process across the bubble interface were investigated. Mass transfer data reported in the literature for non-circulating carbon dioxide bubbles was verified. A mathematical model predicting the mass transfer process for the single bubble system used in this study was formulated and this model provided a reasonable fit for experimental data obtained for the dissolution of a carbon dioxide bubble into an aqueous solution of a second sparingly soluble gas. The fate of a hypothetical air bubble in an aerator was briefly considered.

ACKNOWLEDGEMENTS

I wish to express my sincere appreciation and gratitude to Dr. K. L. Murphy for his good guidance and council in the preparation of this work.

The financial assistance provided by the Department of National Health and Welfare through a Professional Training Bursary and the National Research Council of Canada is greatfully acknowledged.

Thanks are due also to the Ontario Water Resources Commission for a leave of absence to complete this work and for the use of their printing and binding facilities.

TABLE OF CONTENTS

	PAGE
ACKNOWLEDGEMENTS	iii
LIST OF FIGURES	vi
LIST OF TABLES	ix
CHAPTER I - INTRODUCTION	1
CHAPTER 2 - LITERATURE REVIEW	4
Development of Theories on the Mechanism of Mass Transfer	4
Development of the Concept of Circulation	10
Measurement of the Mass Transfer Coefficient k_L	13
k_L Variations in Waste Treatment Aeration Systems	17
CHAPTER 3 - EXPERIMENTAL	20
CHAPTER 4 - DATA ANALYSIS	34
CHAPTER 5 - RESULTS	41
Carbon Dioxide - Degasified Water	41
Carbon Dioxide - Aqueous Nitrogen Solution	44
Carbon Dioxide - Aqueous Oxygen Solution	50
Surfactant Runs	50
CHAPTER 6 - APPLICATION	57
CHAPTER 7 - CONCLUSIONS, DISCUSSION AND RECOMMENDATIONS	62
REFERENCES	65

PAGE

APPENDIX "A" - ORIFICE PLATE CALIBRATION CURVES 69

APPENDIX "B" - OPTICAL DISTORTION CALIBRATION CURVE 73

APPENDIX "C" - BUBBLE AREA AND VOLUME DETERMINATIONS 75

APPENDIX "D" - ABS CALIBRATION CURVE 83

APPENDIX "E" - SOLUBILITIES AND DIFFUSIVITIES OF VARIOUS GASES IN WATER 85

APPENDIX "F" - KINEMATIC VISCOSITY OF WATER 88

APPENDIX "G" - BUBBLE RISE RATE VARIATION WITH DIAMETER . 90

APPENDIX "H" - COMPUTER PROGRAMS USED FOR ANALYSES 92

APPENDIX "I" - TABLES OF DATA, CALCULATIONS AND RESULTS . 108

APPENDIX "J" - NOMENCLATURE 120

LIST OF FIGURES

Figure Number	Title	Page
1	SKETCH OF APPARATUS	21
2	SKETCH OF TEST SECTION	22
3a	BUBBLE SUPPORT AND FEEDER ASSEMBLY	23
3b	GAS FEEDING EQUIPMENT	23
4	RATIO OF AVERAGE VELOCITY TO CENTER-LINE VELOCITY	26
5	CARBON DIOXIDE - DEGASIFIED WATER DATA	42
6	COMPARISON OF CO_2 DATA IN THIS STUDY TO GRIFFITH'S: $Sh = 2.0 + 0.72\ Re^{1/2}\ Sc^{1/3}$	43
7	CARBON DIOXIDE - AQUEOUS NITROGEN SOLUTION DATA - RUN #38	45
8	CARBON DIOXIDE - AQUEOUS NITROGEN SOLUTION DATA - RUN #38	46
9	CARBON DIOXIDE - AQUEOUS NITROGEN SOLUTION DATA - RUN #41	47
10	CARBON DIOXIDE - AQUEOUS NITROGEN SOLUTION DATA - RUN #45	48
11	CARBON DIOXIDE - AQUEOUS NITROGEN SOLUTION DATA - RUN #48	49
12	CARBON DIOXIDE - AQUEOUS OXYGEN SOLUTION DATA - RUN #52	51
13	CARBON DIOXIDE - AQUEOUS OXYGEN SOLUTION DATA - RUN #56	52
14	CARBON DIOXIDE - AQUEOUS OXYGEN SOLUTION DATA - RUN #57	53
15	CARBON DIOXIDE - AQUEOUS OXYGEN SOLUTION DATA - RUN #61	54

LIST OF FIGURES (cont'd)

Figure Number	Title	Page
16	MASS FEED RATE VS TIME FOR VARIOUS ABS CONCENTRATIONS	56
17	FATE OF A HYPOTHETICAL AIR BUBBLE 0.206 CM DIAMETER	59
18	FATE OF A HYPOTHETICAL AIR BUBBLE 0.600 CM DIAMETER	60
19	ORIFICE PLATE CALIBRATION CURVES FLOW VS DIFFERENTIAL	70
20	ORIFICE PLATE CALIBRATION CURVES ORIFICE DIFFERENTIAL VS AVERAGE (Q/A) VELOCITY.	71
21	ORIFICE PLATE CALIBRATION CURVES ORIFICE DIFFERENTIAL VS PIPE CENTER-LINE VELOCITY	72
22	OPTICAL DISTORTION CALIBRATION CURVE	74
23a	PHOTOGRAPH OF TYPICAL BUBBLE	78
23b	TRACING OF PROJECTED BUBBLE IMAGE	78
24	BUBBLE HEIGHT VS AREA - ERECT BUBBLE	79
25	BUBBLE HEIGHT VS VOLUME - ERECT BUBBLE	80
26	BUBBLE HEIGHT VS AREA - INVERTED BUBBLE	81
27	BUBBLE HEIGHT VS VOLUME - INVERTED BUBBLE	82
28	SATURATION SOLUBILITIES OF CO_2, O_2, AND N_2 IN WATER	86
29	DIFFUSIVITIES OF VARIOUS GASES IN WATER	87

LIST OF FIGURES (cont'd)

Figure Number	Title	Page
30	KINEMATIC VISCOSITY OF WATER VS TEMPERATURE	89
31	ABS CALIBRATION CURVE	84
32	RISE VELOCITIES OF VARIOUS SIZE INDIVIDUAL BUBBLES	91

LIST OF TABLES

TABLE	TITLE	PAGE
TABLE I	SUMMARY OF EXPERIMENTAL CONDITIONS	33
TABLE II	BUBBLE AREA AND VOLUME DETERMINATIONS BY COMPUTER PROGRAM	76
TABLE III	CALCULATIONS OF DIAMETER OF SPHERES OF EQUIVALENT SURFACE AREA	109
TABLE IV	CALCULATIONS OF AVERAGE k_L VALUES FOR THE CO_2 - DEGASIFIED WATER RUNS	110
TABLE V	CALCULATIONS FOR CO_2 - SULFITE DATA	111
TABLE VI	k_L VALUES USED IN FITTING THE EXPERIMENTAL DATA	113
TABLE VII	SURFACTANT DETERMINATIONS	114
TABLE VIII	EXPERIMENTAL CONDITIONS FOR THE SURFACTANT RUNS	115
TABLE IX	$\frac{dm}{dt}$ CALCULATIONS FOR VARIOUS SURFACTANT LEVELS	116

CHAPTER I

INTRODUCTION

In the activated sludge waste treatment process, microbiological floc and organic wastes are mixed in an aerobic reactor or aeration tank to facilitate the utilization of the waste products as substrate or food for the microorganisms thus purifying the carrier liquid. In the conventional process, the floc and the treated water are separated and the micro-organisms are returned to be mixed with additional untreated waste. A continuous process is maintained wherein the aerobic "bio-mass" grows at the expense of the substrate utilizing the dissolved oxygen in the liquid as a hydrogen acceptor.

There are three basic requirements for an aeration tank, namely (1) an adequate volume to provide the required time for the substrate removal reactions to occur, (2) adequate mixing to keep the biological floc in suspension and promote contact with the waste, and (3) an adequate oxygen supply to keep the process aerobic. At present there are two conventional means of maintaining both the mixing and the oxygen requirements surface - mechanical and diffused air aerators. The former relies on a rotor which splashes

droplets of liquid into the atmosphere and vigorously mixes the liquid thereby keeping the microorganisms in suspension and promoting a high degree of surface renewal to maximize oxygen transfer into the liquid. With the latter, air bubbles are introduced into the liquid some distance beneath the surface. During their formation and subsequent rise, oxygen is transferred across the interfacial boundary and into the liquid. The drag of the rising bubbles creates a "roll" of the tank contents which keeps the tank contents in homogeneous suspension. The bulk flow causes some surface turbulence which, coupled with the action of bubbles bursting at the surface, promotes further transfer of oxygen from the atmosphere.

In a diffused air system, the mass transfer properties of the aerator are governed by the mass transfer coefficient, the total bubble interfacial area, and the mass transfer driving force. It is believed that tank geometry and diffuser submergence have some effect as well. To eliminate many of the variables that necessarily must be considered in studies on aerators, it was considered desirable to study the mass transfer process using a single bubble under controlled conditions. To obtain a more detailed knowledge of the mass transfer process associated with a single bubble of known interfacial area in a continuous liquid

phase, the effects of velocity, bubble size, and surfactant levels on the gas transfer across the interface were investigated. A simplified model illustrating the fate of an air bubble in a hypothetical aerator is briefly presented.

CHAPTER 2

LITERATURE REVIEW

Development of Theories on the Mechanism of Mass Transfer

The generally accepted physical law governing the diffusion process is Fick's Law:

$$\frac{dm}{dt} = - D A \frac{dc}{dy} \qquad (1)$$

where: $\frac{dm}{dt}$ = the rate of mass transfer,

A = the cross-sectional area perpendicular to the direction of diffusion,

$\frac{dc}{dy}$ = the concentration gradient, and

D = a proportionality factor known as the diffusivity.

The negative sign indicates that the diffusion proceeds in a direction opposite to that of the increasing concentration gradient $\frac{dc}{dy}$.

Starting with Fick's Law, Lewis and Whitman (1924) proposed a two-film theory for mass transfer across a gaseous-liquid interface. They assumed that two thin films on either side of the interface provided an "in series" diffusional resistance to mass transfer. The rate of mass transfer through each film must be equal for steady state, consequently:

$$\frac{dm}{dt} = - D_G \; A \; \left(\frac{dc}{dy}\right)_G = - D_L \; A \; \left(\frac{dc}{dy}\right)_L \qquad (2)$$

where: D_G and D_L are the diffusivities of the transferring substance in the gas and liquid phases respectively, and

$\left(\frac{dc}{dy}\right)_G$ and $\left(\frac{dc}{dy}\right)_L$ are the concentration gradients of the transferring substance in the gas and liquid respectively.

If the concentration in the gas phase is expressed as a partial pressure and if the concentration gradients through both films are assumed to be linear, then equation 2 may be rewritten as:

$$\frac{dm}{dt} = - D_G \; A \; \frac{(P_i - P_G)}{Y_G} = - D_L \; A \frac{(C_L - C_i)}{Y_L} \qquad (3)$$

where P_i = the partial pressure of the transferring substance at the interface,

P_G = the partial pressure of the transferring substance in the atmosphere above the interface,

Y_G = the gaseous film thickness,

C_L = the concentration of the transferring substance in the bulk of the liquid,

C_i = the interfacial concentration of the transferring substance, and

Y_L = is the liquid film thickness.

Lewis and Whitman defined the mass transfer coefficients for the gas and liquid phases as $k_G = \frac{D_G}{Y_G}$ and $k_L = \frac{D_L}{Y_L}$ respectively.

The resulting equation is:

$$\frac{dm}{dt} = k_G \quad A \quad (P_G - P_i) = k_L \quad A \ (C_i - C_L) \qquad (4)$$

They applied this equation to the mass transfer of gases of low, intermediate, and high solubility. With gases of low solubility, only a small concentration gradient can be established across the liquid film. The liquid at the interface is essentially saturated with solute and the gas film may be neglected in any calculations. The resulting mass transfer equation becomes:

$$\frac{dm}{dt} = k_L \quad A \ (C_i - C_L) \qquad (5)$$

Lewis and Whitman assumed that a steady state equilibrium existed in the two films; however, upon formation of the interface, some time would be required to establish equilibrium conditions throughout the film. To account for this non equilibrium period Higbie (1935) proposed a "penetration theory" wherein the penetration period was defined as the initial unsteady-state period of gas absorption which preceeded the steady state period described by the Lewis and Whitman two-film theory. If the penetration period was in order of the time of contact of an element of liquid at the interface, deviations from the two - film model

occurred. Starting with Fick's Law of Diffusion, Higbie arrived at the following equation for the mass of solute gas (m) absorbed in time "t_e" into a stagnant liquid:

$$m = 2\sqrt{\frac{D_L}{\pi\, t_e}}\; A\; (C_i - C_L) \qquad (6)$$

where: t_e = the time of exposure of the liquid to the gas, and,

C_i = that concentration of solute corresponding to the partial pressure of solute gas in the gaseous phase.

Higbie concluded that the mass transfer coefficient (k_L) was directly proportional to the square root of the diffusivity (D_L) and inversely proportional to the square root of the time of exposure (t_e) of the gas at the surface. In support of his postulate, he stated that it was

> "consistent with common experience that agitation and shortening the period of exposure increase the coefficient."

Higbie attempted to verify the penetration theory with data obtained from a carbon dioxide - water system. He noticed that invariably, the experimental $\frac{dm}{dt}$ values were lower than those predicted by the penetration theory for small time of exposures (t_e), but that as t_e increased, the experimental results approached the theoretical penetration

theory prediction. To account for this deviation, he discarded the assumption of equilibrium at the surface and imposed a "first order process surface resistance phenomenon." This model had a rate that was proportional to the degree of unsaturation or removal from equilibrium at the surface and fit his experimental data. This illustrated that as the time of exposure decreased, the absorption coefficient did not increase indefinitely as was predicted by the penetration theory, but approached some maximum finite initial value. He concluded that in an aeration system, more agitation beyond a certain degree would be useless unless new interfacial area was created.

Danckwerts (1951) arrived at the general equation for mass transfer (equation 1) without considering two stagnant films. He proposed a model for absorption into a turbulent liquid where eddies continually exposed fresh surface to the gas, then returned to the bulk of the liquid. Considering equation 6 for a stagnant liquid, he noted that if the scale of turbulence in a turbulent liquid were greatly in excess of the depth of penetration of the solute, the relative motion of the liquid beneath the surface could be disregarded. He then defined a rate of surface renewal (r) and proceeded to show that:

$$k_L = \sqrt{D_L r}$$

Dobbins (1956) noted discrepancies in all of the previous theories. His principal objections to the Lewis and Whitman theory was the assumption of steady state mass transfer. It was certain that turbulence in the bulk of the liquid promoted film renewal and at the instant of renewal, an unsteady state mass transfer condition would exist. The Higbie and Danckwerts penetration theories were based on the assumption that the transfer rate across the surface could be taken as that for an infinite liquid depth. This would be true as long as r were large enough so that the gas which penetrated would be largely confined to a surface layer much smaller than the actual depth. Dobbins went on to show that this assumption was unnecessary. Using the age distribution functions that Danckwerts employed in developing his theory, and assuming that the film was always maintained in a statistical sense but its composition was continuously changed by the liquid from beneath the surface, Dobbins arrived at the following expression for k_L:

$$k_L = \sqrt{D\ r}\ \coth\ \left(\frac{rL^2}{D}\right) \qquad (7)$$

where L = liquid film thickness.

It is apparent that the Lewis and Whitman and the penetration theories are two special cases of equation 7. As the renewal rate r approached zero, equation 7 approaches the film model

equation ($k_L = \frac{D}{L}$), and when the coth term exceeds 3.0, equation 7 reduces to the Danckwerts equation ($k_L = \sqrt{D\ r}$).

Development of the Concept of Circulation

In 1928, Bond and Newton (1928) investigated the rise of rates of bubbles. They cited Hadamard's (1911) modification of Stoke's Law for spherical globules:

$$V_t = \frac{1}{K}\left(\frac{2}{9}\ \frac{(\rho_1 - \rho_2)\, g\, r^2}{\mu_2}\right) \qquad (8)$$

where: V_t = the terminal velocity of the falling drop or rising bubble,

ρ_1 = the density of the dispersed (drop or bubble) phase,

ρ_2 = the density of the continuous phase,

g = the gravitational constant,

r = the radius of the drop or bubble,

μ_2 = the viscosity of the continuous phase, and

$$K = \frac{2/3 + \frac{\mu_1}{\mu_2}}{1 + \frac{\mu_1}{\mu_2}}$$

where μ_1 is the viscosity of the dispersed phase,

and noted that if $\mu_1 >> \mu_2$, rigid sphere behaviour occurred because $\frac{1}{K} \longrightarrow 1.0$. However, if the fluid drop were very inviscous (i.e. - air), then $\mu_1 << \mu_2$ and $\frac{1}{K} \longrightarrow 1.5$.

Consequently, the rise rates for air bubbles should be about 150% of those predicted for rigid spheres of equivalent mass. Experimental data showed that for less than some critical bubble diameter, rigid sphere behaviour occurred and $\frac{1}{K} \simeq 1.0$. Bond and Newton attributed this to surface tension (σ) forces and using dimensional analysis, they predicted a critical radius $\bar{r}$ at which the transition would occur:

$$\bar{r} = \frac{\sigma}{(\rho_1 - \rho_2)\, g} \qquad (9)$$

In their discussion, they stated that when $\frac{1}{K} \simeq 1.5$ and when the critical radius $\bar{r}$ was exceeded,

> " the fluid just inside and outside of the interface had a common tangential velocity."

In other words, circulation was occurring in the droplet or bubble.

Rosenberg (1950) made a comprehensive study of the drag and shape of air bubbles rising in liquids. He noticed that the drag coefficient (C_D) for air bubbles was considerably lower than that predicted using rigid sphere behaviour for the range of Reynolds numbers between 70 and 400. This he attributed to "slip at the boundary of the fluid sphere."

Using photographic methods to observe the fall of

droplets and the diffusion patterns within the droplets, Garner (1950) concluded that air bubbles of diameter greater than about 0.02 cm. circulated and the rise rate of the bubble increased over that predicted for a rigid sphere. Garner stated that for rigid sphere behaviour, the fluid in contact with the sphere had the same velocity as the sphere and since no boundary layer slip could occur, the fluid would have zero velocity with respect to the surface of the sphere. For fluid sphere behaviour (circulation), the viscous drag acting on the surface caused a motion of the fluid within the sphere and again no slip occurred at the surface.

In an effort to rectify some of the discrepancies in the literature about the transition from non-circulating to circulating conditions, Garner and Hammerton (1954) studied bubble rise rates and used ammonium chloride fog, introduced into the bubble upon formation, to observe any circulation. They found that for air bubbles in clean water, circulation commenced at bubble diameters of 0.015 to 0.03 cm and reached a maximum at 0.25 cm diameter. It was halted by the addition of very small amounts of surface active matter for all bubbles with diameters less than 0.6 cm. They concluded that the Bond and Newton critical radius (equation 9) failed to predict the transition diameter. Garner and Hammerton attributed the discrepancies in previous data to

four possible factors: temperature, rate of formation, wall effect, and surface active contaminants.

Haberman and Morton (1954) studied the rise rates of single bubbles in water and noticed that for tiny bubbles, the drag coefficients were essentially the same as for rigid spheres. As bubble size increased, a decrease in the drag below that of rigid spheres was observed indicative of circulation. With further increases in bubble size, viscous and hydrodynamics forces predominated over the surface tension forces, which had originally maintained the smaller bubbles in a spherical shape, and flattening of the bubble occurred to form a "cap" having a higher drag coefficient than a rigid sphere of equivalent volume.

Griffith (1962) proposed an "Insoluble film Theory" where surfactants adsorbed on a fluid globule moving in a liquid accumulated at the rear of the globule to form a cap of immobile surface. He then showed that it was the reduction in surface tension by a surfactant rather than the resultant surface tension alone that was the criterion for the transition from a circulating to a non-circulating state upon the addition of surfactants. Experimental evidence was presented that provided good agreement with his model.

Measurement of the Mass Transfer Coefficient k_L

It wasn't until the mid-century mark that reliable and reproduceable measurements of mass transfer coefficients

(k_L) were made. Among others, Datta et al. (1950) recorded mass transfer coefficients for carbon dioxide dissolving into water. The k_L values obtained were indicative of circulating conditions within the bubbles.

Coppock and Meiklejohn (1951) began with the mass transfer equation (equation 1) and noted that for a stream of bubbles aerating a liquid:

$$V\,dc = dm\,N\,\frac{h}{V_\infty} \qquad (10)$$

where: V = volume of liquid in the aerator,

dc and dm - incremental changes in concentration of the solute in the liquid and mass of the solute in the gas respectively,

N = number of bubbles produced per unit time,

h = height of the aerator, and

V_∞ = rise rate of the bubbles.

They combined equations 5 and 10 to obtain:

$$\frac{dc}{dt} = k_L\,\frac{A}{V}\,N\,\frac{h}{V_\infty}\,(C_i - C_L) \qquad (11)$$

where A = average surface area of each bubble.

As was expected, a plot of log $(C_i - C_L)$ versus time for a given set of conditions in an aerator was linear, the slope being equal to:

$$\text{slope} = k_L\,\left(\frac{A}{V}\,N\,\frac{h}{V_\infty}\right) \qquad (12)$$

More recently, the terms within the bracket in equation 12 have been combined and defined as the specific surface area (a). Equation 12 then becomes:

$$\text{slope} = k_L a \qquad (13)$$

The term $k_L a$ has been defined as the overall mass transfer coefficient for a particular aeration system.

Downing and Trusdale (1955) in an effort to understand reaeration in the Thames estuary in England, studied the effect of various factors on k_L values. Wind velocity, wave height, and submerged turbulence were shown to have a positive effect on k_L. Temperatures also increased k_L, but to a lesser degree. Oil films were found to have a depressing effect on k_L and it was hypothesized that this was due to the added diffusional resistance. Surfactants also depressed k_L, but only up to a certain limiting concentration beyond which no further depression occurred.

A Theoretical development from first principles was made by Garner and Keey (1958) to determine the local mass transfer rates at any angle θ from the forward stagnation point around a rising sphere.

Griffith (1960) presented several correlations using the Reynolds $\left(\frac{V \quad d}{\nu}\right)$, Sherwood $\left(\frac{k_L \quad V_\infty}{D}\right)$, and Schmidt $\left(\frac{\nu}{D}\right)$ numbers, the shear viscosity (μ), and the surface tension (σ) for both laminar ($R < 1.0$) and turbulent ($R > 1.0$)

spheres and for varying degrees of circulation from rigid sphere to fully circulating behaviour. He determined the empirical constants for his correlations using experimental data obtained with a water tunnel apparatus similar to the one used in this study. For rigid sphere behaviour, he found the following correlation :

$$Sh = a + b\, Re^{1/2}\, Sc^{1/3} \qquad (14)$$

where: Sh = Sherwood number,

Re = Reynolds number,

Sc = Schmidt number, and

a & b - empirical constants depending on the constituent of the bubble phase.

Eckenfelder and O'Connor (1961) and Rich (1961) correlated the Sherwood, Reynolds and Schmidt numbers in a different fashion for application to diffused air aeration systems. They added a depth factor L (depth to the diffusers) and manipulated terms so that the overall mass transfer coefficient (k_La) for an aeration system was a function of the tank volume (V), tank depth (L), and air flow rate (q) as follows:

$$k_La = B\, \frac{L^{(1-m)}\, q^{(1-n)}}{V} \qquad (15)$$

where: B = a constant characteristic of the aeration system, and

(1-m) and (1-n) = exponents also characteristic of the aeration system.

Dobbin (1964), and later Metzger and Dobbins (1967), studied mass transfer across an atmospheric surface into a turbulent liquid. They obtained data from which they calculated the rate of surface renewal (r) and film depth (L) in equation 7 developed by Dobbins (1956) for the mass transfer coefficient (k_L).

k_L Variations in Waste Treatment Aeration Systems:

Doing both laboratory and prototype studies, several investigators in the sanitary engineering literature have attempted to determine the effects of many factors, including surface active agents, on k_L values. Lynch and Sawyer (1954) performed batch aeration studies on solutions of tap water containing known concentrations of various household synthetic detergents (syndets). They noted that each retail syndet had different foaming characteristics and each varied in their effect on oxygen transfer.

A decrease in the "oxygenation capacity" of diffused air aerators with the addition of detergents was observed by Baars (1955). However, he noticed that the oxygenation capacity of a Kessener Brush pilot plant was increased by the addition of detergents. This he attributed to the fact that detergents induced rigid sphere behaviour in rising bubbles from a diffuser while with the Kessener Brush, the vigorous turbulence around the teeth of the rotating brush caused rapid stripping and renewal of the surface layers.

Downing et al. (1957) made experimental studies on the surface aeration of deaerated water using various concentrations of household detergents from 0.1 to 15.0 mg/l. In all cases, he found that increasing concentration of the detergents depressed the reaeration rate. In further studies, Downing and Scragg (1958) found that the performance of a pilot activated sludge treatment plant was impaired by the addition of small concentrations of detergents when compared to the performance of a detergent-free plant. This they attributed to a decrease in the oxygenation capacity of the aerator caused by the surface active properties of detergents.

A comprehensive investigation of the effects of increasing surfactant concentration on the overall mass transfer coefficient for a given diffused air aerator (k_La) was made by Mancy and Okun (1960). Generally, with initial increases in surfactant concentrations, a very marked drop in k_La was noticed. The overall coefficient reached a minimum value and then gradually increased as the surfactant concentration was increased further. They also noticed that for a given air flow rate and diffuser orifice, increasing the surfactant concentration lowered the surface tension and resulted in a more rapid formation of bubbles of smaller volume. In this and in subsequent paper (Mancy and Okun, 1963), they theorized that the original rapid drop of k_La could be the result of

the cessation of circulation inside the bubble. Surface active agents, owing to the polar nature of their molecules, are attracted to interfaces and would coat a bubble thereby impeding surface flow and stopping circulation. Once circulation has stopped, increasing the concentration of surfactant would no longer affect k_L; however, the lower surface tension and subsequent formation of smaller bubbles would increase the total bubble interfacial area. In an aerator of constant volume, this would cause an increase in the specific bubble surface (a) and result in the observed gradual increase in k_La.

Eckenfelder and O'Connor (1961) and other investigators have established a ratio relating the k_La value obtained with a waste containing surfactants to that value obtained in clear tap water

$$\alpha = \frac{k_La \text{ (for waste)}}{k_La \text{ (for tap water)}} \qquad (16)$$

For most waste, α varies between 0.25 and 1.0 and is dependent upon the type of waste, the type of aeration device used, and the geometry of the tank.

CHAPTER 3

EXPERIMENTAL

To study the mass transfer with single dispersed bubbles, a water tunnel was constructed using concepts employed by Griffith (1960), Houghton (1967) and other workers. The apparatus, sketched in figure 1, consisted of $1\frac{1}{2}$ inch nominal inside diameter glass pipe separated by neoprene gaskets. All piping was manufactured by Q.V.F. Limited, England. Incorporated in the loop were a centrifugal pump with variable speed drive, an orifice plate, a thermometer, a scintered glass diffuser, and a modified test section. Flexible tygon tubing adapted the pump to the rigid glass piping.

Figure 2 shows the test section in which the gas bubble was suspended on a teflon tip supported by fine stainless steel tubing. During the tests, the size of the bubble was kept constant by feeding gas through a three-way glass valve from a "Manostat" micropipet (1.0 cc capacity, accurate to $\pm$ 0.001 cc). A cross-sectional drawing of the teflon tip and stainless steel tubing is sketched in figure 3a. The tip had a diameter of approximately 0.170 cm. at the top with an expanding taper to approximately 0.320 cm at about the

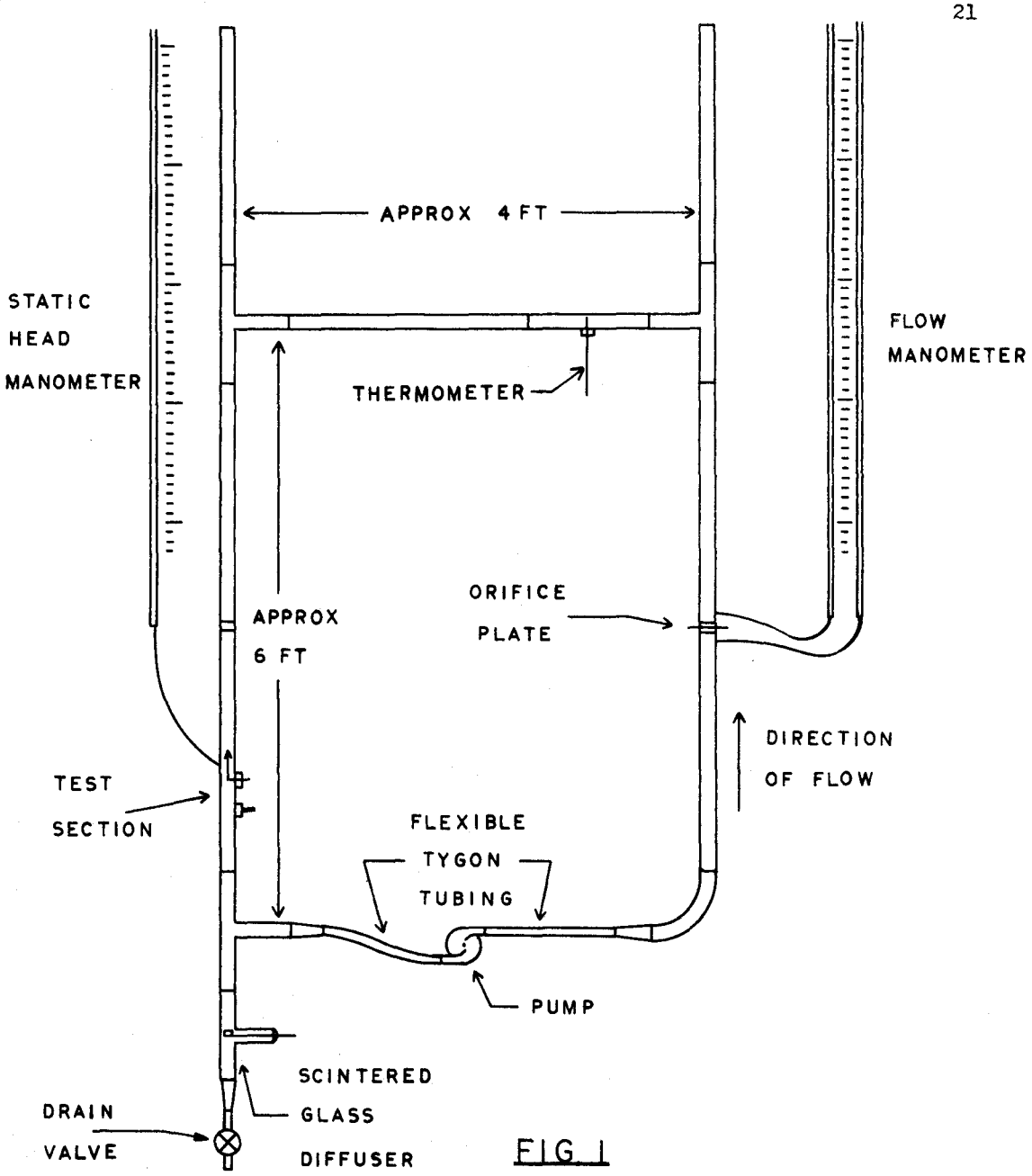

FIG 1

SKETCH OF APPARATUS

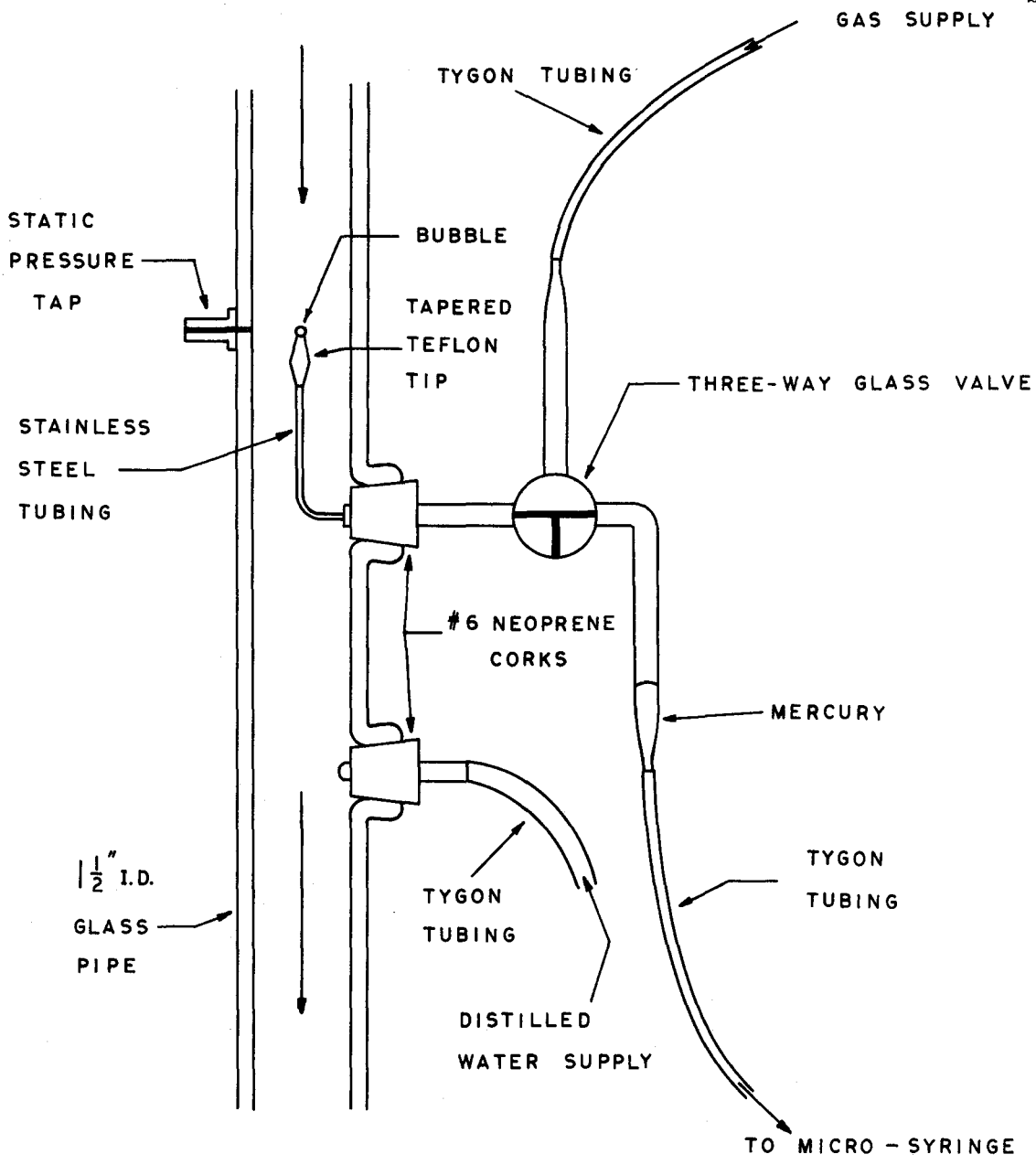

FIG. 2

SKETCH OF TEST SECTION

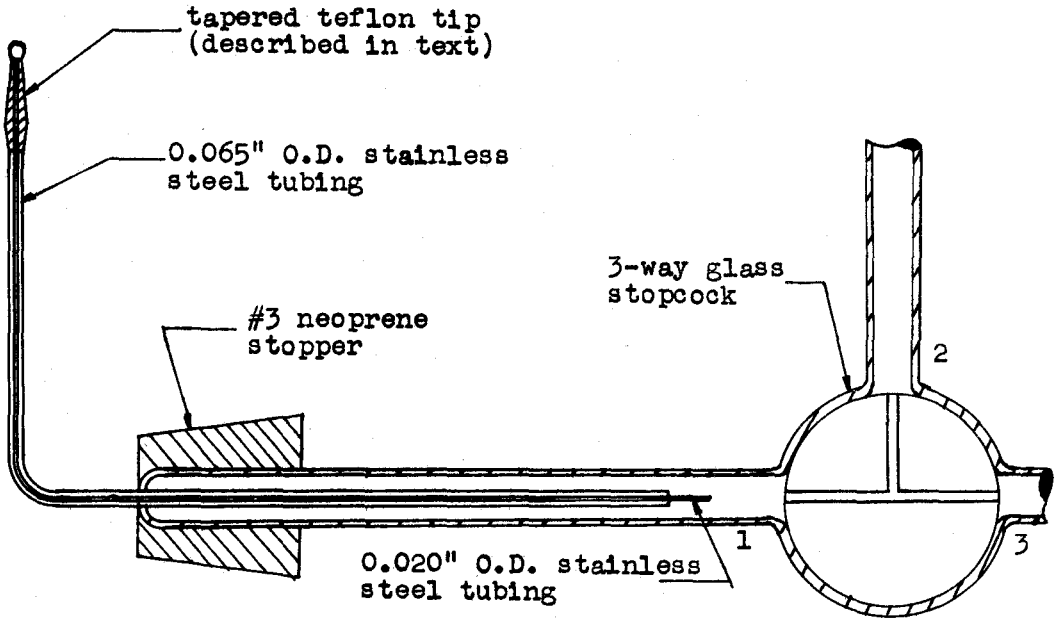

FIGURE 3a

BUBBLE SUPPORT AND FEEDER ASSEMBLY

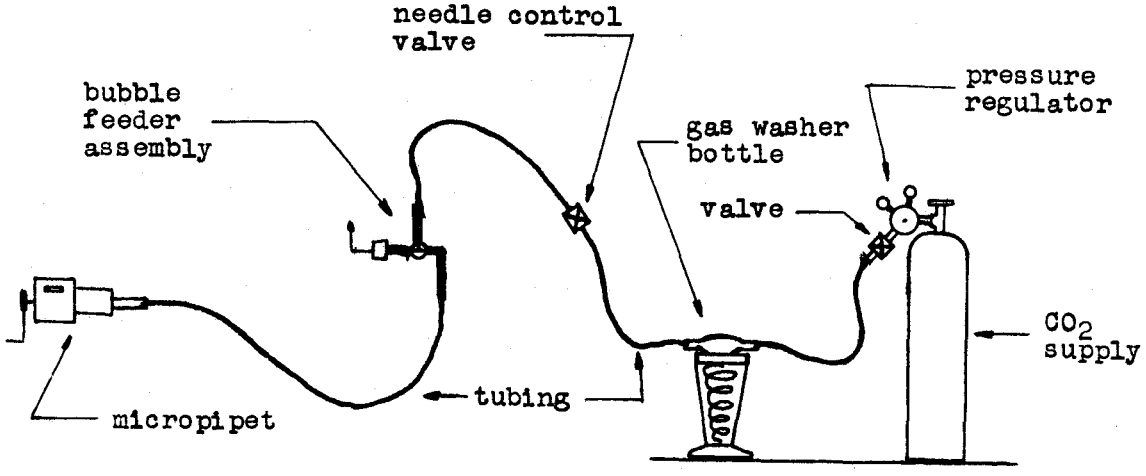

FIGURE 3b

GAS FEEDING EQUIPMENT

three-quarter point and a reducing taper to approximately 0.25 cm at the base. It is seen that two stainless steel tubes were connected to the tip, one inside the other. The outer one (0.065" O.D.) was for structural support while the inner one (0.020" O.D. and approximately 0.012" I.D.) carried gas to the bubble. Neoprene stoppers and gaskets were used wherever required in the apparatus.

Equipment associated with the gas feeder assembly is pictured in figure 3b. A regulated gas cylinder fed gas through a Fisher-Milligan Gas Washer Bottle to saturate the feed gas with water vapour. A needle valve controlled the gas flow to the bubble feeder assembly when a fresh supply of gas was required. A second pressure - regulated supply of gas was connected to the glass diffuser in the bottom leg of the apparatus.

Two orifice plates (5/16" and 3/16" diameter) were calibrated in place by pumping from a constant-head reservoir, through the orifice, and into a tank mounted on a scale. The time taken to pump a given weight of water for a constant head differential across the orifice plate was measured. The flow was calculated and calibration curves for the 5/16" and 7/16" orifices were plotted (Appendix "A"). Calibration curves giving the average or Q/A velocity in the pipe for a given orifice differential also appear on Appendix "A".

A study of pipe centre-line velocities was made using red acid Rhodamine B dye. The thermometer was removed from the top horizontal of the apparatus and inserted in place of the bubble feeder assembly. A hypodermic syringe was used to inject small "pulse" inputs of dye into a pre-set flowing stream of water in the loop through a stopper at the former location of the thermometer. The front of this input of tracer was taken to be the centre-line velocity in the pipe and was timed over a distance of 61.1 cm along the top horizontal pipe for various Q/A flow rates set using a constant orifice differential. The ratio of $\frac{\text{Q/A velocity}}{\text{centre-line velocity}}$ versus Reynolds number was plotted in figure 4. Within the scatter of the data, there is essentially no visible discontinuity between the plotted points for each orifice plate and a continuous curve was constructed through all points.

Streeter (1961, page 3 - 15) presented the following formula for turbulent flow conditions:

$$\frac{V_{max}}{V_{Q/A}} = \frac{1.0 + 4.07\sqrt{\frac{f}{8}}}{1.0} \qquad (17)$$

where V_{max} = maximum pipe velocity (centre-line),

$V_{Q/A}$ = average pipe velocity, and

f = Fanning friction factor,

For high Reynolds numbers ($R \geq 10^4$) values of f=0.031 have been given for smooth pipes (Eskinazi 1962, page 390).

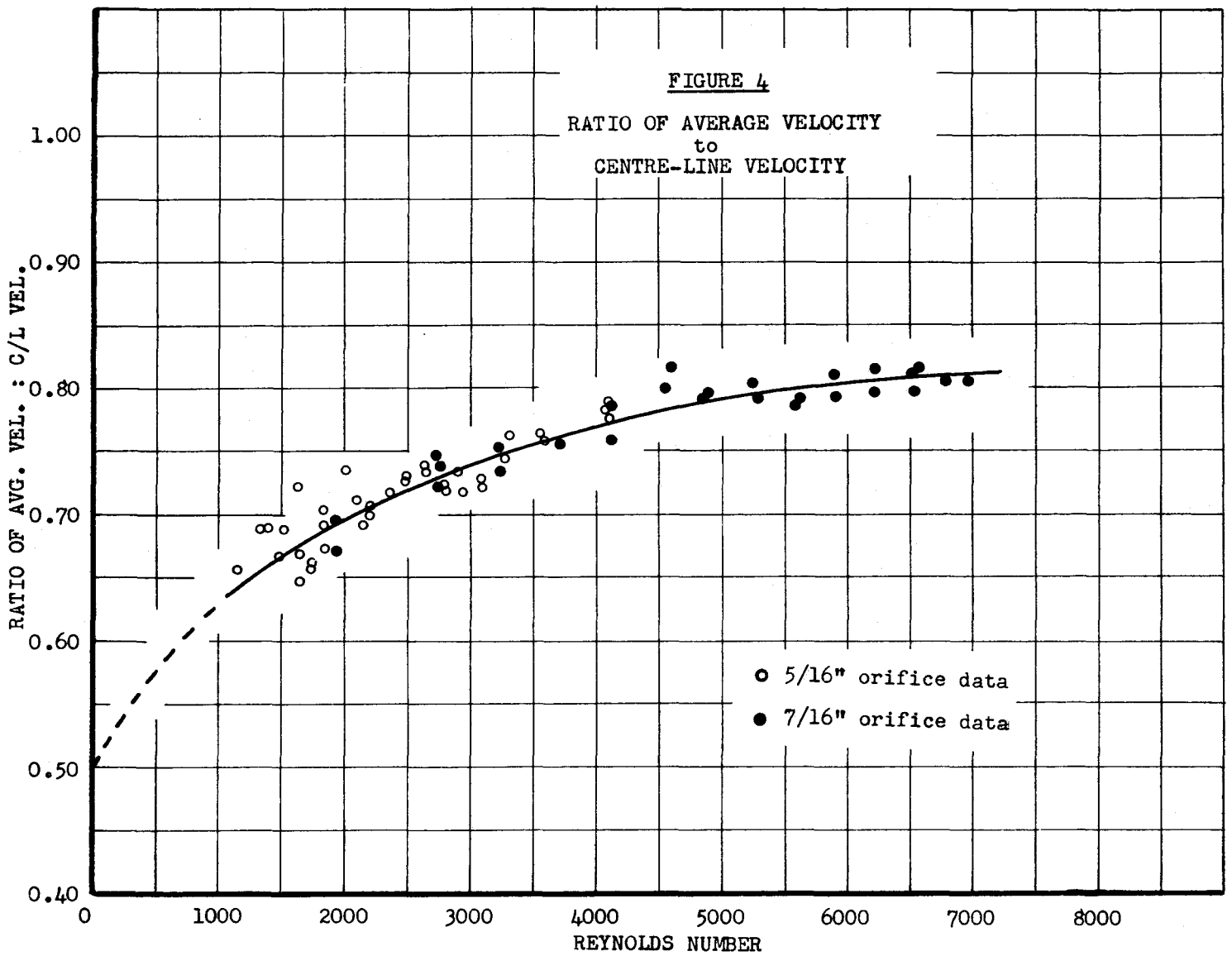
FIGURE 4
RATIO OF AVERAGE VELOCITY
to
CENTRE-LINE VELOCITY
RATIO OF AVG. VEL. : C/L VEL.
1.00
0.90
0.80
0.70
0.60
0.50
0.40
0
1000
2000
3000
4000
5000
6000
7000
8000
REYNOLDS NUMBER
5/16" orifice data
7/16" orifice data

Substituting into equation 17, we obtain:

$$\frac{V_{max}}{V_{Q/A}} = 1.25 \quad \text{or} \quad \frac{V_{Q/A}}{V_{max}} = 0.80$$

Figure 4 indicates that the estimated curve through the experimental points approaches $\frac{V_{Q/A}}{V_{max}} = 0.82$ at Re $= 10^4$. The relatively small difference between the experimental results and those predicted by equation 17 are not considered significant.

For small Reynolds numbers (laminar flow conditions), the velocity profile was assumed to be parabolic (Eskinazi, 1962), and the average velocity was taken to be one-half the maximum or centre-line velocity;

$$\frac{V_{Q/A}}{V_{max}} = 0.50 \qquad (18)$$

for the limiting condition. For this apparatus, it was assumed that the average pipe velocity increases, there was a gradual tendency to progress from a parabolic profile, where $\frac{V_{Q/A}}{V_{max}} = 0.50$ at low Reynolds numbers, to a fully developed turbulent profile, where $\frac{V_{Q/A}}{V_{max}} = 0.82$ at high Reynolds numbers. Figure 4 was used to plot a second calibration curve for the orifice plates of centre-line velocity versus orifice differential which appears in Appendix "A". The

5/16" orifice plate was used for the duration of this study.

Dye studies were also made by suspending a potassium permanganate crystal in the centre of the pipe and observing the resulting stream line for various flow velocities. Visual observations indicated that the flow regime was essentially laminar up to a pipe Reynolds number of 2300 when turbulent flow patterns were first observed.

The bubble was observed through a Brunson #605936 telescope equipped with an optical micrometer. At the test section, the surface of the $1\frac{1}{2}$ I.D. glass pipe had a prominent curvature about the vertical axis. This refraction widened the observed image of the tip and bubble inside the pipe when the pipe was filled with water. Using the optical micrometer, the actual width of various objects was measured in air outside the pipe and compared to the equivalent width, measured inside the water-filled test section. A calibration curve was plotted and appears in Appendix "B". A straight line was fitted through the origin by least squares, and from the slope, the following relationship was obtained.

$$W = 0.732\ W' \qquad (19)$$

where W = actual width

W' = apparent width in water-filled test section.

This correction factor was used to reduce all widths measured in the test section throughout this work.

Areas and volumes of various bubble sizes under various centre-line pipe velocities were determined. Photographs were taken of bubbles ranging from 0.127 cm to 0.216 cm in height above the teflon tip and using centre-line pipe velocities from 4.0 to 11.0 cm/second. The photographic negatives were mounted on 35 mm slides and then projected on a screen. The outline of each bubble was traced from the screen projection (Appendix "C"). Co-ordinates of the circumference of the traced projection of the bubble were transferred to computer data cards with the aid of a Benson-Lehner Oscar Model F. A computer program was developed utilizing the summation of successive volumes and areas of incremental frustrums of a cone to approximate the bubble area and volumes (see Appendix "H"). The accuracy of this program was checked by tracing the co-ordinates of a two-dimensional projection of a sphere (a circle in two dimensions) of known size. It was found that for a sphere of 0.270 cm diameter on the tracing, the area and volume calculated with the Oscar and computer program was 0.2293 cm^2 and 0.01024 cm^3 respectively whereas the standard formulae of Area = πd^2 and Volume = $\frac{\pi}{6} d^3$ gave 0.2290 cm^2 and 0.01031 cm^3 respectively. Therefore, the computer program was considered reliable.

Plots of bubble height versus bubble area and volume appear in Appendix "C". Parabolic second order regression lines for each of the four centre-line pipe velocities were fitted. In fitting the data, it was assumed that at the limiting condition of zero bubble height, the area and volume were independent of the range of velocities used.

Likewise, the photographic and regression fitting methods described above were used for an inverted bubble. The results also appear in Appendix "C".

Prior to testing, the apparatus was dismantled and thoroughly cleaned. The glass pipe was soaked in an acid - chromate cleaning solution and all pipes and fittings were rinsed with distilled water.

In preparation for an experimental run, high purity oxygen or nitrogen gas was bubbled from the scintered glass diffuser up one side of the loop for approximately two hours in order to saturate the distilled water with either oxygen or nitrogen and strip other dissolved gases. The three-way valve was set in the 1-2-3 position and high purity carbon dioxide was connected to the bubble feeder assembly and allowed to escape at a low rate from the teflon tip to prevent water from entering the feeder assembly. Immediately prior to a run, the nitrogen (or oxygen) flow was stopped, the desired water velocity was set, and the temperature of the water, barometric pressure, and static head at the bubble

elevation, were recorded.

The 3-way valve in the feeder assembly was set in the 1-3 position and then a CO_2 bubble was formed on the teflon tip and fed appropriate quantities of CO_2 from the micro-pipet to replace that gas which transferred from the bubble into the liquid to maintain the bubble at a constant size. The quantity of gas fed to the bubble was recorded every 30 seconds and a volumetric feed rate, that was proportional to the rate of CO_2 mass transfer across the interfacial area of the bubble, was calculated. Normally, the duration of a run would be 40 minutes. Immediately following a run, several 20 micro-liter samples of liquid were taken from the water tunnel and injected into a Beckman Infra-red Carbon Analyser. The carbon concentrations obtained were used to calculate the dissolved CO_2 level in the water tunnel for that run.

Runs were made with the teflon tip positioned both erect and inverted. No difference was noticed in the results of either configuration so it was decided to employ an erect bubble tip as the bubble appeared more stable. Two bubble heights (0.165 cm and 0.203 cm) and two centre-line pipe velocities (5 and 10 cm/sec.) were selected. Combinations of these yielded bubble Reynolds numbers of 104, 121, 212, and 246. All runs were made with pure carbon dioxide initially in the bubble. A set of runs for the Reynolds numbers

specified above was made with nitrogen dissolved in the water of the loop. Another set of runs was made with oxygen in the liquid phase. A third set of runs was made with the liquid phase deaerated. This was accomplished by first saturating the water with oxygen and then adding sodium sulfite to a concentration of approximately 75 mg/l to deoxygenate, and hence degasify, the water. Some runs were repeated with the addition of concentrations of ABS, a surface active agent, in varying concentrations to a maximum of 7.4 mg/l. Generally, at least three repeated runs were made for each condition.

The "Methylene Blue" technique as outlined in Standard Methods for the examination of Water and Wastewater (12th edition) was used for determination of the surfactant concentration. A Coleman Model 14 Universal Spectrophotometer with 20 mm rectangular curvettes was used for the colour comparison. The calibration curve of percent transmitting versus ABS concentration is shown in Appendix "D".

As it was felt that the interfacial area would directly affect the rate of mass transfer from a given bubble, the diameter of a sphere of equivalent surface area was chosen to characterize the test bubble. A summary of the experimental conditions for each series of runs made appears in Table I.

TABLE (I)

SUMMARY OF EXPERIMENTAL CONDITIONS

Bubble Height (cm)	Centre-Line Pipe Velocity (cm/sec.)	Reynolds Numbers	Bubble Volume (cm^3)	Bubble Area (cm^2)	Charateristic Bubble Dia. for a sphere of Equivalent Surface Area (cm)
0.165	5.0	104	0.00345	0.096	0.174
0.165	10.0	212	0.00360	0.099	0.1775
0.203	5.0	121	0.00525	0.130	0.203
0.203	10.0	246	0.00550	0.134	0.206

CHAPTER 4

DATA ANALYSIS

Before analyzing the data, the cumulative gas volumes recorded every 30 seconds from the micro-pipet during the course of a run were transposed to volumetric feed rates $\left(\frac{dV}{dt}\right)$ and plotted with time.

Throughout this study, the temperature could not be controlled, but varied between the limits of 27.0°C and 31.5 °C with a mathematical average of 28.67°C over all runs. The temperature for each run was recorded and used to select the dissolved gas saturation concentration value in the liquid. This value was picked from the curves plotted in Appendix "E" using data taken from the Handbook of Physics and Chemistry. However, to select the appropriate viscosity and diffusivity values to use for calculating the Reynolds, Sherwood, Schmidt and Peclet numbers in each series of runs, the arithmetic average temperature of 28.67°C was used. The viscosity ν was selected from data supplied by Eskinazi (1962) and the diffusivity D from data by several workers - Davidson and Cullen (1957), Baird and Davidson (1962), and Metzger and Dobbins (1967). Plots showing the temperature dependence of the diffusivity and viscosity appear in Appendicies "E" and "F". The values used were

ν = 8.36 x 10^{-3} cm^2/sec and D = 2.2 x 10^{-5} cm^2/sec. for carbon dioxide, D = 2.28 x 10^{-5} cm^2/sec. for nitrogen, and D = 2.65 x 10^{-5} cm^2/sec. for oxygen.

The data for a carbon dioxide bubble dissolving into degasified (oxygenated and then deoxygenated with sodium sulfite) water was analyzed first. Knowing the molecular weight of carbon dioxide, the temperature and the pressure in the immediate vicinity of the bubble, $\frac{dV}{dt}$ may be changed to a mass feed rate $\frac{dm}{dt}$. This is the mass rate at which carbon dioxide transfers across the interface of the bubble in question and corresponds to the left hand side of equation 1.

$$\frac{dm}{dt} = k_L A (C_i - C_L) \qquad (1)$$

The interfacial area A can be determined from figure 23; the interfacial CO_2 concentration C_i is equal to the saturation value of CO_2 in distilled water (C_s) at the given temperature and pressure(from Appendix "E"), and the concentration of dissolved gas in the bulk of the liquid C_L was obtained using the carbon analyzer. Knowing this, the unknown mass transfer coefficient k_L was calculated using equation 1 for the experimental conditions. These k_L values were then used to verify Griffith's CO_2 correlations for Reynolds, Schmidt and Sherwood numbers.

Because the Fisher-Milligan gas washer bottle was employed in the gas feeding apparatus, it was assumed that both the gas in the bubble and the feed gas were saturated with water vapour and in equilibrium with the liquid phase. Hence, a volume correction was applied to the volume of gas fed to the bubble using water vapour pressure data taken from the Handbook of Physics and Chemistry. This correction amounted to approximately a 4% decrease in $\frac{dV}{dt}$ for the static heads encountered in this study. It was not necessary to correct the partial pressures of gases in the bubble because the data used for saturation concentration values (Appendix "E") taken from the Handbook of Physics and Chemistry, were adjusted for vapour gases saturated with water vapour.

A mathematical model for two-way mass transfer was developed based on a volume balance on the single bubble system used in the experiment (figure 3a). The direction of mass transfer for gases A and B across the bubble interface can occur either way depending on the relative gas concentration values at the interface and in the bulk of the liquid. As before, transfer into the bubble was assumed positive. Then for a volume balance on this system:

$$\begin{pmatrix}\text{Volume Rate of}\\ \text{Input of A}\\ \text{from bubble}\\ \text{Feeder Assembly}\end{pmatrix} = \begin{pmatrix}\text{Volume Rate of}\\ \text{Change of A}\\ \text{in the bubble}\end{pmatrix} + \begin{pmatrix}\text{Volume Rate of}\\ \text{Change of B}\\ \text{in the bubble}\end{pmatrix} \quad (20)$$

$$\text{or} \quad \left(\frac{dV_a}{dt}\right)_{IN} = \left(\frac{dV_a}{dt}\right) + \left(\frac{dV_b}{dt}\right) \quad (21)$$

From the rate of mass transfer equation (equation 1), we may now write: $\frac{dm_A}{dt} = k_{LA} \cdot A \cdot (C_{iA} - C_{LA})$

$$\text{or:} \quad dm_A = k_{LA} \cdot A \cdot \left(\frac{V_A}{V_A+V_B} \cdot C_{SA} - C_{LA}\right) \quad (22)$$

$$\text{and similarily:} \quad \frac{dm_B}{dt} = k_{LB} \cdot A \cdot \left(\frac{V_B}{V_A+V_B} \cdot C_{SB} - C_{LB}\right) \quad (23)$$

where the subscripts A and B refer to gases A and B respectively. These rates of mass transfer (equations 22 and 23) may be transposed into corresponding rates of volume transfer by giving proper consideration to the gas molecular weight (MW), barometric pressure (P) at the bubble elevation, and the temperature (T) of the system. Then we have for equations 22 and 23 respectively:

$$\left(\frac{dV_a}{dt}\right) = \frac{MW_A}{22.4} \times \frac{P}{760.0} \times \frac{273.0}{T} \times k_{LA} \times A \cdot \left(\frac{V_A}{V_A+V_B} \times C_{SA} - C_{LA}\right) \quad (24)$$

and:

$$\frac{dV_A}{dt} = \frac{MW_B}{22.4} \times \frac{P}{760.0} \times 273.0 \times k_{LB} \times A \cdot \left(\frac{V_B}{V_A+V_B} \cdot C_{SB} - C_{LB} \right) \quad (25)$$

substituting into equation 21:

$$\frac{dV_A}{dt} = \frac{A}{22.4} \times \frac{P}{760.0} \times \frac{273.0}{T} \times \left(MW_A \times k_{LA} \cdot \left\{ \frac{V_A}{V_A+V_B} \times C_{SA} - C_{LA} \right\} + MW_B \times k_{LB} \cdot \left\{ \frac{V_B}{V_A+V_B} \times C_{SB} - C_{LB} \right\} \right) \quad (26)$$

Equation 26 was integrated to find V_A, the cumulative volume fed to the bubble at any time from the micropipet.

On examining equations 24 and 25, it is seen that there will be no transfer of gas A when:

$$\left(\frac{V_A}{V_A+V_B} \times C_{SA} \right) = \left(C_{LA} \right),$$

and that there will be no transfer of gas B when:

$$\left(\frac{V_B}{V_A+V_B} \times C_{SB} \right) = \left(C_{LB} \right).$$

For the experimental conditions, gas A is carbon dioxide and occupies 100% of the bubble volume at the time zero while only dissolved to a relatively small extent in the water. Gas B (either oxygen or nitrogen) exists at something less

than a saturated concentration value at the static head at the bubble elevation. It was assumed that gas B was dissolved to an amount equal to the saturation concentration of B at the static head in the upper horizontal pipe of the apparatus. Consequently, two driving forces result whereby carbon dioxide dissolves from the bubble into the liquid and gas B comes out of solution and begins to occupy some of the bubble volume. During the course of a run, the term $\left(\frac{V_B}{V_A + V_B}\right)$ progressively becomes larger until a steady state is reached where:

$$\left(\frac{V_B}{V_A + V_B} \times C_{SB}\right) = (C_{LB})$$

and no further transfer of B occurs and a system is maintained whereby a small fraction of the bubble volume is occupied by carbon dioxide and the rate of CO_2 input from the micro-pipet has a finite value equal to the rate of transfer of CO_2 from the bubble.

A computer program was developed to simulate an experimental run where the bubble contained 100% by volume of gas A immediately upon formation and a second gas B was dissolved in the liquid phase. Equation 26 was used as a

mathematical model to establish the program. The program is given in Appendix "H". All known or measured experimental variables were specified for each run and used as input data for the program. The variables included bubble area and volume, flow velocity, barometric pressure, static head above the bubble, temperature, molecular weight of both gases A and B, the mass transfer coefficients k_{LA} and k_{LB} for gases A and B respectively, the existing concentration of gas A in the liquid phase, and the saturation concentration of both gases A and B in the liquid phase. Also specified in the data input for the computer solution were the length of the simulated experimental run desired and the increments of time with which the integration is made.

The program prints out the volumetric feed rate from the micropipet $\left(\frac{dV_A}{dt}\right)_{IN}$ at any time during the course of a run. Incidental to this computation, the volumes of gases A and B in the bubble during a run were calculated as well as other pertinent variables. A typical print out of results from the program also appears in Appendix "H".

CHAPTER 5

RESULTS

Carbon Dioxide - Degasified Water

A typical plot of the volumetric feed rate of the micro-pipet versus time for the solution of CO_2 into degasified water (the sodium sulfite runs) appears in figure 5. It was noticed that after a small initial decline, the feed rate approached a constant value in three to four minutes. At least three repeat runs were made for each set of experimental conditions and the arithmetical average of all experimental points for each run beyond the initial three to four minute period was used to calculate the k_L value for that run. Average k_L values for each set of repeat runs were calculated and the appropriate Reynolds, Sherwood, and Schmidt numbers were determined. These were compared to those correlations advanced by Griffith in figure 6. The calculations appear in Appendix "I". It may be seen that the CO_2 - degasified water data compares favourably with Griffith's values. It was decided to use Griffith's correlations to obtain CO_2, N_2, and O_2 k_L values for the conditions of this experiment.

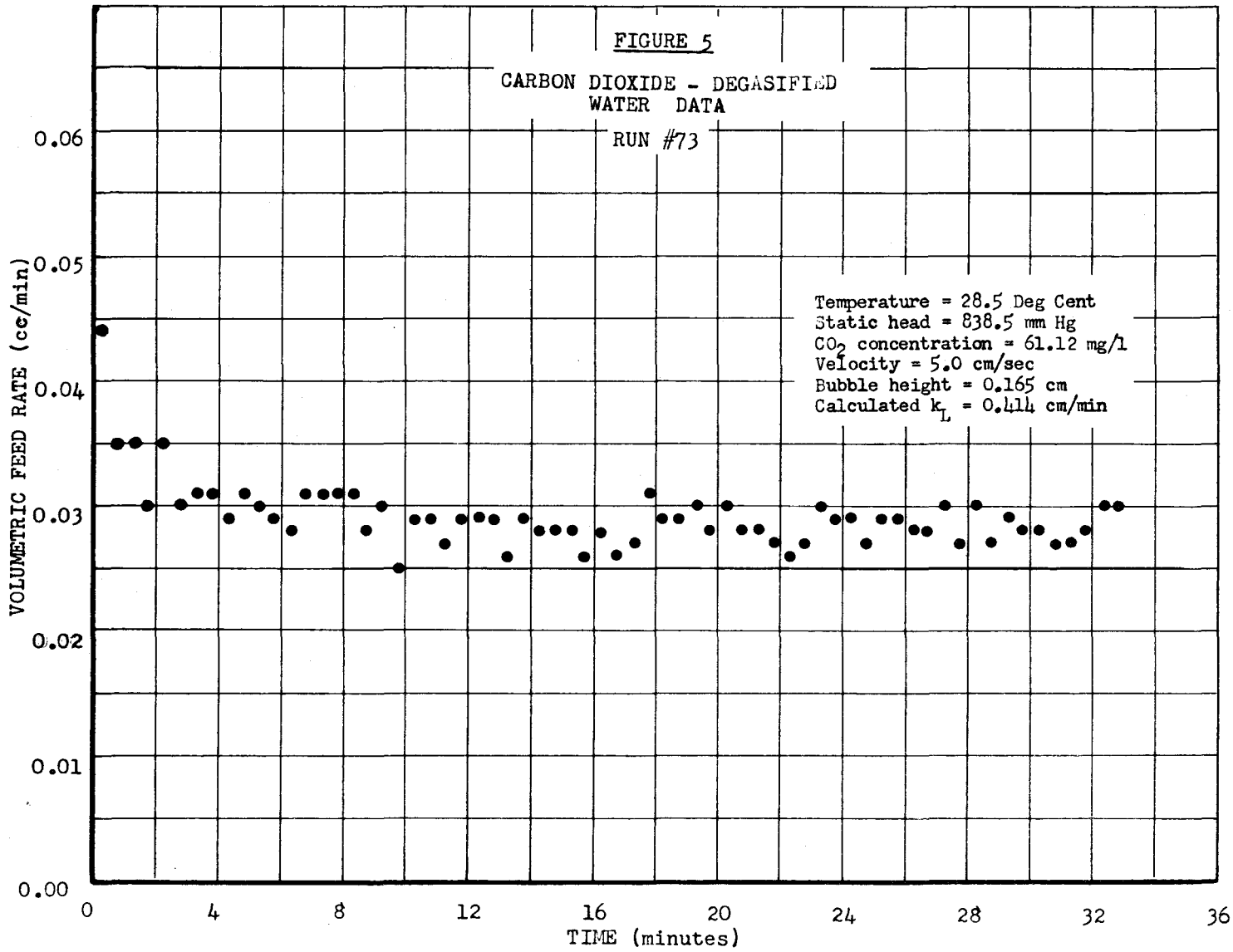
FIGURE 5
CARBON DIOXIDE - DEGASIFIED WATER DATA
RUN #73
Temperature = 28.5 Deg Cent
Static head = 838.5 mm Hg
CO_2 concentration = 61.12 mg/l
Velocity = 5.0 cm/sec
Bubble height = 0.165 cm
Calculated k_L = 0.414 cm/min
VOLUMETRIC FEED RATE (cc/min)
0.00
0.01
0.02
0.03
0.04
0.05
0.06
0
4
8
12
16
20
24
28
32
36
TIME (minutes)

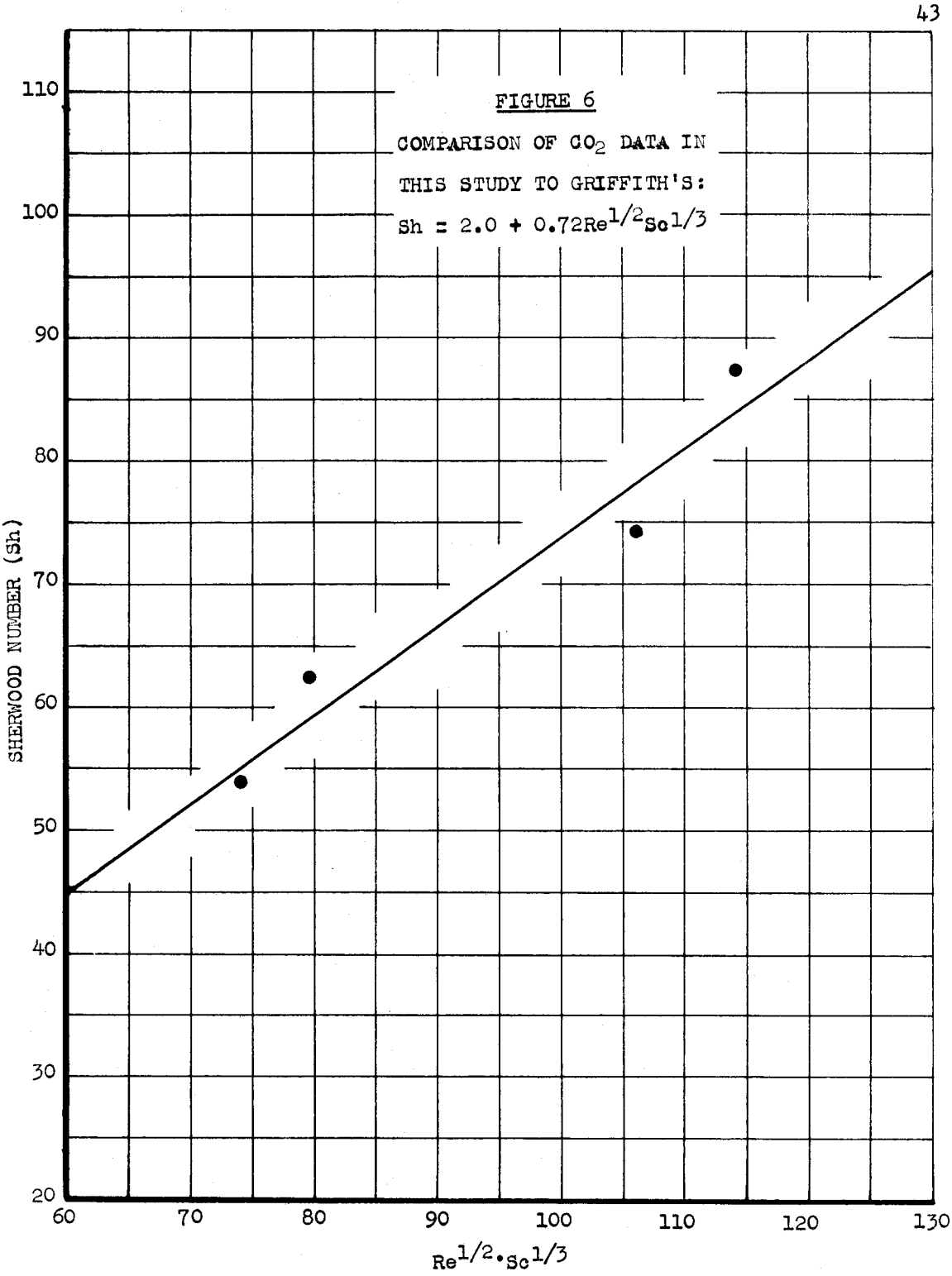
FIGURE 6
COMPARISON OF CO_2 DATA IN THIS STUDY TO GRIFFITH'S:
$Sh = 2.0 + 0.72Re^{1/2}Sc^{1/3}$
SHERWOOD NUMBER (Sh)
110
100
90
80
70
60
50
40
30
20
60
70
80
90
100
110
120
130
$Re^{1/2} \cdot Sc^{1/3}$

Carbon Dioxide - Aqueous Nitrogen Solution (CO_2-N_2 data)

Typical plots of the experimental results for a Reynolds number of 247 appear in figure 7. Superimposed on the experimental data points are two curves obtained from the mathematical model with k_L values representative of circulating ($Sh = 1.13\ Pe^{1/2}$) and non-circulating ($Sh = a + b\ Re^{1/2} Sc^{1/3}$) conditions. Neither curve provides close agreement with the experimental data - the initial rate of volume transfer lying somewhere between the non-circulating and circulating curves. From this comparison coupled with the observed apparent initial decay in feed rate with the CO_2 - degasified water data, it was postulated that the turbulence associated with the bubble formation resulted in initial bubble circulation which was rapidly damped. Consequently, an exponential decay from circulating conditions to non-circulating conditions, at the beginning of the run was arbitrarily imposed upon the mathematical model and fitted by a trial-and-error solution. Figures 8 through 11 indicate the fit obtained with typical runs for each of the four Reynolds Numbers used in this study when 99% of the decay from the circulating to the non-circulating case occurred in the first half minute.

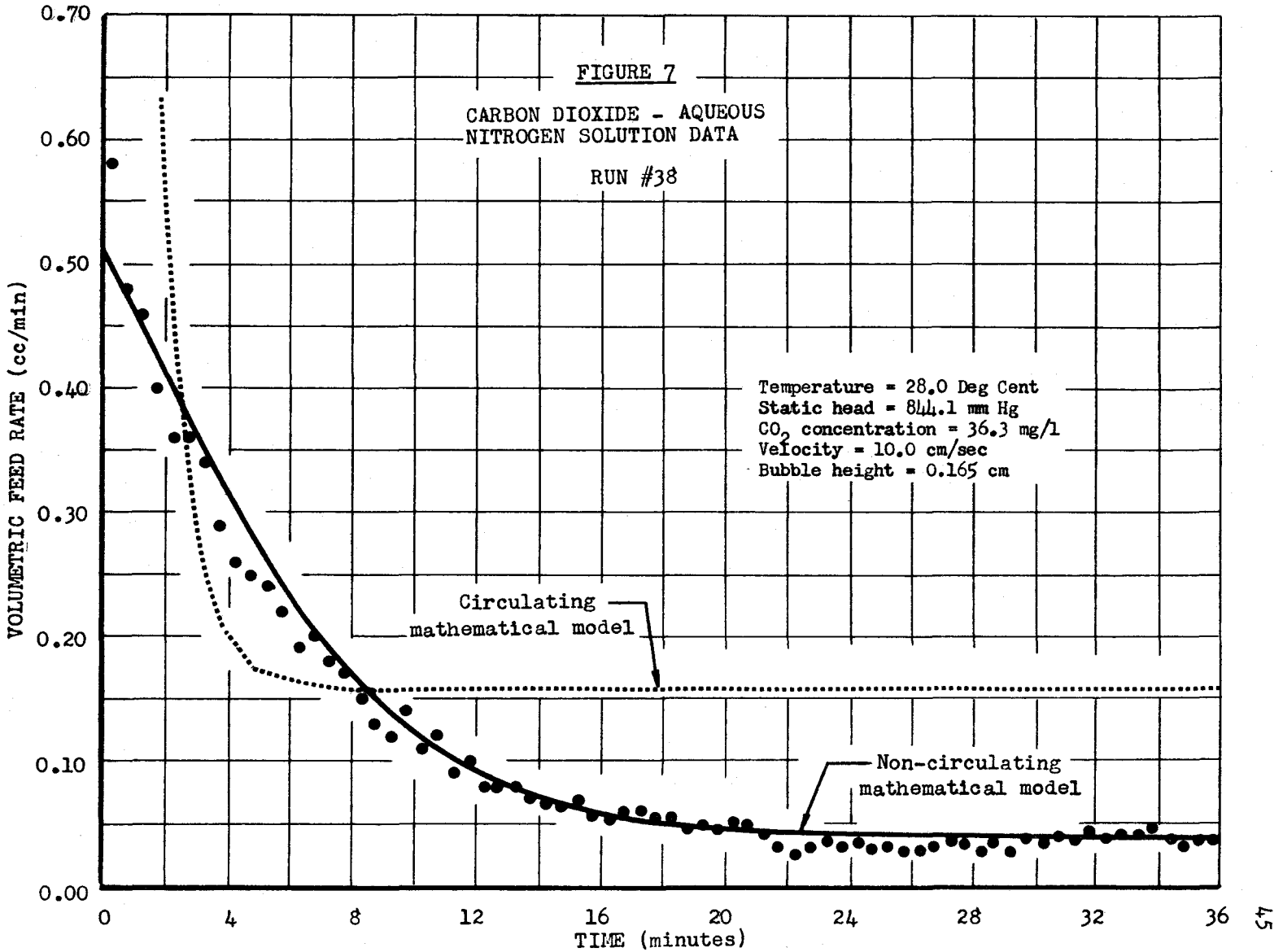
FIGURE 7
CARBON DIOXIDE - AQUEOUS NITROGEN SOLUTION DATA
RUN #38
Temperature = 28.0 Deg Cent
Static head = 844.1 mm Hg
CO_2 concentration = 36.3 mg/l
Velocity = 10.0 cm/sec
Bubble height = 0.165 cm
Circulating mathematical model
Non-circulating mathematical model
VOLUMETRIC FEED RATE (cc/min)
0.70
0.60
0.50
0.40
0.30
0.20
0.10
0.00
0
4
8
12
16
20
24
28
32
36
TIME (minutes)

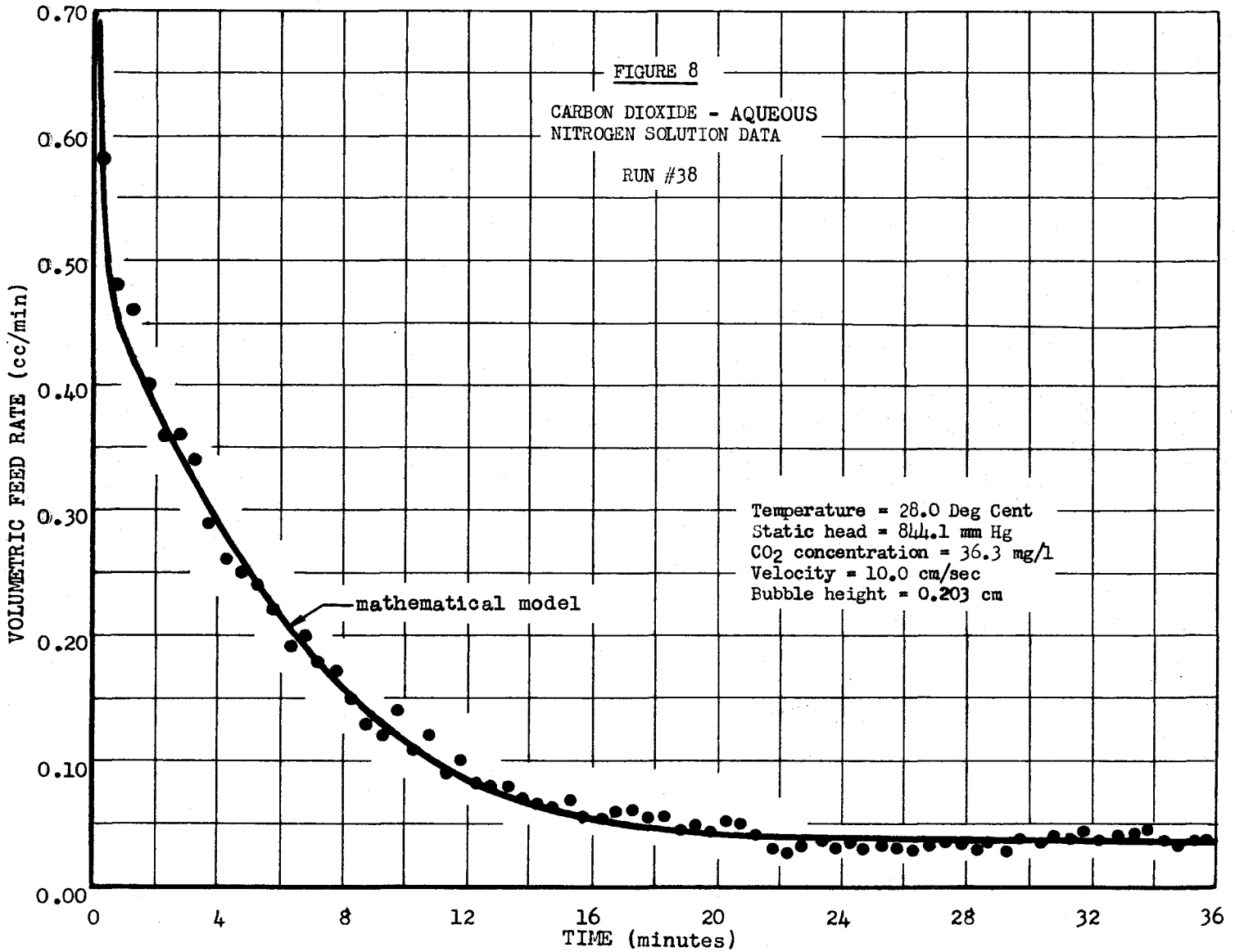
FIGURE 8
CARBON DIOXIDE - AQUEOUS NITROGEN SOLUTION DATA
RUN #38
Temperature = 28.0 Deg Cent
Static head = 844.1 mm Hg
CO_2 concentration = 36.3 mg/l
Velocity = 10.0 cm/sec
Bubble height = 0.203 cm
mathematical model
VOLUMETRIC FEED RATE (cc/min)
0.70
0.60
0.50
0.40
0.30
0.20
0.10
0.00
0
4
8
12
16
20
24
28
32
36
TIME (minutes)

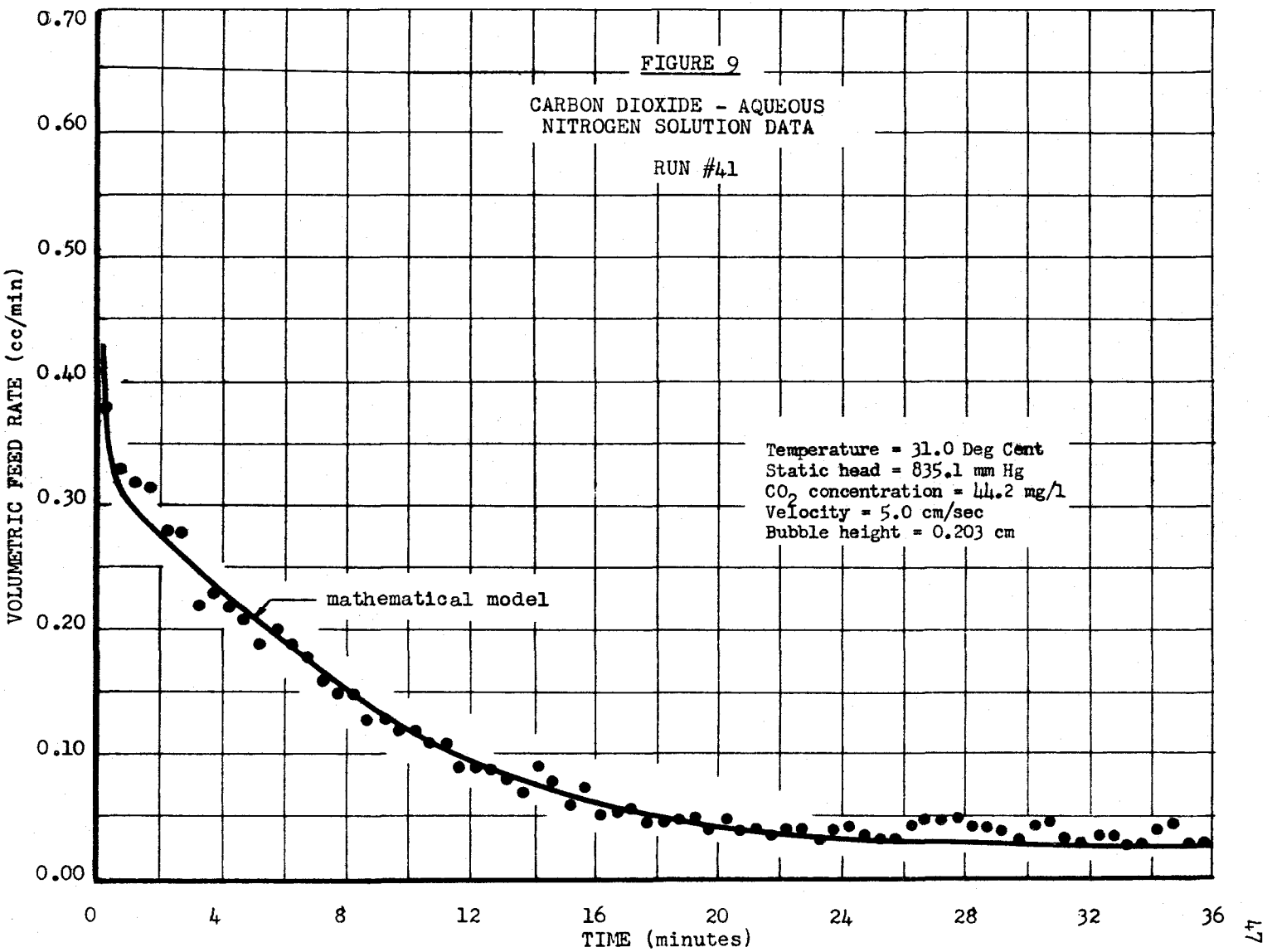
FIGURE 9
CARBON DIOXIDE - AQUEOUS NITROGEN SOLUTION DATA
RUN #41
Temperature = 31.0 Deg Cent
Static head = 835.1 mm Hg
CO_2 concentration = 44.2 mg/l
Velocity = 5.0 cm/sec
Bubble height = 0.203 cm
mathematical model
VOLUMETRIC FEED RATE (cc/min)
0.70
0.60
0.50
0.40
0.30
0.20
0.10
0.00
0
4
8
12
16
20
24
28
32
36
TIME (minutes)

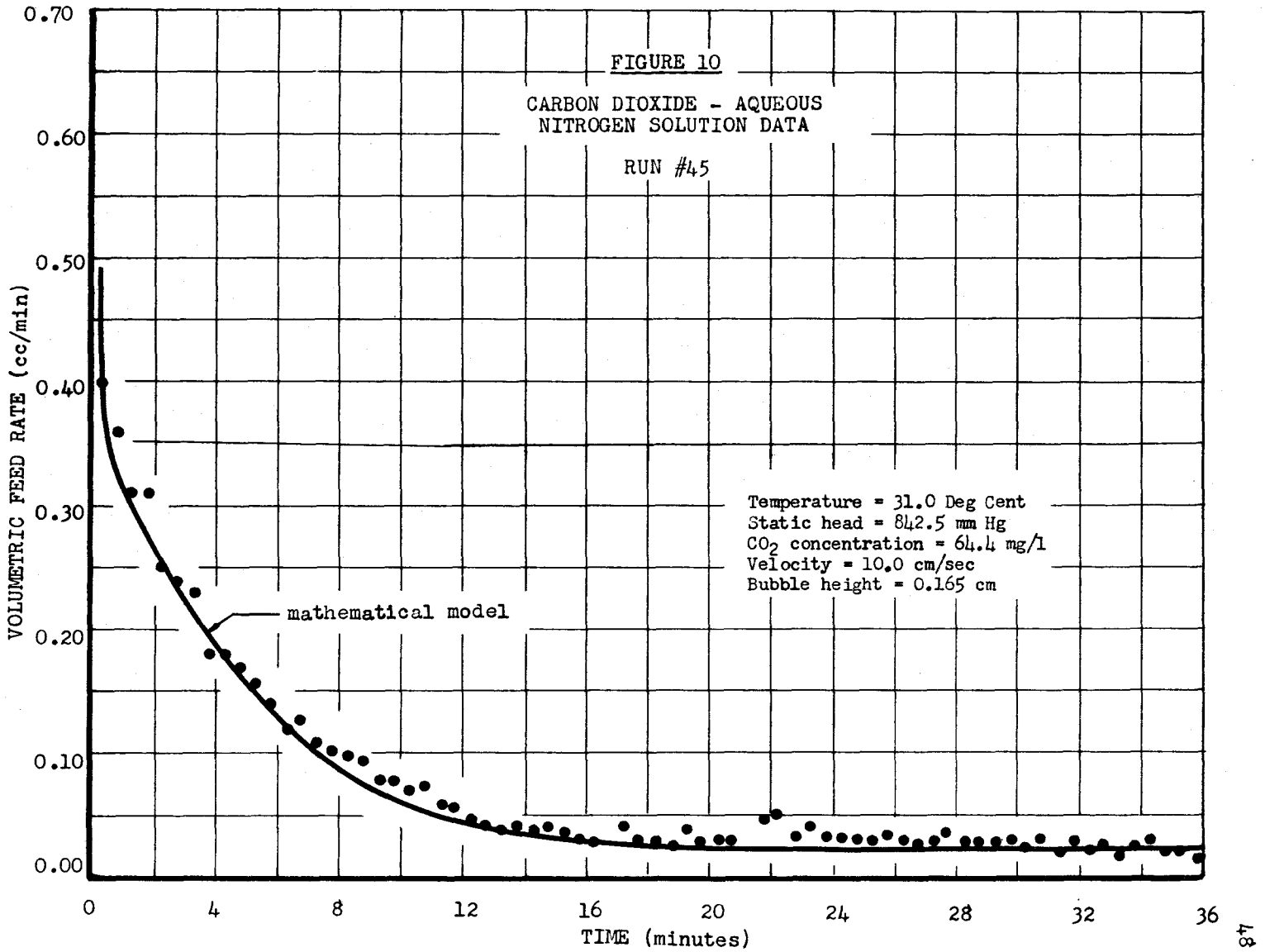
FIGURE 10
CARBON DIOXIDE - AQUEOUS NITROGEN SOLUTION DATA
RUN #45
Temperature = 31.0 Deg Cent
Static head = 842.5 mm Hg
CO_2 concentration = 64.4 mg/l
Velocity = 10.0 cm/sec
Bubble height = 0.165 cm
mathematical model
VOLUMETRIC FEED RATE (cc/min)
0.70
0.60
0.50
0.40
0.30
0.20
0.10
0.00
0
4
8
12
16
20
24
28
32
36
TIME (minutes)

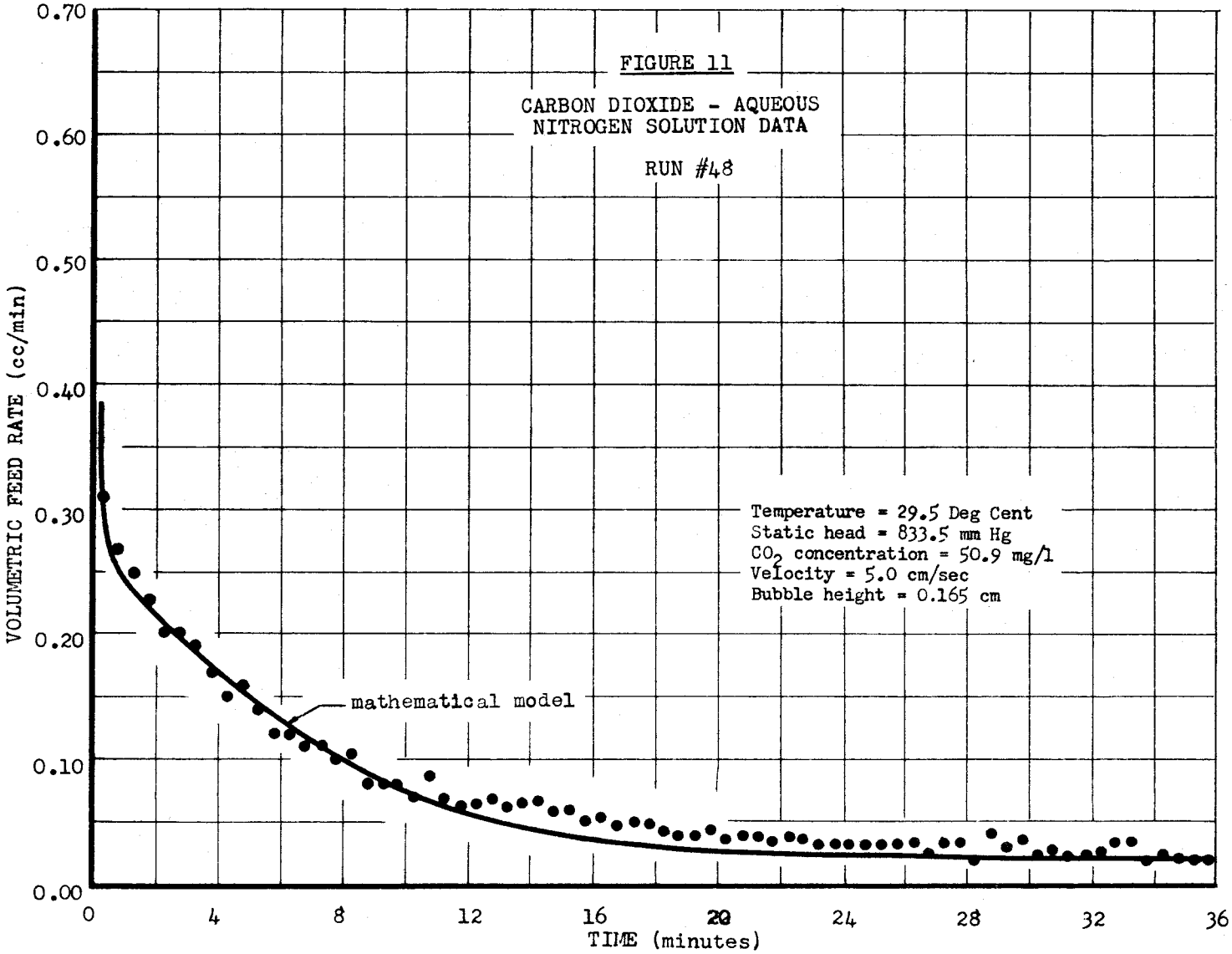
FIGURE 11
CARBON DIOXIDE - AQUEOUS NITROGEN SOLUTION DATA
RUN #48
Temperature = 29.5 Deg Cent
Static head = 833.5 mm Hg
CO_2 concentration = 50.9 mg/l
Velocity = 5.0 cm/sec
Bubble height = 0.165 cm
mathematical model
VOLUMETRIC FEED RATE (cc/min)
0.70
0.60
0.50
0.40
0.30
0.20
0.10
0.00
0
4
8
12
16
20
24
28
32
36
TIME (minutes)

Carbon Dioxide - Aqueous Oxygen Solution (CO_2 - O_2 data)

Figures 12 through 15 show the experimental data for some of the runs made with a carbon dioxide bubble and oxygen dissolved in the liquid phase. The solid line is the plot of the results obtained when the mathematical model again incorporates the same initial half-minute decay from circulating to non-circulating ^{k}L values as was done with the CO_2 - N_2 data.

When comparing the CO_2 - O_2 data with the equivalent CO_2 - N_2 data, the former volumetric feed rate decreases to a steady state at a faster rate than the latter. This would be predicted from the mathematical model, as the driving force for the accumulation of oxygen in the bubble, $\left(\frac{V_B}{(V_A + V_B}\right) \cdot C_{SB} - C_{LB})$ from equation 26, is greater than that for nitrogen as C_{SB} is 36.73 mg/l for oxygen and 16.56 mg/l for nitrogen at 28.67^{o}C.

Surfactant Runs -

A series of runs using the larger bubble size and larger flow velocity (Re = 247) were made with alkyl benzene sulfonate (ABS) concentrations varying from 0.0 to 7.4 mg/l. Table VII shows the results of the ABS determinations for these runs. The rate of mass transfer $\left(\frac{dm}{dt}\right)$ for a CO_2 - N_2 system is calculated from volumetric feed rate data in Table IX , and presented in figure 16 for the different surfactant

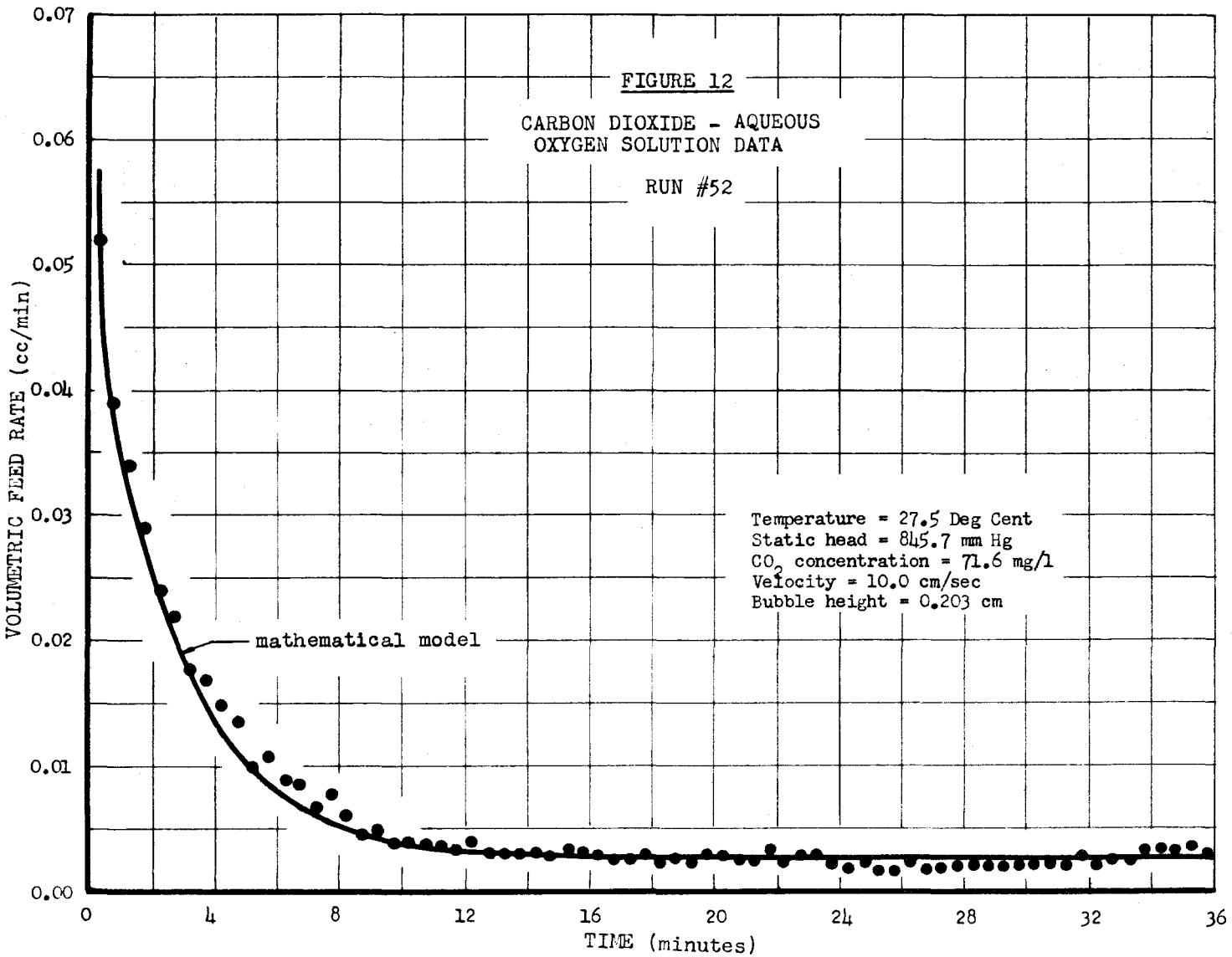
FIGURE 12
CARBON DIOXIDE - AQUEOUS OXYGEN SOLUTION DATA
RUN #52
Temperature = 27.5 Deg Cent
Static head = 845.7 mm Hg
CO_2 concentration = 71.6 mg/l
Velocity = 10.0 cm/sec
Bubble height = 0.203 cm
mathematical model
VOLUMETRIC FEED RATE (cc/min)
0.07
0.06
0.05
0.04
0.03
0.02
0.01
0.00
0
4
8
12
16
20
24
28
32
36
TIME (minutes)

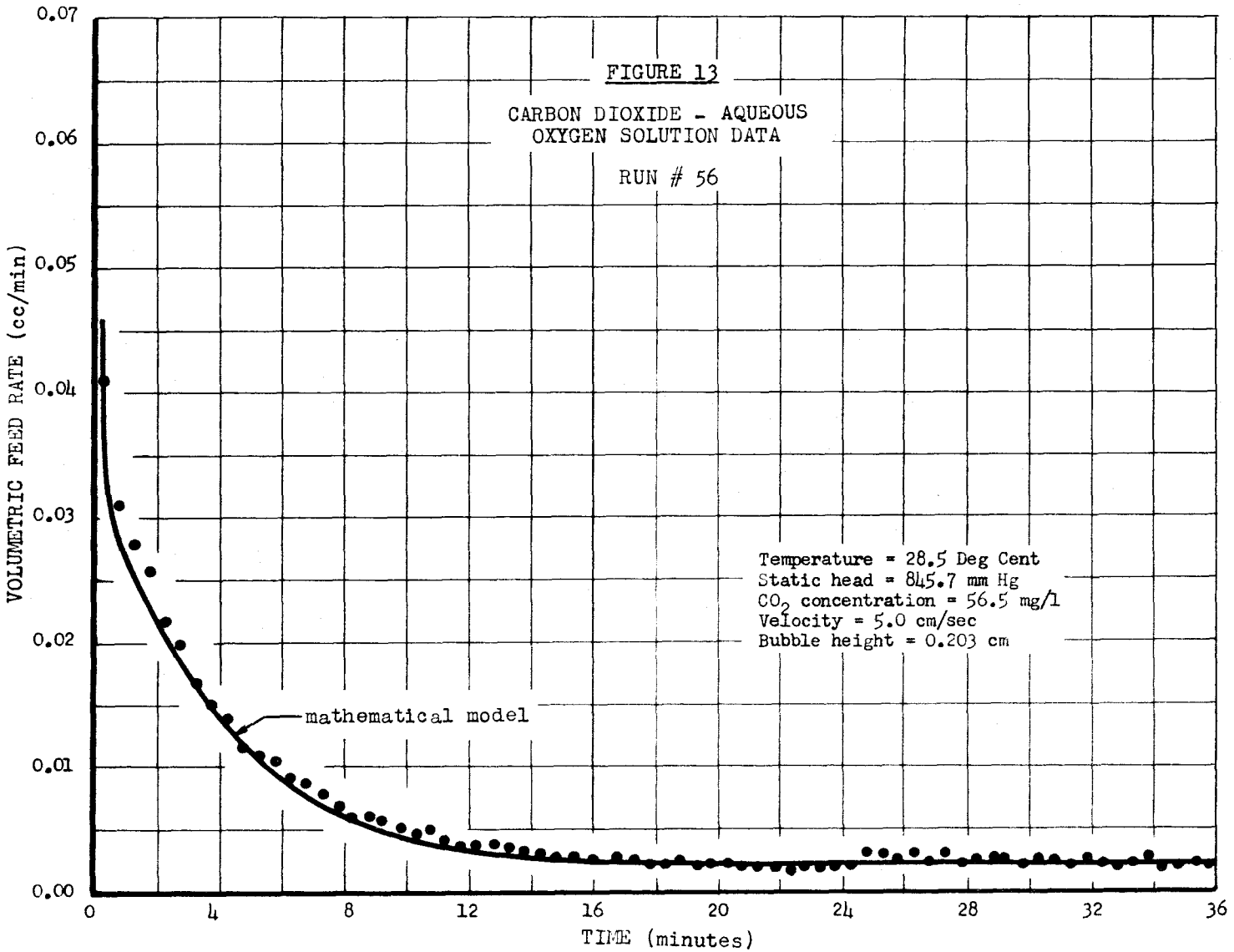
FIGURE 13
CARBON DIOXIDE - AQUEOUS OXYGEN SOLUTION DATA
RUN # 56
VOLUMETRIC FEED RATE (cc/min)
0.07
0.06
0.05
0.04
0.03
0.02
0.01
0.00
0
4
8
12
16
20
24
28
32
36
TIME (minutes)
mathematical model
Temperature = 28.5 Deg Cent
Static head = 845.7 mm Hg
CO_2 concentration = 56.5 mg/l
Velocity = 5.0 cm/sec
Bubble height = 0.203 cm

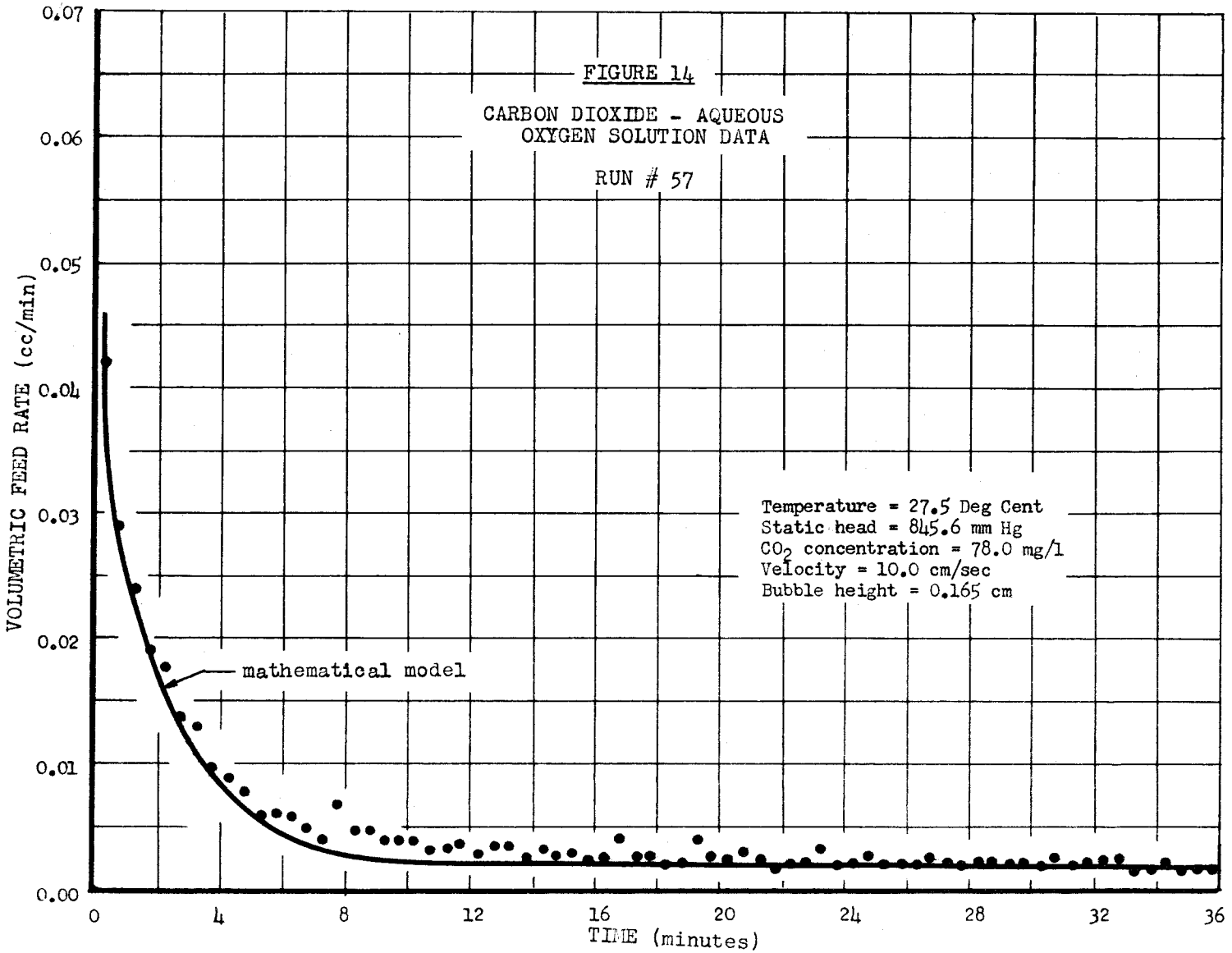
FIGURE 14
CARBON DIOXIDE - AQUEOUS OXYGEN SOLUTION DATA
RUN # 57
Temperature = 27.5 Deg Cent
Static head = 845.6 mm Hg
CO_2 concentration = 78.0 mg/l
Velocity = 10.0 cm/sec
Bubble height = 0.165 cm
mathematical model
VOLUMETRIC FEED RATE (cc/min)
0.07
0.06
0.05
0.04
0.03
0.02
0.01
0.00
0
4
8
12
16
20
24
28
32
36
TIME (minutes)

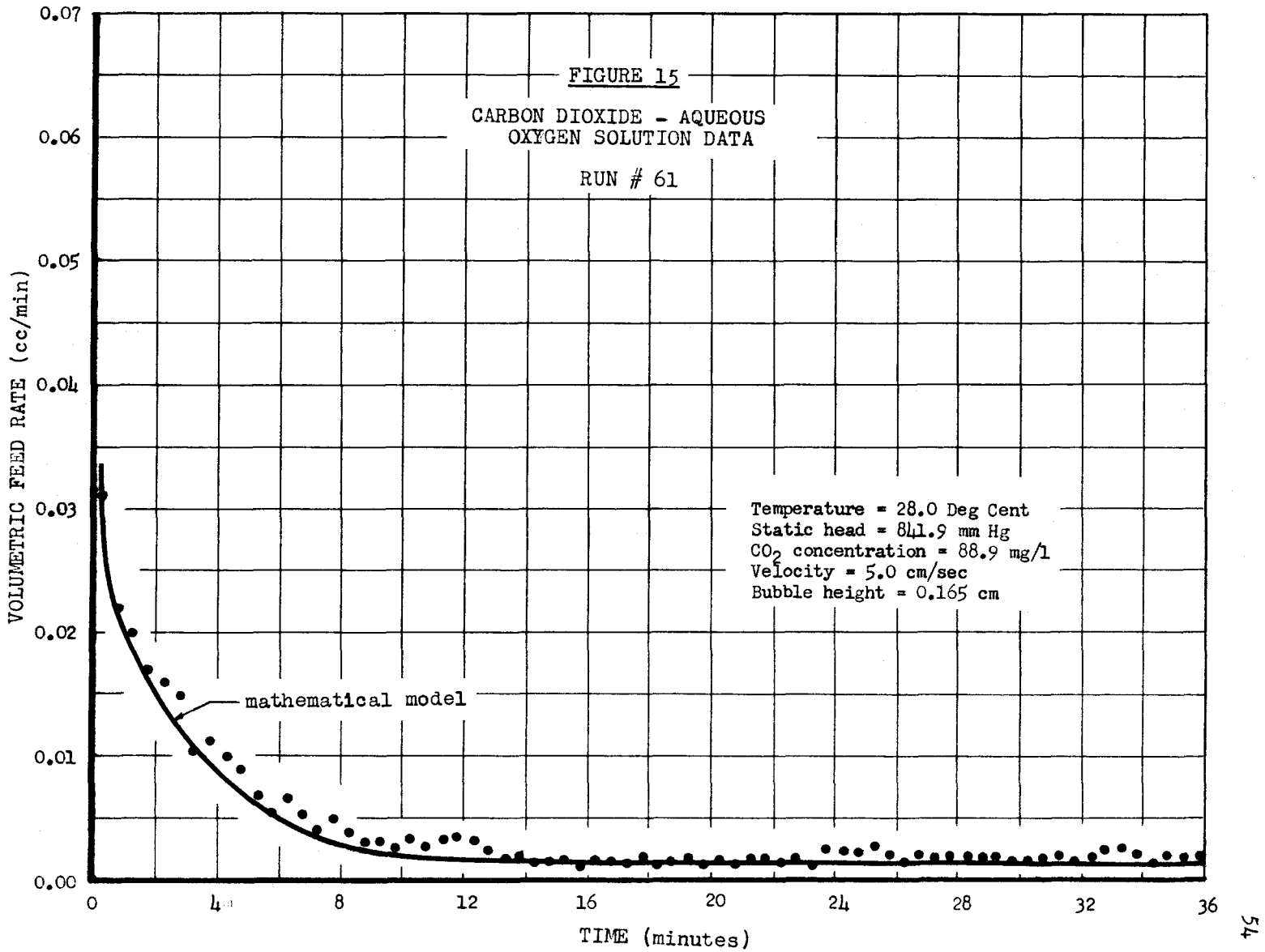
FIGURE 15
CARBON DIOXIDE - AQUEOUS OXYGEN SOLUTION DATA
RUN # 61
Temperature = 28.0 Deg Cent
Static head = 841.9 mm Hg
CO_2 concentration = 88.9 mg/l
Velocity = 5.0 cm/sec
Bubble height = 0.165 cm
mathematical model
VOLUMETRIC FEED RATE (cc/min)
0.07
0.06
0.05
0.04
0.03
0.02
0.01
0.00
0
4
8
12
16
20
24
28
32
36
TIME (minutes)

concentrations. The level of surfactants had no significant influence on the results as the runs for various levels could be superimposed with no marked deviation. The slightly different dissolved CO_2 levels in the liquid phase could change the driving force and thereby affect the rate of mass transfer $\left(\frac{dm}{dt}\right)$, but the dissolved CO_2 levels for these runs only varied between the limits of approximately 35 mg/l and 85 mg/l and this variation would not significantly affect the fit of the experimental data.

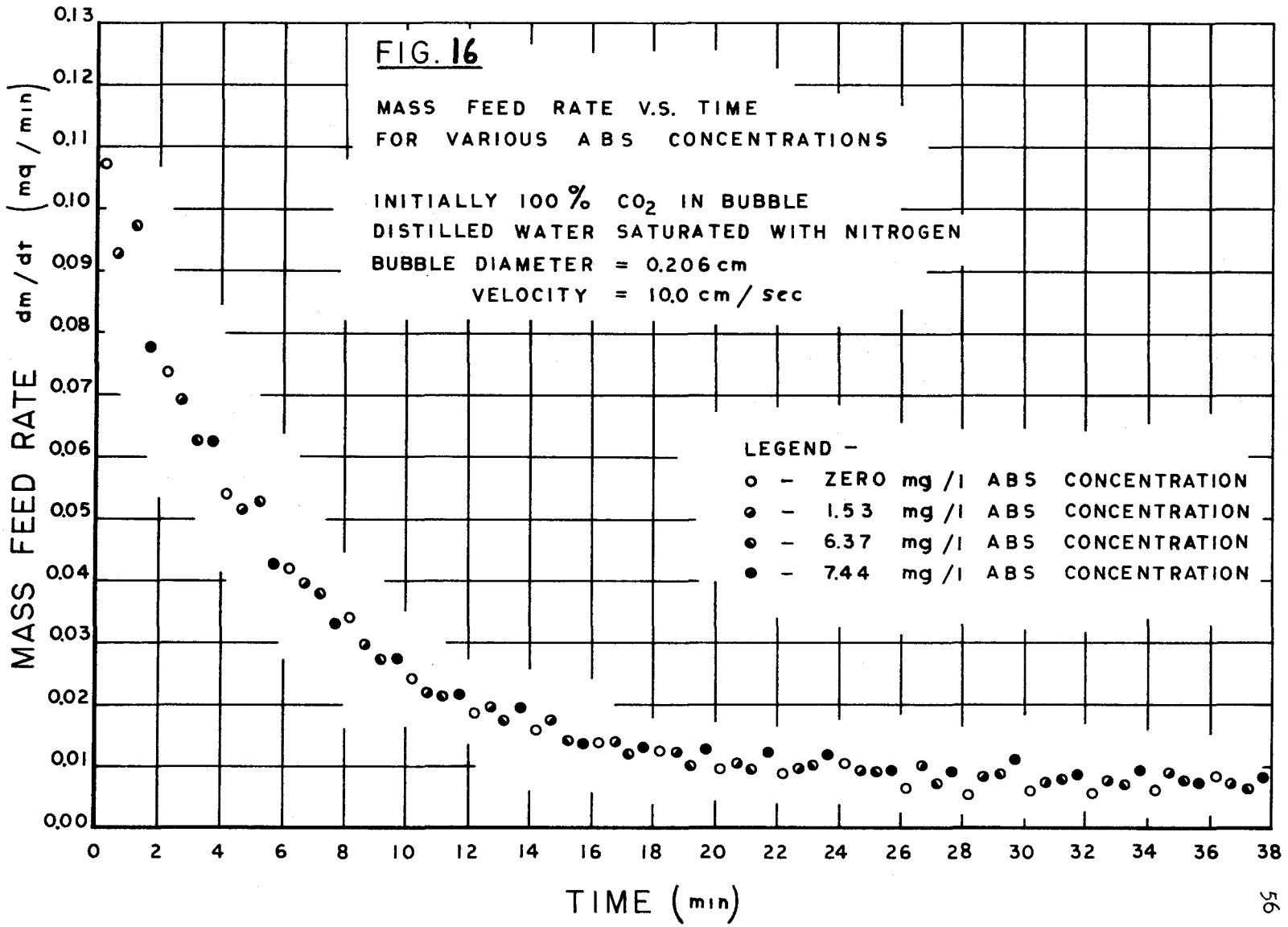
FIG. 16
MASS FEED RATE V.S. TIME
FOR VARIOUS ABS CONCENTRATIONS
INITIALLY 100 % CO_2 IN BUBBLE
DISTILLED WATER SATURATED WITH NITROGEN
BUBBLE DIAMETER = 0.206 cm
VELOCITY = 10.0 cm / sec
LEGEND –
o – ZERO mg / l ABS CONCENTRATION
– 1.53 mg / l ABS CONCENTRATION
– 6.37 mg / l ABS CONCENTRATION
● – 7.44 mg / l ABS CONCENTRATION
MASS FEED RATE dm / dt (mg / min)
0.13
0.12
0.11
0.10
0.09
0.08
0.07
0.06
0.05
0.04
0.03
0.02
0.01
0.00
0 2 4 6 8 10 12 14 16 18 20 22 24 26 28 30 32 34 36 38
TIME (min)

CHAPTER 6

APPLICATION

Since the simultaneous diffusion of two or more gases into or out of a bubble was predicted successfully by considering each gas individually, it was thought to be of interest to consider the fate of an air bubble in an aerator. Another computer program was developed to simulate mass transfer from a hypothetical air bubble rising in an aeration tank. The program appears in Appendix "I".

Several simplifying assumptions were made, the major one being:

i) Temperature = 20^0C
   Kinematic viscosity ν = 0.01 cm^2/sec.for water
   Diffusivity D = 2.14 x 10^{-5} cm^2/sec. for oxygen
   Diffusivity D = 1.88 x 10^{-5} cm^2/sec. for nitrogen

ii) Constant static head of 760 mm. Hg.

iii) The process is not diffusion - limiting in the gaseous phase as the oxygen approaches depletion in the bubble.

iv) The dissolved oxygen in the liquid phase is zero.

v) The dissolved nitrogen in the liquid phase is equivalent to the saturation value for the partial pressure of nitrogen in air.

vi) Initially the bubble composition is 80% nitrogen and 20% oxygen.

vii) No transition from the circulating to the non-circulating state occurs.

The mass transfer coefficient (k_L) values were calculated from the Boussinesq relationship ($Sh = 1.13\ Pe^{1/3}$) for circulating bubbles and from the Griffith relationship (equation 14) for non-circulating bubbles. Two bubble diameters were selected for consideration 0.206 cm and 0.600 cm., the former being a bubble diameter used previously in this work, and the latter being the largest bubble diameter in which the circulation could be stopped by the addition of small amounts of surface active materials (Garner and Hammerton 1954). Rise rates of 18.0 cm/sec. and 22.0 cm/sec. were used (Appendix "G") for the smaller and the larger bubble diameters respectively.

Plots of the volume of the constituent gases at the end of various retention times appear in figures 17 and 18. For a circulating bubble of 0.206 cm diameter, over half of the oxygen in the bubble is depleted in 0.24 minutes, and for a 0.600 cm. diameter circulating bubble, half of the oxygen is depleted in 1.07 minutes. Nitrogen also dissolves from the bubble into the liquid as the retention time increases. The initial transfer of oxygen increases the

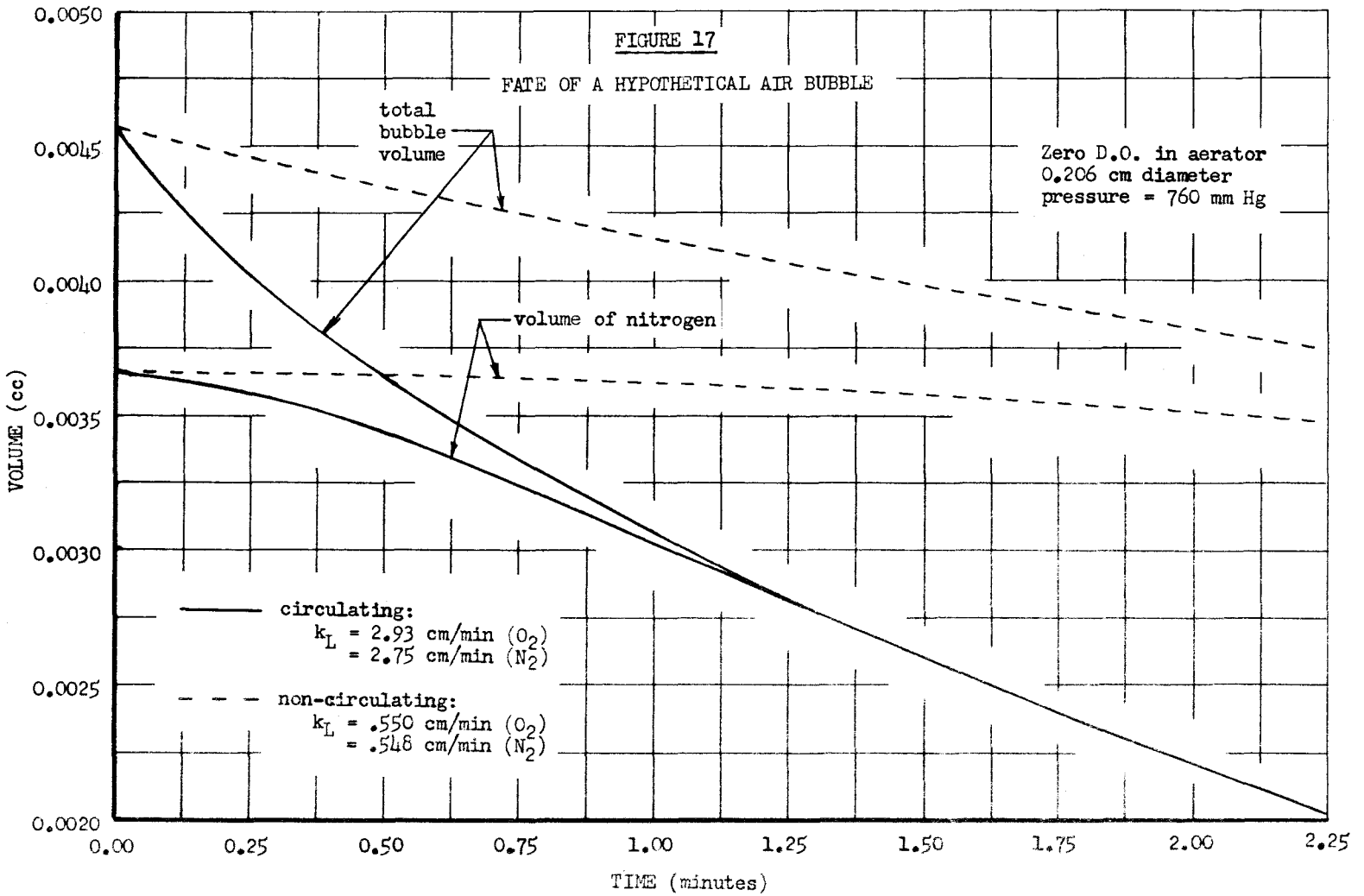
FIGURE 17
FATE OF A HYPOTHETICAL AIR BUBBLE
total bubble volume
volume of nitrogen
Zero D.O. in aerator
0.206 cm diameter
pressure = 760 mm Hg
circulating:
k_L = 2.93 cm/min (O_2)
= 2.75 cm/min (N_2)
non-circulating:
k_L = .550 cm/min (O_2)
= .548 cm/min (N_2)
VOLUME (cc)
0.0050
0.0045
0.0040
0.0035
0.0030
0.0025
0.0020
0.00
0.25
0.50
0.75
1.00
1.25
1.50
1.75
2.00
2.25
TIME (minutes)

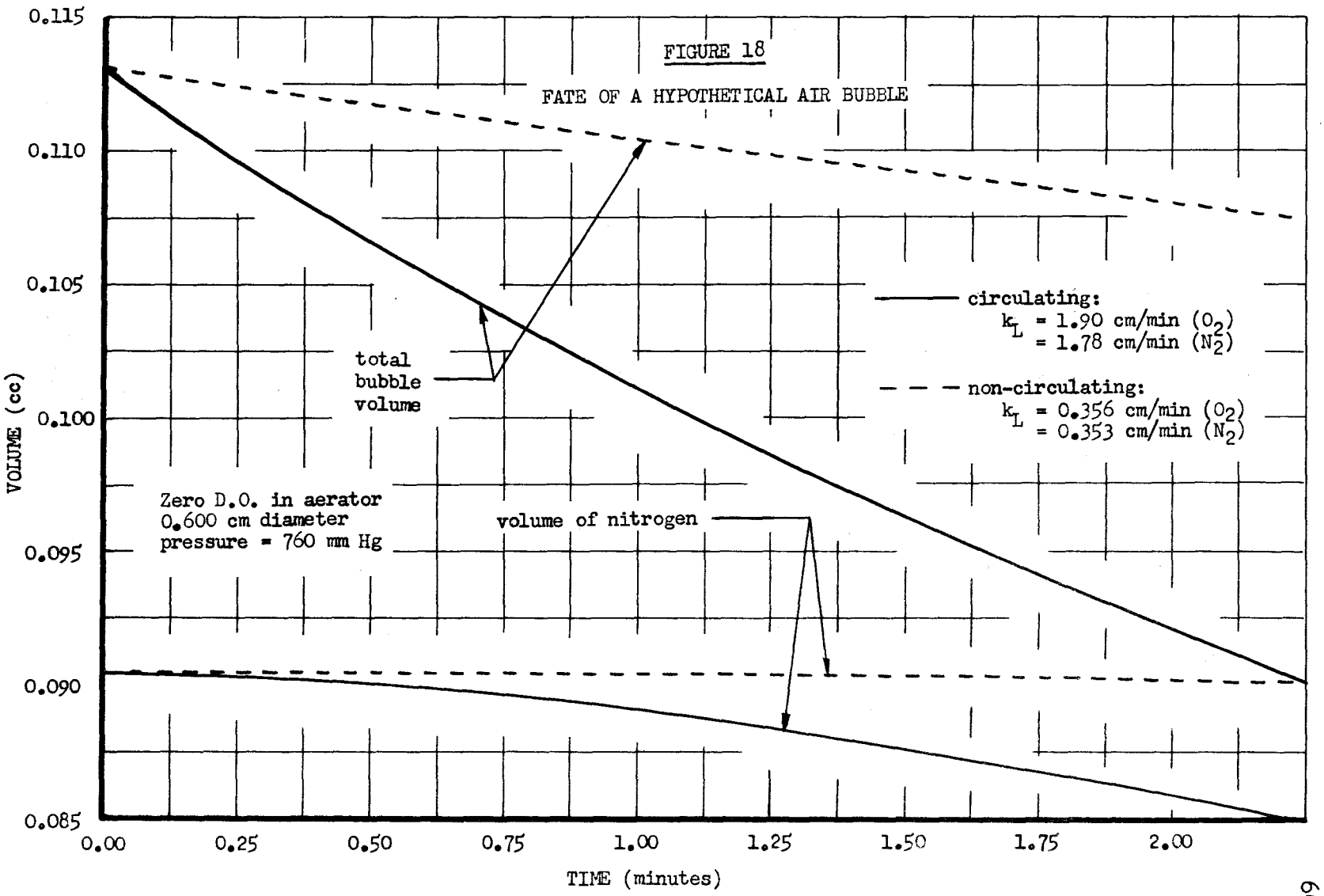
FIGURE 18
FATE OF A HYPOTHETICAL AIR BUBBLE
circulating:
k_L = 1.90 cm/min (O_2)
= 1.78 cm/min (N_2)
non-circulating:
k_L = 0.356 cm/min (O_2)
= 0.353 cm/min (N_2)
total bubble volume
volume of nitrogen
Zero D.O. in aerator
0.600 cm diameter
pressure = 760 mm Hg
VOLUME (cc)
0.115
0.110
0.105
0.100
0.095
0.090
0.085
0.00
0.25
0.50
0.75
1.00
1.25
1.50
1.75
2.00
TIME (minutes)

partial pressure of nitrogen and this causes a concurrent transfer of nitrogen from the bubble. Decreases in bubble volume would result from the transfer of both oxygen and nitrogen gases.

The foregoing suggests that consideration must be given to bubble retention times in an aerator as oxygen depletion may result from extended bubble hold-up. The assumption of atmospheric pressure in figures 17 and 18 decreases the rate of gas depletion in comparison to rates in actual aerators with higher static heads. The higher pressures would increase the aqueous saturation concentration values of the gases in the bubble and cause a higher driving force for mass transfer which would result in a more rapid dissolution rate of the bubble.

CHAPTER 7

CONCLUSIONS, DISCUSSION AND RECOMMENDATIONS

For a single bubble suspended in a liquid flow regime, it has been established that:

1. The mass transfer data obtained by Griffith (1960)for carbon dioxide bubbles could be reproduced.
2. A mathematical model could be formulated that predicted the two-way mass transfer process for a pure bubble dissolving into an aqueous solution of a different gas. This model provided a good fit for the experimental data obtained.
3. Backdiffusion of the gas in the aqueous solution into the bubble must be considered unless some means of completely degasifying the liquid is provided.
4. For the system described, a rapid decay in initial circulation caused a reduction in the initial mass transfer coefficient (^{k}L) to that of a non-circulating bubble. Approximately 99% of the decay occurred in the first half minute of a run.

5. No significant effect in the resultant mass transfer coefficient (^{k}L) or the rate of decay could be observed for surfactant (ABS) concentrations up to 7.4 mg/l. Any variations in the overall mass transfer coefficient ($^{k}L^{a}$) for non-circulating bubbles must be associated with an increase in specific surface area (a).

Extending the model of concurrent mass transfer to or from a bubble when two or more gases are involved to a hypothetical bubble in an aerator:

6. In actual aerators, a substantial decrease in the rate of oxygen transfer would result with bubble hold-up from the depletion of oxygen in the bubble. This effect is more pronounced with smaller bubbles than with larger ones. For the circulating hypothetical bubble considered in this investigation, at least one half of the oxygen content of the bubble would be depleted in 0.24 minutes for an initial bubble diameter of 0.206 cm., and in 0.87 minutes for an initial bubble diameter of 0.600 cm.
7. Decreases in bubble volume with bubble hold-up are caused by the transfer of both oxygen and nitrogen from the bubble accelerating the reductions in area (A) through which transfer

can occur and reducing further the overall oxygen transfer coefficient ($k_L a$).

Future work with this apparatus could possibly be directed toward using different bubble sizes and/or larger liquid flow velocities in an effort to induce circulation in the bubble and study the corresponding mass transfer properties of the system. Modification of the bubble supporting tip may be necessary to facilitate this.

Increasing the static head at the bubble elevation while still maintaining the same level of dissolved gas in the liquid would result in higher terminal steady state volumetric feed rates of the carbon dioxide - aqueous oxygen or nitrogen solution runs. This would reduce the possibility of error when recording the relatively low volumetric feed rates once the system has reached a steady state.

REFERENCES

1. Baars, J. K., "The Effect of Detergents on Aeration: A Photographic Approach to the Problem," Journ. Inst. of Sewage Purification, part 4, 358 (1955).

2. Bond, W. N. and Newton, D. A., "Bubbles, Drops and Stokes' Law," Philosophical Magazine, Series 7, 5, 794 (1928).

3. Coppock, P. D., and Meiklejohn, G.T., "Behaviour of Gas Bubbles in Relation to Mass Transfer," Trans. Inst. of Chem. Engrs. (London), 24, 75 (1951).

4. Danckwerts, P.V., "Significance of Liquid Film Coefficients in Gas Absorption," Ind. and Engr. Chem., 43, 1460 (1951).

5. Datta, R.L., Napier, D. H., and Newitt, D.M., "The Properties and Behaviour of Gas Bubbles formed at a Circular Orifice," Trans. Inst. of Chem. Engrs. (London), 28, 14 (1950).

6. Davidson, J. F., and Cullen, E.J., "The Determination of Diffusion Coefficients for Sparingly Soluble Gases in Liquids," Trans. Inst. of Chem. Engrs. (London), 35, 51 (1957).

7. Degens, P. N., Jr., Vander Zee, H., and Kommer, J. D., "Influence of Anionic Detergents on the Diffused Air Activated Sludge Process," Journ. of Sewage and Industrial Wastes, 27, 10 (1955).

8. Dobbins, W.E., "Mechanism of Gas Absorption by Turbulant Liquids," Proc. International Conference on Water Pollution, London, England, 1962, Pergamon Press, New York,(1964).

9. Dobbins, W. E., "The Nature of the Oxygen Transfer Coefficient in Aeration Systems," Biological Waste Treatment of Sewage and Industrial Wastes, Reinhold, New York, (1956).

10. Downing, A. L., Melbourne, K. V., and Bruce, A.M., "The Effect of Contaminants on the Rate of Aeration of Water," Journ. of Applied Chemistry (Brit.), 7, 590 (1957).

11. Downing, A.L., and Scragg, L. J., "The Effect of Synthetic Detergents on the Rate of Aeration in Diffused Air Activated Sludge Plants,"Water and Waste Treatment Journal, 7, 102 (1958).

12. Downing, A. L. and Truesdale, G. A., "Some Factors Affecting the Rate of Solution of Oxygen in Water," Journal of Applied Chemistry, 5, 570 (1955).

13. Eckenfelder, W. W., "Absorption of Oxygen from Air Bubbles in Water," Journ. San. Engr. Div., A.S.C.E., SA4, 85, 89 (1959).

14. Eckenfelder, W. W., and O'Connor, O. J., Biological Waste Treatment, Pergamon Press, New York, (1961).

15. Eskinazi, S., Principles of Fluid Mechanics, Allyn and Bacon, Boston, (1962).

16. Garner, F. H., "Diffusion Mechanism in the Mixing of Fluids," Trans. Inst. Chem. Engrs. (London), 28, 88 (1950).

17. Garner, F. H., and Hammerton, D., "Circulation Inside Gas Bubbles," Chem. Eng. Sci, 3, 1 (1954).

18. Garner, F. H., and Keey, R. B., "Mass Transfer from Single Solid Spheres - I. Transfer of Low Reynolds Numbers," Chem. Eng. Sci., 9, 119 (1958).

19. Garner, F. H., and Keey, R. B., "Mass Transfer from Single Solid Spheres - II. Transfer in Free Convection," Chem. Eng. Sci., 9, 218 (1958).

20. Griffith, R. M., "Mass Transfer from Drops and Bubbles," Chem. Eng. Sci, 12, 198 (1960).

21. Griffith, R. M., "The Effect of Surfactants on the Terminal Velocity of Drops and Bubbles," Chem. Eng., Sci., 17, 1057 (1962).

22. Haberman, W.L.,and Morton, R. K., "An Experimental Study of Bubbles Moving in Liquids," Proc. A.S.C.E., 80, (1954).

23. Handbook of Physics and Chemistry, 39th Ed., edited by C. D. Hodgman, Chemical Rubber Publishing Company, Cleveland,(1957).

24. Higbie, R., "The Rate of Absorption of a Pure Gas into a Still Liquid During Short Periods of Exposure," Trans. Amer. Inst. of Chem. Engrs., 31, 365 (1935).

25. Holroyd, A., and Parker, H. B., "Investigations on the Dynamics of Aeration: The Effects of Some Surface Contaminants." Journ. Inst. of Sewage Purification, Part 4, 280 (1952).

26. Ippen, A. T., and Carver, C. E., "Basic Factors of Oxygen Transfer in Aeration Systems," Journ. Sewage and Industrial Wastes, 26, 813, (1954).

27. Lewis, W. K., and Whitman, W. G., "Principles of Gas Absorption," Industrial and Engineering Chemistry, Absorption Symposium, 16, 1215 (1924).

28. Lynch, W. O., and Sawyer, C. H., "Physical Behaviour of Synthetic Detergents," Journ. Sewage and Industrial Wastes, 26, 1193 (1954).

29. Lynch, W. O. and Sawyer, C. N., "Effects of Detergents on Oxygen Transfer in Bubble Aeration," Journ. Water Pollution Control Federation, 32, 25 (1960).

30. Mancy, K. H. and Okun, D. A., "Effects of Surface Active Agents on Bubble Aeration," Journ. Water Pollution Control Federation, 32, 351 (1960).

31. Mancy, K. H., and Okun D. A., "Effects of Surface Active Agents on the Rate of Oxygen Transfer," Advances in Water Pollution Research, ed. by McCabe and Eckenfelder, 111, Pergamon Press, New York,(1963).

32. McKeown, J. J. and Okun, D. A., "Effects of Surface Active Agents on Oxygen Bubble Characteristics," Advances in Biological Waste Treatment, ed. by McCabe and Eckenfelder, 113, Pergamon Press, New York, (1963).

33. Metzger, and Dobbins, W. E., "Role of Fluid Properties in Gas Transfer," Environmental Science and Technology, 1, 57 (1967).

34. Pattle, R. E., "Aeration of Liquids I: the Solution of Gas from Rising Bubbles," Trans. Inst. of Chem. Engrs. (London), 28, 27 (1950).

35. Rich, L. G., Unit Operations in Sanitary Engineering, John Wiley and Sons, New York, (1961).

36. Rosenberg, B., "The Drag and Shape of Air Bubbles Moving in Liquids," Report 727, Navy Department, David Taylor Model Basin, Washington, D. D., (September, 1950).

37. Sawyer, C. N., "The Effect of Synthetic Detergents on Sewage Treatment Processes," Journ. Sewage and Industrial Wastes, 30, 757 (1958).

38. Standard Methods for the Examination of Water and Waste Water, Americal Public Health Association, 12 Ed. New York, (1965).

39. Streeter, V. L., ed. Handbook of Fluid Dynamics, McGraw-Hill, New York, (1961).

APPENDIX "A"

ORIFICE PLATE CALIBRATION CURVES

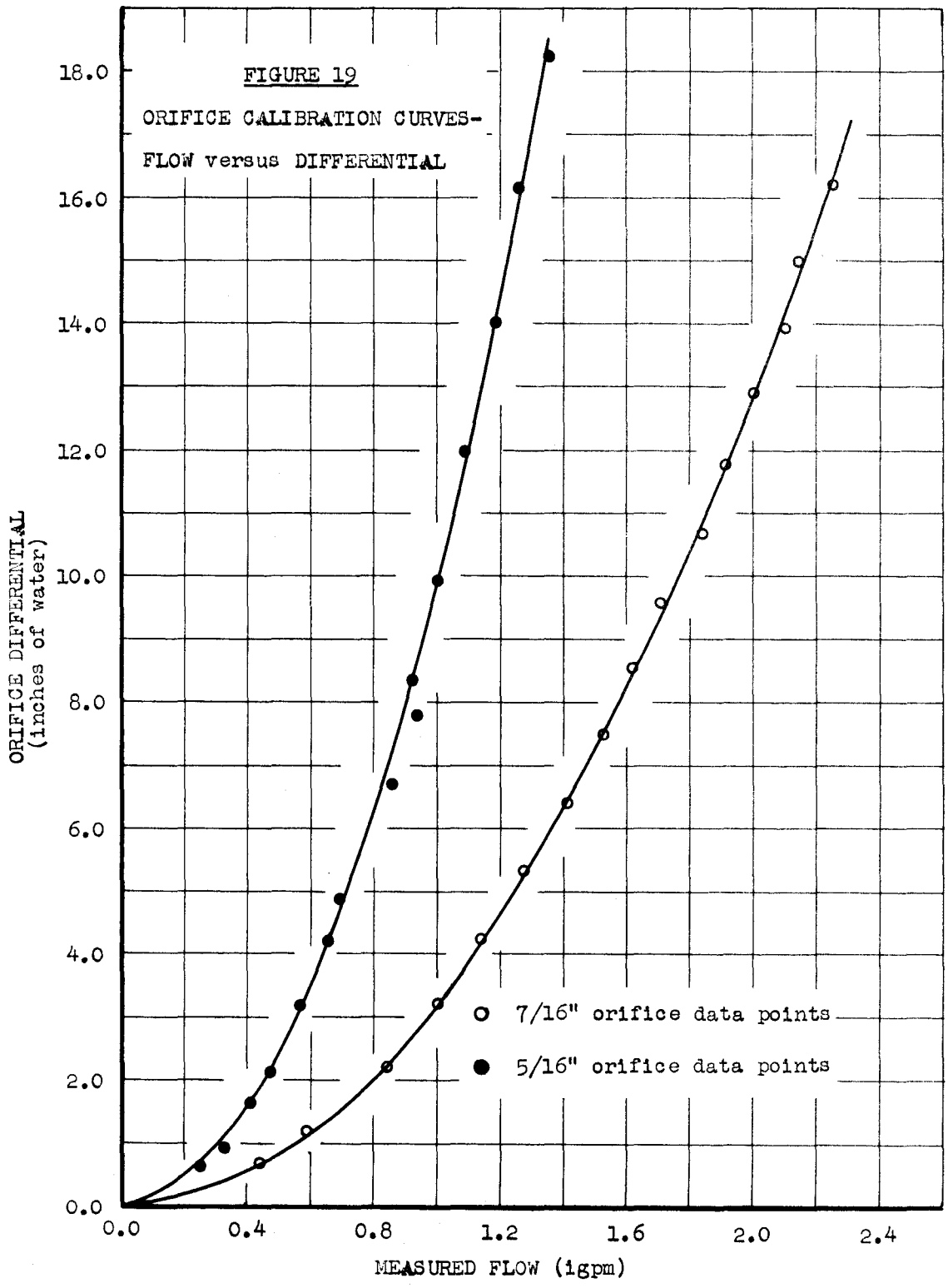
FIGURE 19
ORIFICE CALIBRATION CURVES-
FLOW versus DIFFERENTIAL
ORIFICE DIFFERENTIAL
(inches of water)
18.0
16.0
14.0
12.0
10.0
8.0
6.0
4.0
2.0
0.0
0.0
0.4
0.8
1.2
1.6
2.0
2.4
MEASURED FLOW (igpm)
7/16" orifice data points
5/16" orifice data points

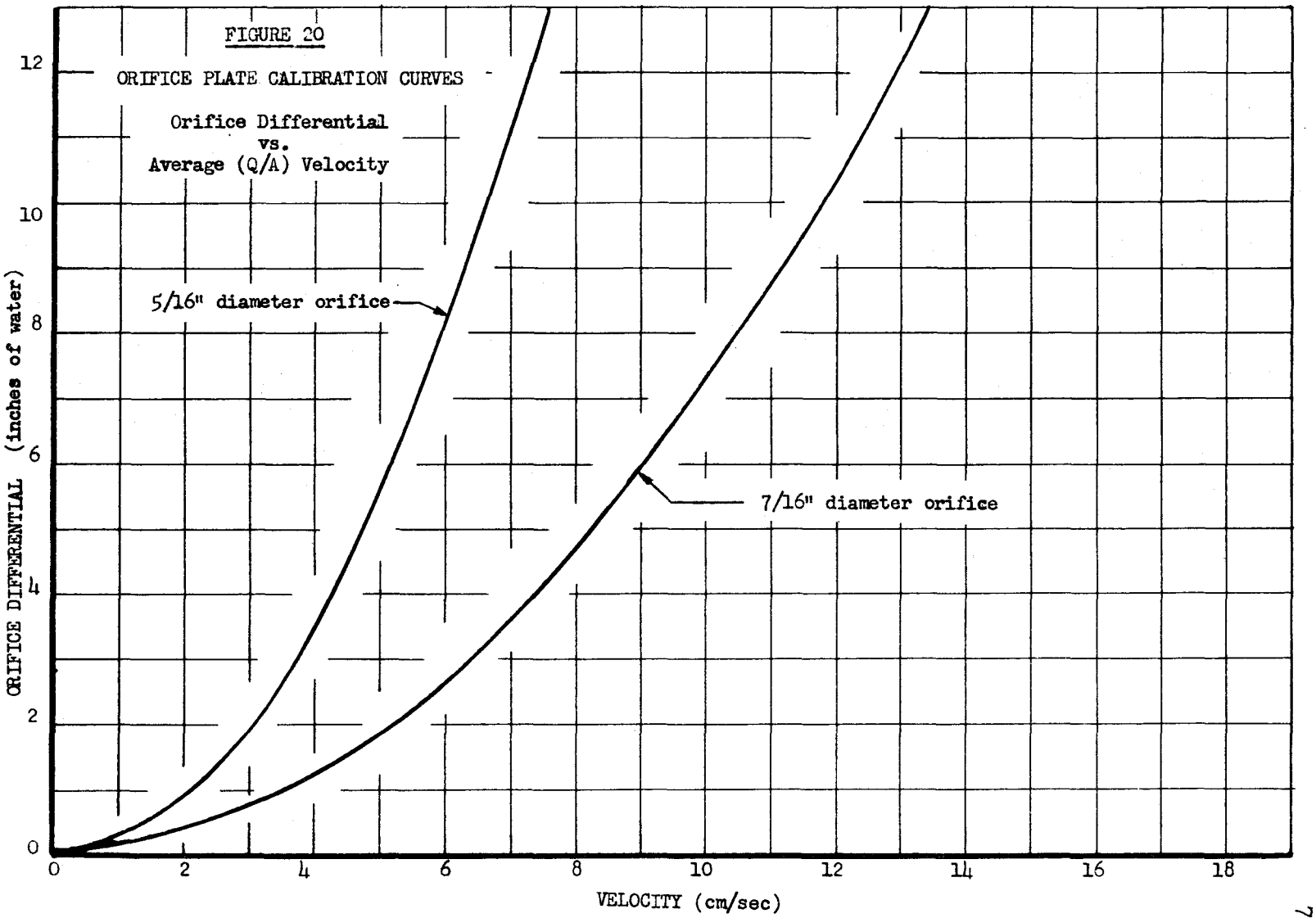
FIGURE 20
ORIFICE PLATE CALIBRATION CURVES
Orifice Differential
vs.
Average (Q/A) Velocity
5/16" diameter orifice
7/16" diameter orifice
ORIFICE DIFFERENTIAL (inches of water)
VELOCITY (cm/sec)
0
2
4
6
8
10
12
14
16
18

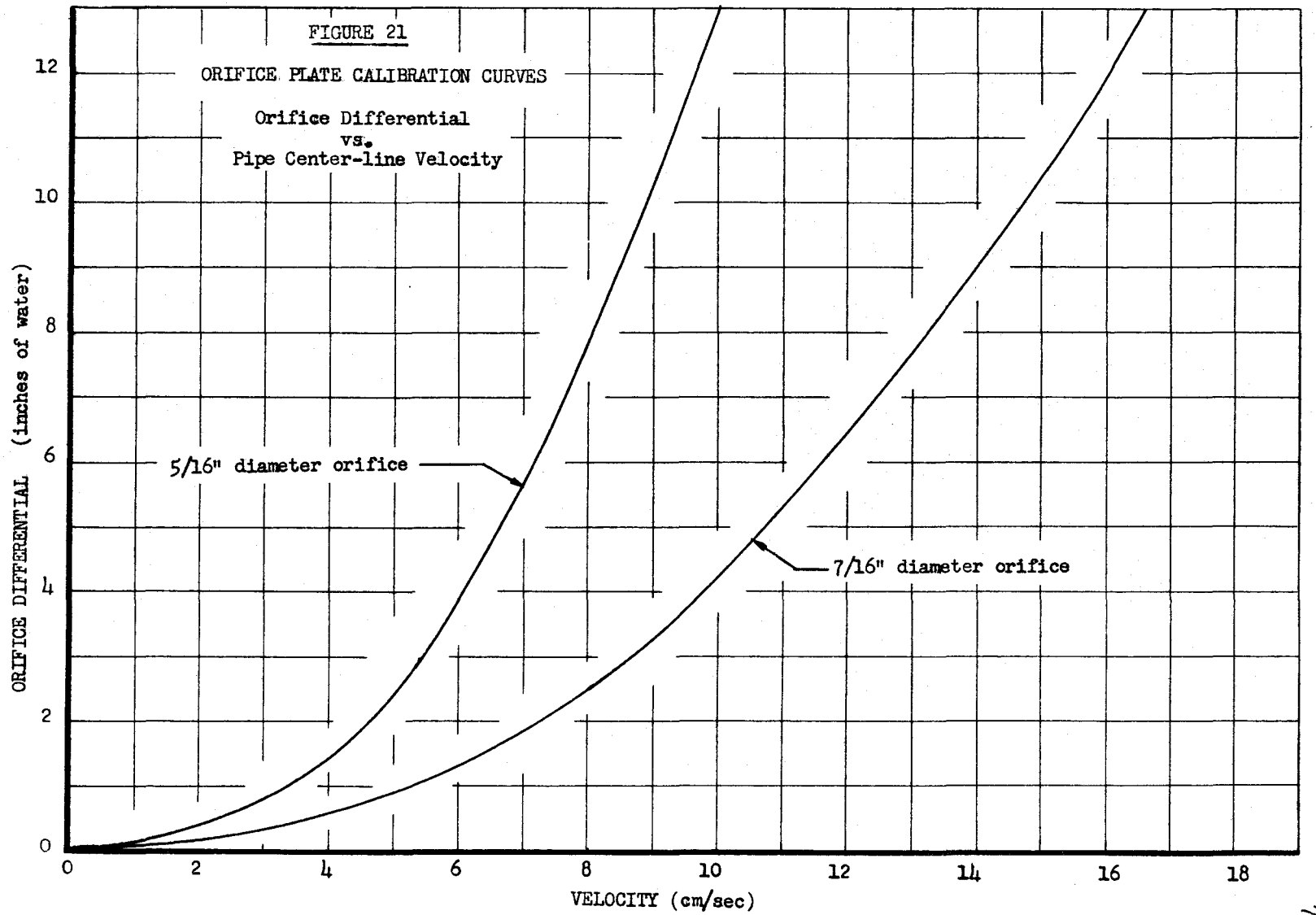
FIGURE 21
ORIFICE PLATE CALIBRATION CURVES
Orifice Differential
vs.
Pipe Center-line Velocity
5/16" diameter orifice
7/16" diameter orifice
ORIFICE DIFFERENTIAL (inches of water)
VELOCITY (cm/sec)
0
2
4
6
8
10
12
14
16
18

APPENDIX "B"

OPTICAL DISTORTION CALIBRATION CURVE

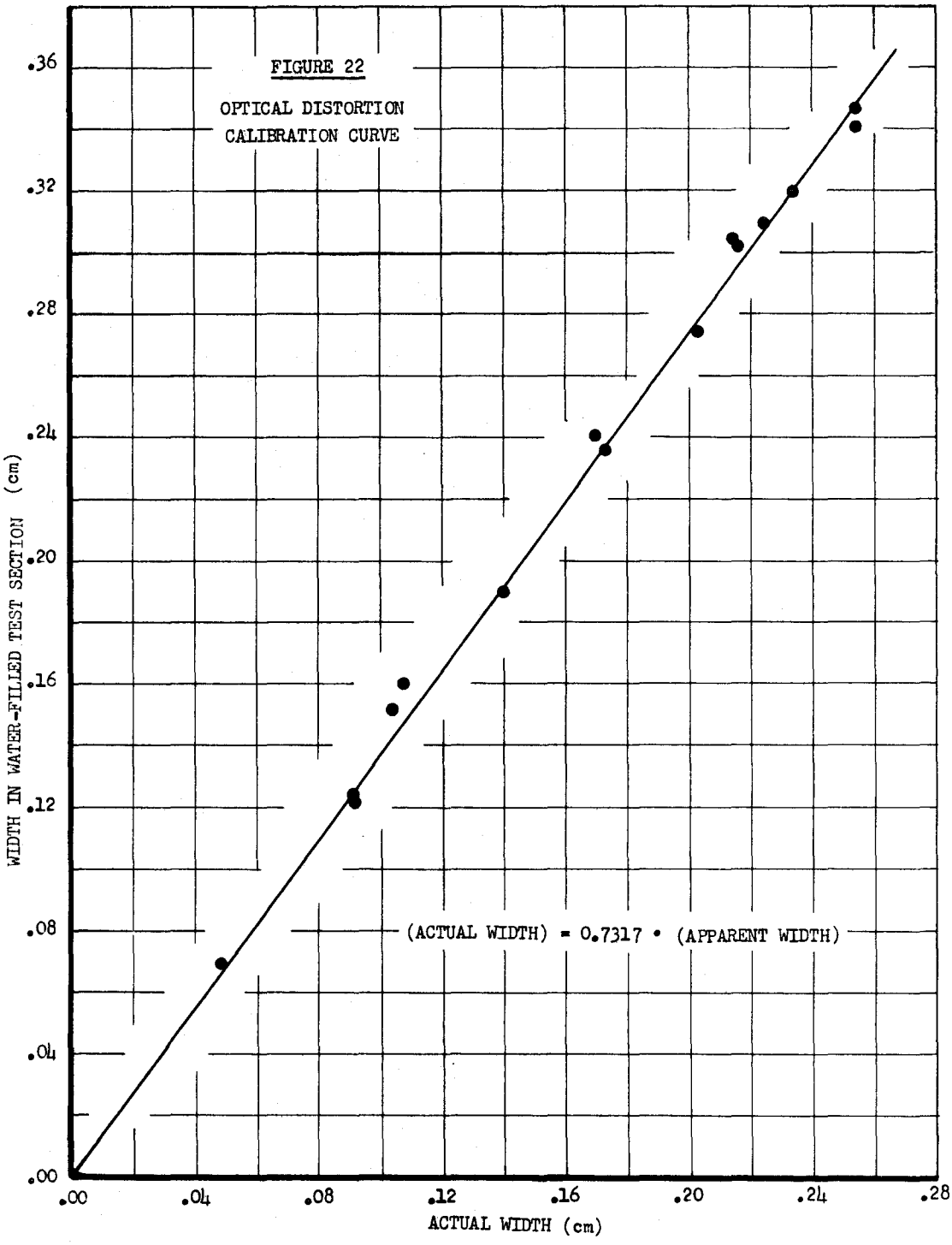
FIGURE 22
OPTICAL DISTORTION
CALIBRATION CURVE
(ACTUAL WIDTH) = 0.7317 • (APPARENT WIDTH)
WIDTH IN WATER-FILLED TEST SECTION (cm)
ACTUAL WIDTH (cm)
.00
.04
.08
.12
.16
.20
.24
.28
.32
.36

APPENDIX "C"

BUBBLE AREA AND VOLUME DETERMINATIONS

TABLE II

BUBBLE AREA AND VOLUME DETERMINATIONS BY COMPUTER PROGRAM

Bubble Height (cm)	Pipe Center-line Velocity (cm/sec.)	ERECT BUBBLE		INVERTED BUBBLE	
		Bubble Area (cm^2)	Bubble Volume (cm^3)	Bubble Area (cm^2)	Bubble Volume (cm^3)
0.127	4.0	0.0649	0.00204	0.0608	0.00182
0.140	4.0			0.0718	0.00229
0.152	4.0	0.0827	0.00283	0.0847	0.00288
0.165	4.0			0.0969	0.00341
0.178	4.0	0.1047	0.00390	0.1081	0.00397
0.190	4.0			0.1228	0.00471
0.203	4.0	0.1267	0.00497		
0.216	4.0			0.1650	0.00718
0.229	4.0	0.1580	0.00677		
0.254	4.0	0.1821	0.00825		
0.279	4.0	0.2049	0.00964		
0.305	4.0	0.2373	0.01186		
0.330	4.0	0.2577	0.01316		
0.127	6.6	0.0671	0.00217	0.0613	0.00184
0.140	6.6			0.0732	0.00236
0.152	6.6	0.0829	0.00285	0.0879	0.00304
0.165	6.6			0.1016	0.00369
0.178	6.6	0.1084	0.00415	0.1098	0.00405
0.190	6.6			0.1306	0.00507
0.203	6.6	0.1306	0.00527	0.1431	0.00591
0.216	6.6			0.1769	0.00762
0.229	6.6	0.1591	0.00694		
0.254	6.6	0.1867	0.00857		
0.279	6.6	0.2100	0.01013		
0.305	6.6	0.2350	0.01174		
0.330	6.6	0.2616	0.01350		
0.127	8.9	0.0643	0.00201	0.0629	0.00191
0.140	8.9			0.0765	0.00253
0.152	8.9	0.0859	0.00300	0.0876	0.00301
0.165	8.9			0.0960	0.00337
0.178	8.9	0.1037	0.00382	0.1126	0.00419
0.190	8.9			0.1263	0.00493
0.203	8.9	0.1308	0.00530	0.1460	0.00604
0.216	8.9			0.1773	0.00800
0.229	8.9	0.1615	0.00712		
0.254	8.9	0.1882	0.00870		
0.279	8.9	0.2137	0.01035		
0.305	8.9	0.2453	0.01250		
0.330	8.9	0.2722	0.01429		
0.127	11.0	0.0632	0.00196	0.0655	0.00202

TABLE II (CONT'D)

Bubble Height (cm)	Pipe Center-line Velocity (cm/sec)	ERECT BUBBLE		INVERTED BUBBLE	
		Bubble Area (cm^2)	Bubble Volume (cm^3)	Bubble Area (cm^2)	Bubble Volume (cm^3)
0.140	11.0			0.0756	0.00247
0.152	11.0	0.0835	0.00286	0.0854	0.00290
0.165	11.0			0.1011	0.00367
0.178	11.0	0.1099	0.00419	0.1139	0.00433
0.190	11.0			0.1335	0.00537
0.203	11.0	0.1370	0.00567	0.1497	0.00629
0.216	11.0			0.1281	0.00801
0.229	11.0	0.1612	0.00701		
0.254	11.0	0.1933	0.00919		
0.279	11.0	0.2155	0.01055		
0.305	11.0	0.2368	0.01184		
0.330	11.0	0.2774	0.01483		

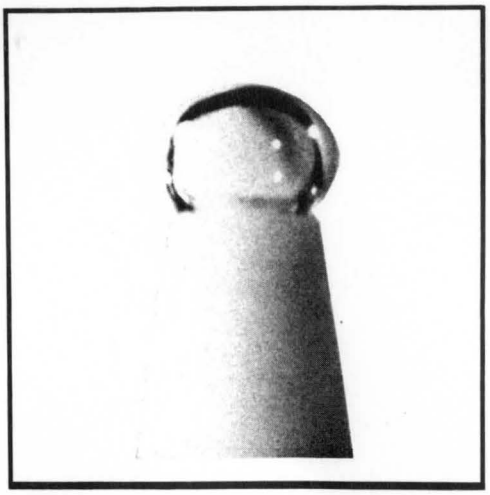

FIGURE 23a

PHOTOGRAPH OF TYPICAL BUBBLE

bubble height = 0.203 cm

velocity = 6.6 cm/sec

erect configuration

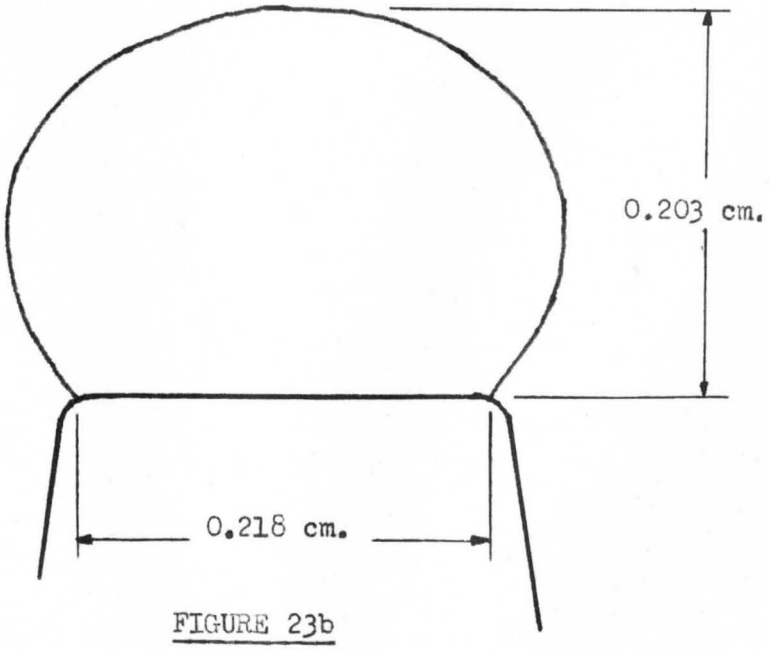

FIGURE 23b

TRACING OF PROJECTED BUBBLE IMAGE

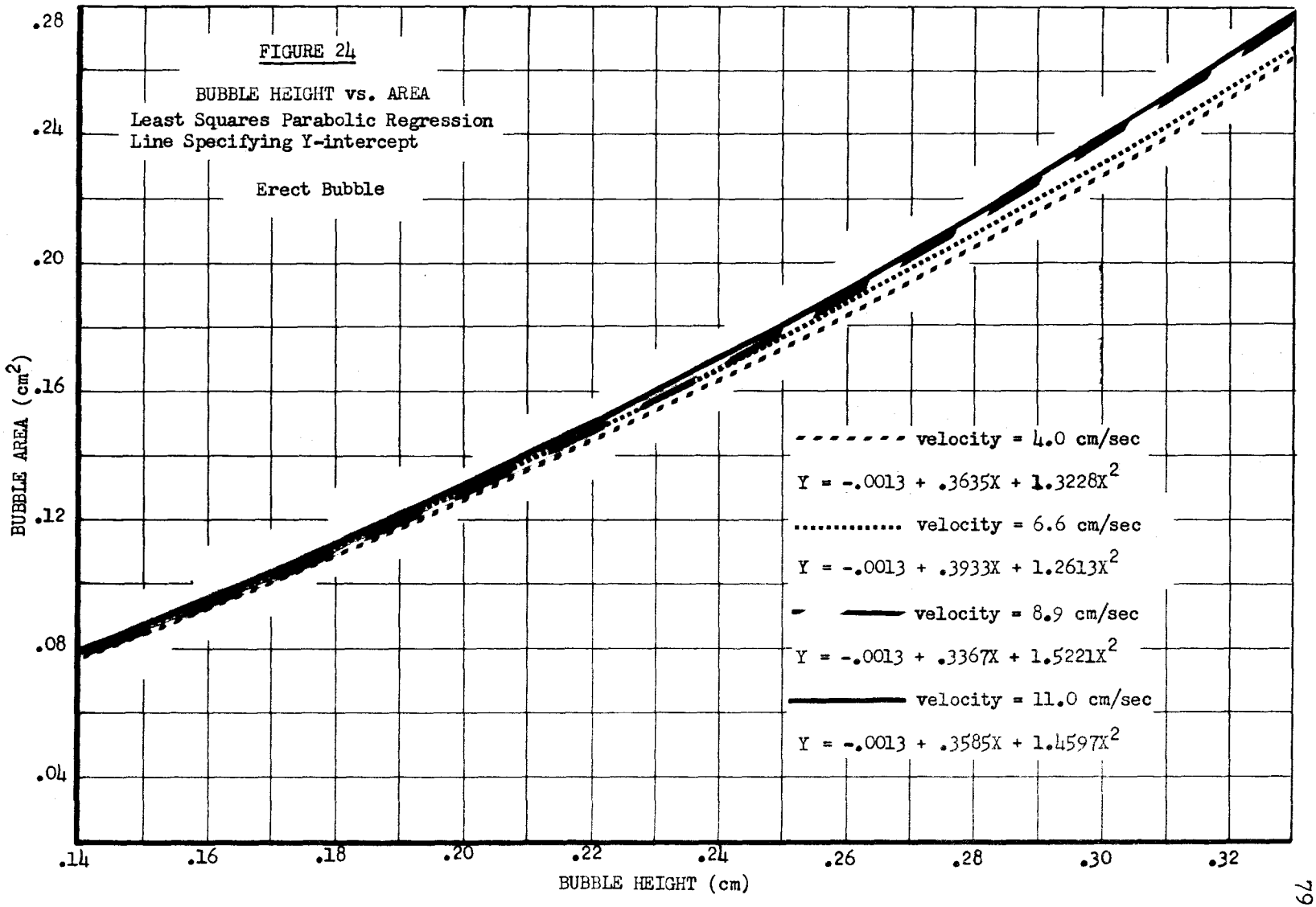
FIGURE 24
BUBBLE HEIGHT vs. AREA
Least Squares Parabolic Regression
Line Specifying Y-intercept
Erect Bubble
velocity = 4.0 cm/sec
Y = -.0013 + .3635X + 1.3228X²
velocity = 6.6 cm/sec
Y = -.0013 + .3933X + 1.2613X²
velocity = 8.9 cm/sec
Y = -.0013 + .3367X + 1.5221X²
velocity = 11.0 cm/sec
Y = -.0013 + .3585X + 1.4597X²
BUBBLE AREA (cm²)
.28
.24
.20
.16
.12
.08
.04
.14
.16
.18
.20
.22
.24
.26
.28
.30
.32
BUBBLE HEIGHT (cm)

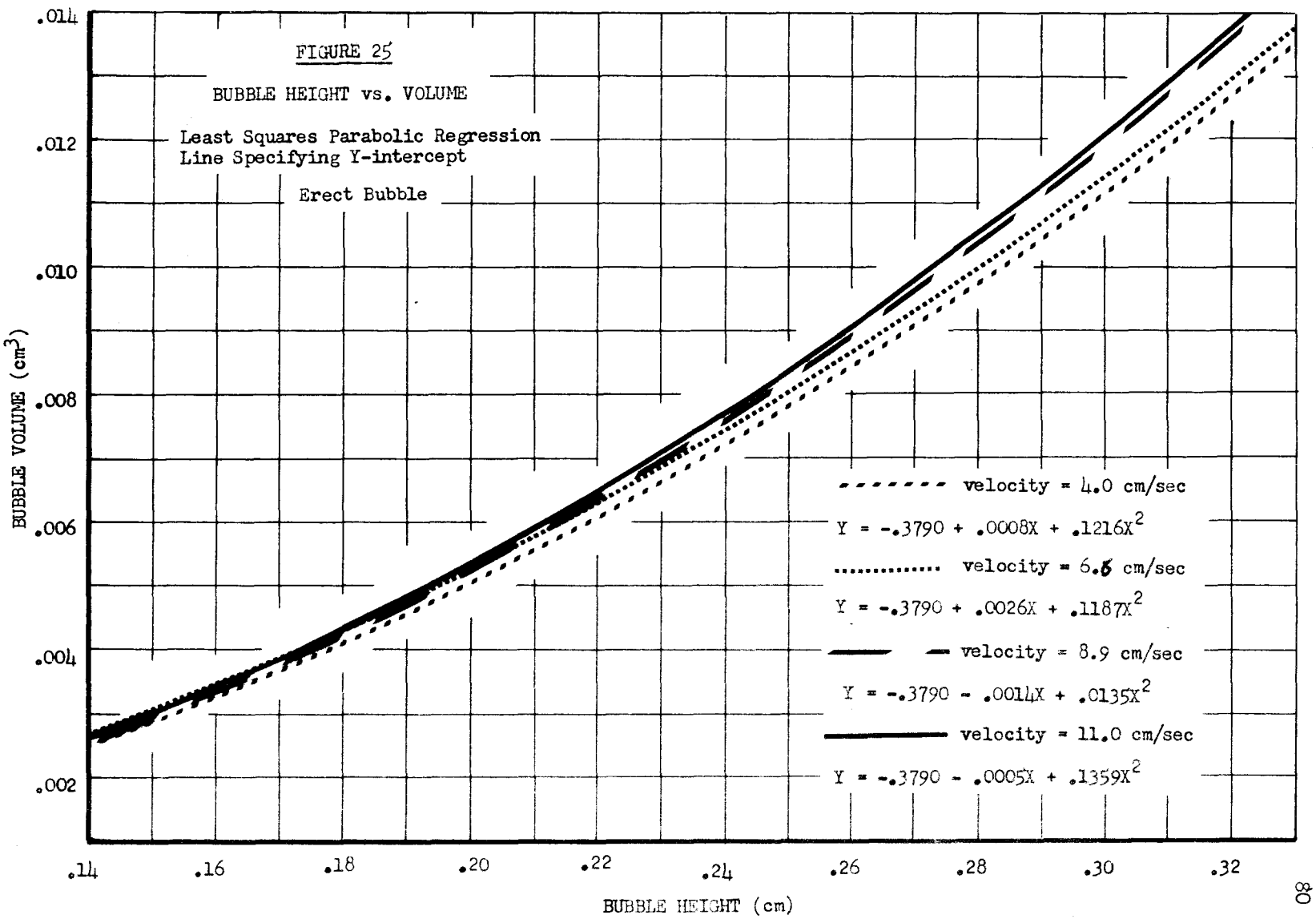
FIGURE 25
BUBBLE HEIGHT vs. VOLUME
Least Squares Parabolic Regression
Line Specifying Y-intercept
Erect Bubble
velocity = 4.0 cm/sec
Y = -.3790 + .0008X + .1216X²
velocity = 6.6 cm/sec
Y = -.3790 + .0026X + .1187X²
velocity = 8.9 cm/sec
Y = -.3790 - .0014X + .0135X²
velocity = 11.0 cm/sec
Y = -.3790 - .0005X + .1359X²
BUBBLE VOLUME (cm³)
.014
.012
.010
.008
.006
.004
.002
.14
.16
.18
.20
.22
.24
.26
.28
.30
.32
BUBBLE HEIGHT (cm)

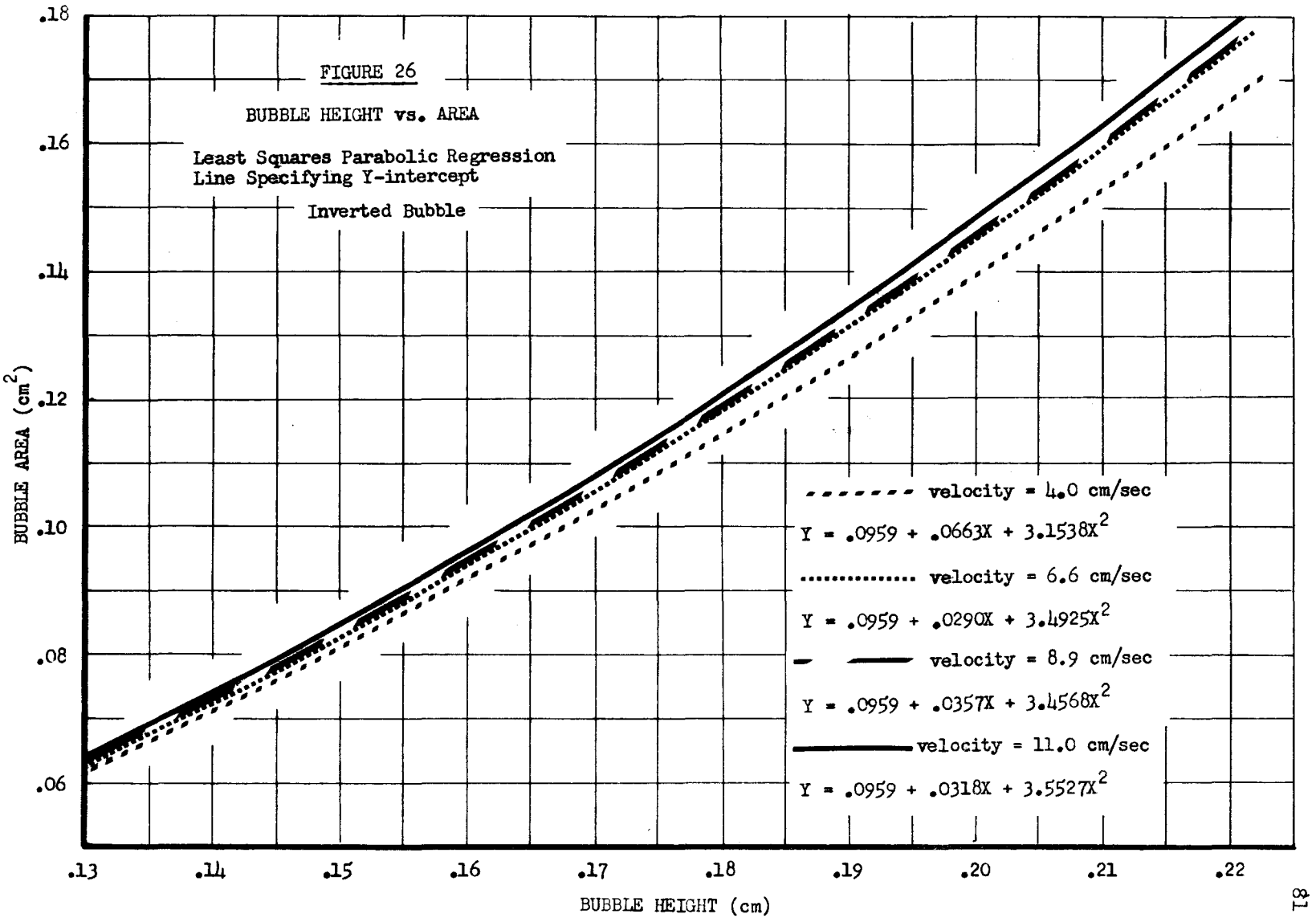
FIGURE 26
BUBBLE HEIGHT vs. AREA
Least Squares Parabolic Regression
Line Specifying Y-intercept
Inverted Bubble
velocity = 4.0 cm/sec
Y = .0959 + .0663X + 3.1538X²
velocity = 6.6 cm/sec
Y = .0959 + .0290X + 3.4925X²
velocity = 8.9 cm/sec
Y = .0959 + .0357X + 3.4568X²
velocity = 11.0 cm/sec
Y = .0959 + .0318X + 3.5527X²
BUBBLE AREA (cm²)
.18
.16
.14
.12
.10
.08
.06
.13
.14
.15
.16
.17
.18
.19
.20
.21
.22
BUBBLE HEIGHT (cm)

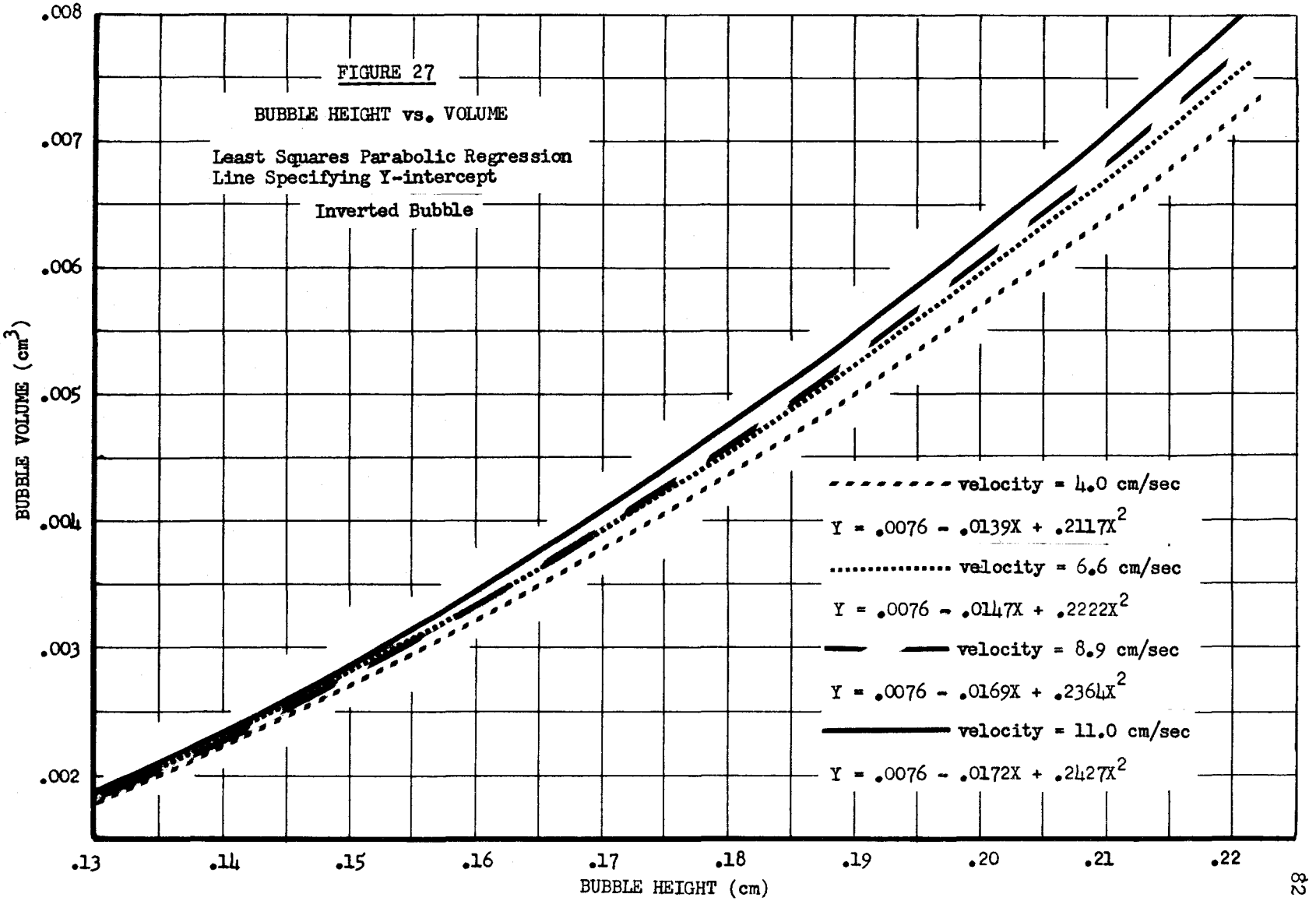
FIGURE 27
BUBBLE HEIGHT vs. VOLUME
Least Squares Parabolic Regression Line Specifying Y-intercept
Inverted Bubble
velocity = 4.0 cm/sec
Y = .0076 - .0139X + .2117X²
velocity = 6.6 cm/sec
Y = .0076 - .0147X + .2222X²
velocity = 8.9 cm/sec
Y = .0076 - .0169X + .2364X²
velocity = 11.0 cm/sec
Y = .0076 - .0172X + .2427X²
BUBBLE VOLUME (cm³)
.008
.007
.006
.005
.004
.003
.002
.13
.14
.15
.16
.17
.18
.19
.20
.21
.22
BUBBLE HEIGHT (cm)

APPENDIX "D"

ALKYL BENZENE SULFONATE CALIBRATION CURVE

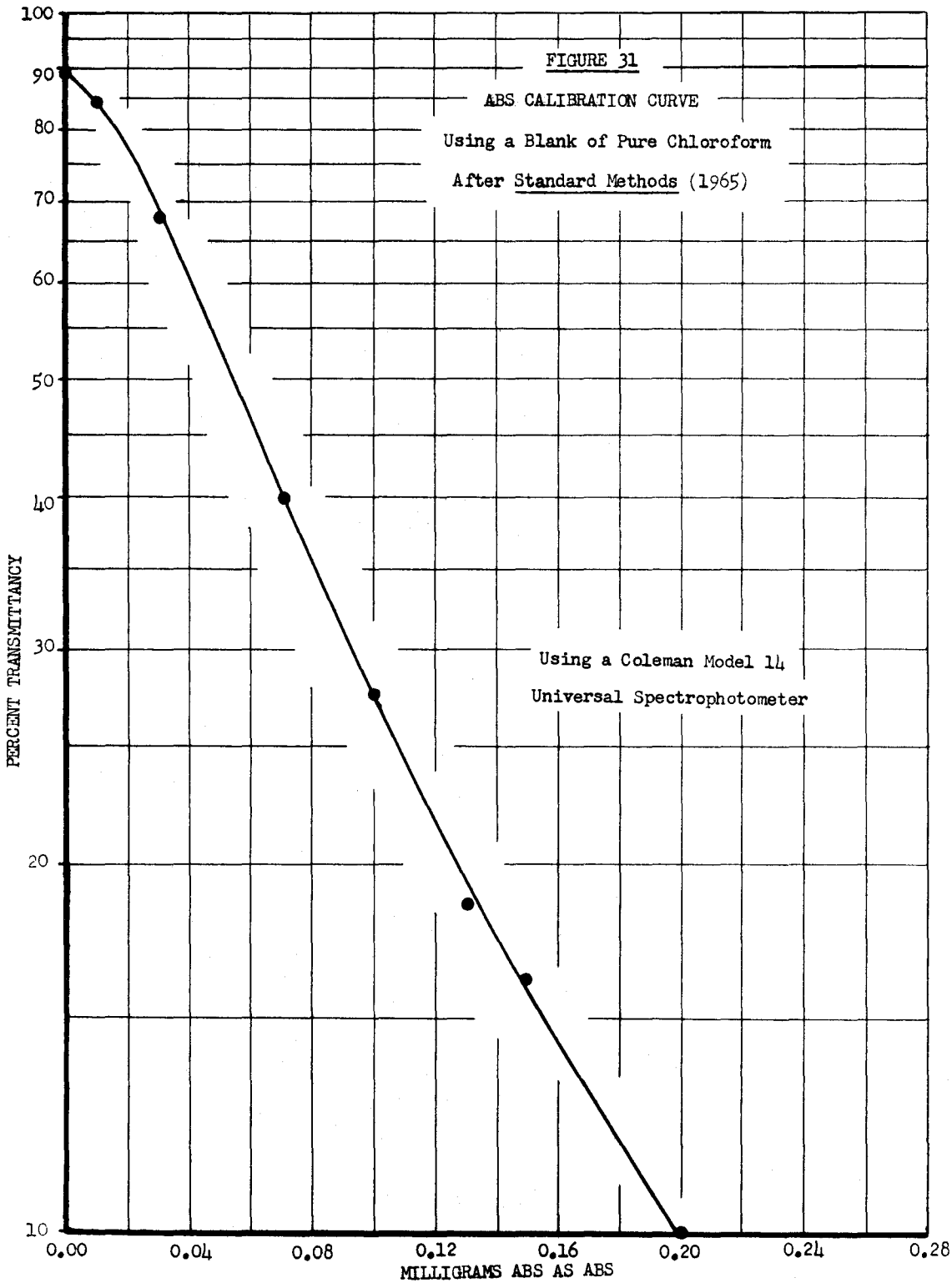
FIGURE 31
ABS CALIBRATION CURVE
Using a Blank of Pure Chloroform
After Standard Methods (1965)
Using a Coleman Model 14
Universal Spectrophotometer
PERCENT TRANSMITTANCY
100
90
80
70
60
50
40
30
20
10
0.00
0.04
0.08
0.12
0.16
0.20
0.24
0.28
MILLIGRAMS ABS AS ABS

APPENDIX "E"

SOLUBILITIES AND DIFFUSIVITIES OF VARIOUS GASES IN WATER

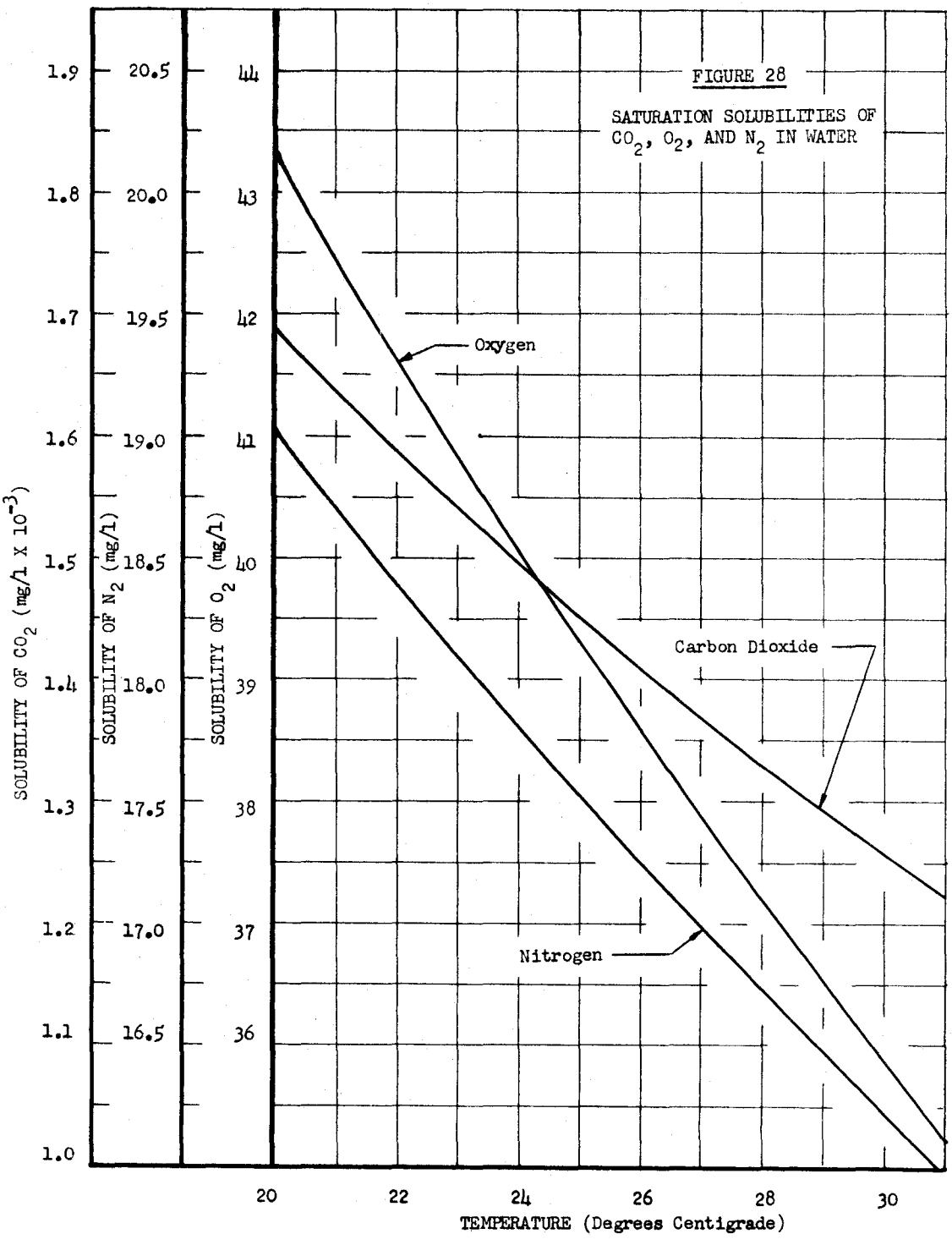
FIGURE 28
SATURATION SOLUBILITIES OF CO_2, O_2, AND N_2 IN WATER
Oxygen
Carbon Dioxide
Nitrogen
SOLUBILITY OF CO_2 (mg/l X 10^{-3})
SOLUBILITY OF N_2 (mg/l)
SOLUBILITY OF O_2 (mg/l)
1.9
1.8
1.7
1.6
1.5
1.4
1.3
1.2
1.1
1.0
20.5
20.0
19.5
19.0
18.5
18.0
17.5
17.0
16.5
44
43
42
41
40
39
38
37
36
20
22
24
26
28
30
TEMPERATURE (Degrees Centigrade)

FIGURE 29

DIFFUSIVITIES OF VARIOUS GASES IN WATER

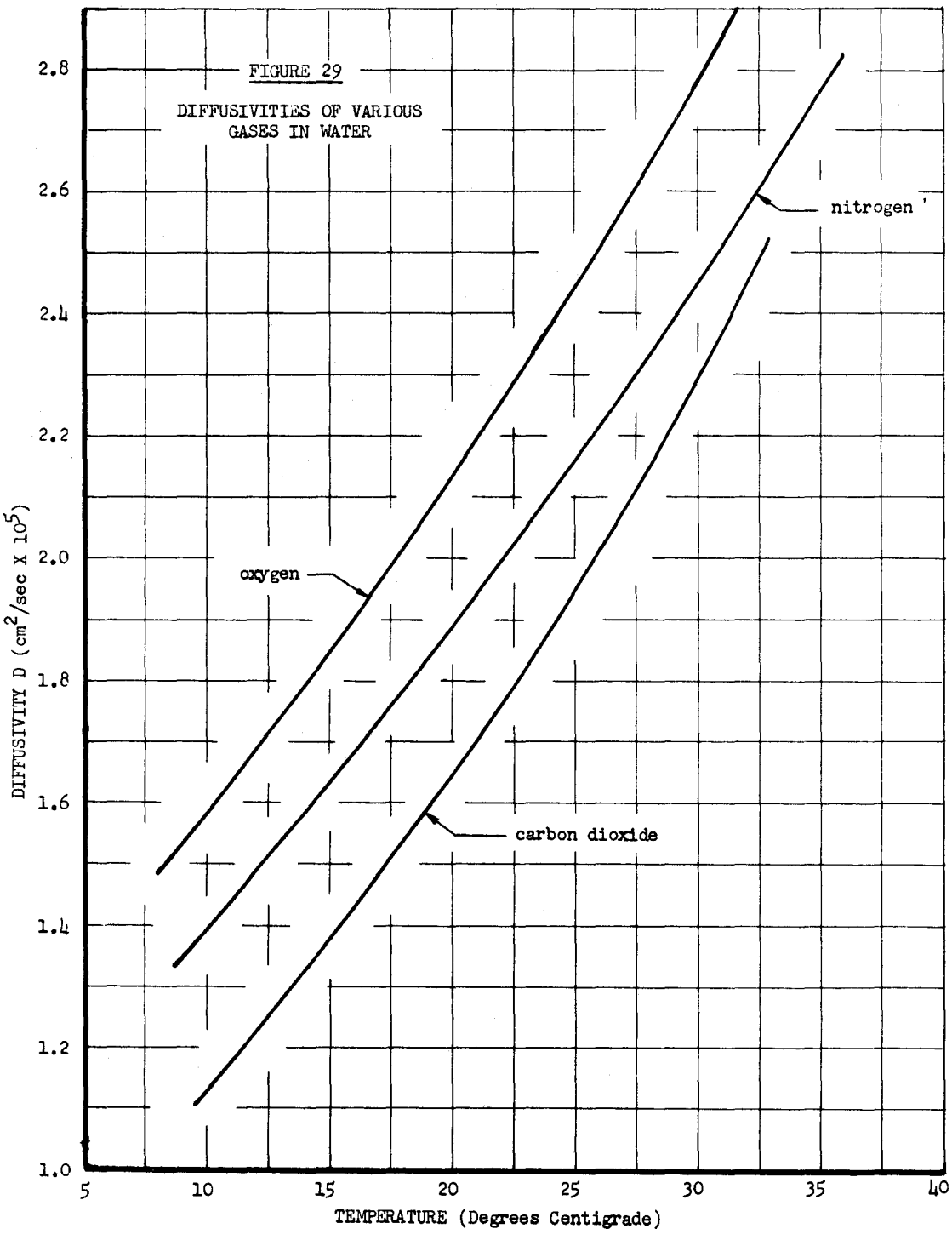

APPENDIX "F"

KINEMATIC VISCOSITY OF WATER

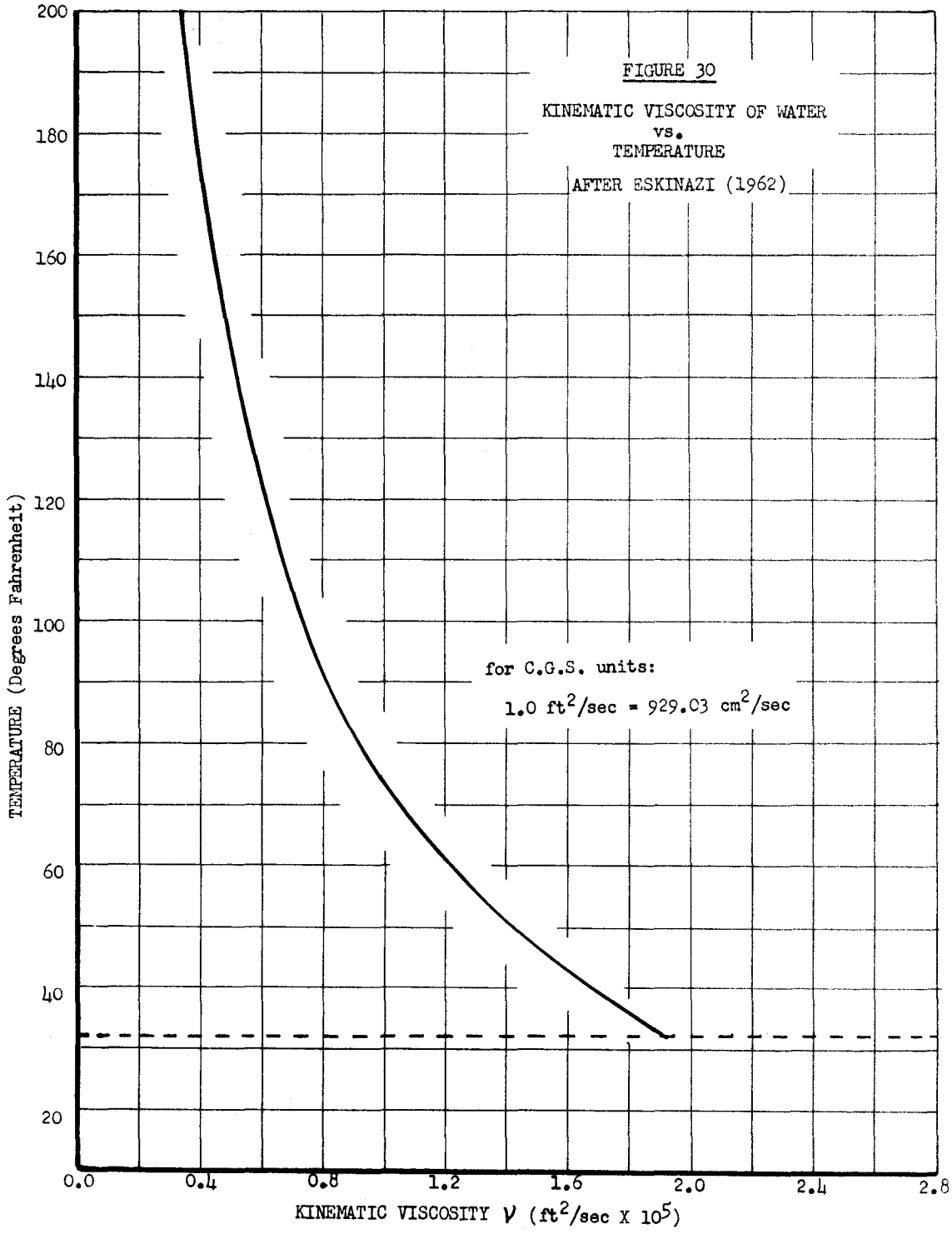
FIGURE 30
KINEMATIC VISCOSITY OF WATER
vs.
TEMPERATURE
AFTER ESKINAZI (1962)
for C.G.S. units:
1.0 ft²/sec = 929.03 cm²/sec
TEMPERATURE (Degrees Fahrenheit)
200
180
160
140
120
100
80
60
40
20
0.0
0.4
0.8
1.2
1.6
2.0
2.4
2.8
KINEMATIC VISCOSITY ν (ft²/sec X 10⁵)

APPENDIX "G"

BUBBLE RISE RATE VARIATION WITH DIAMETER

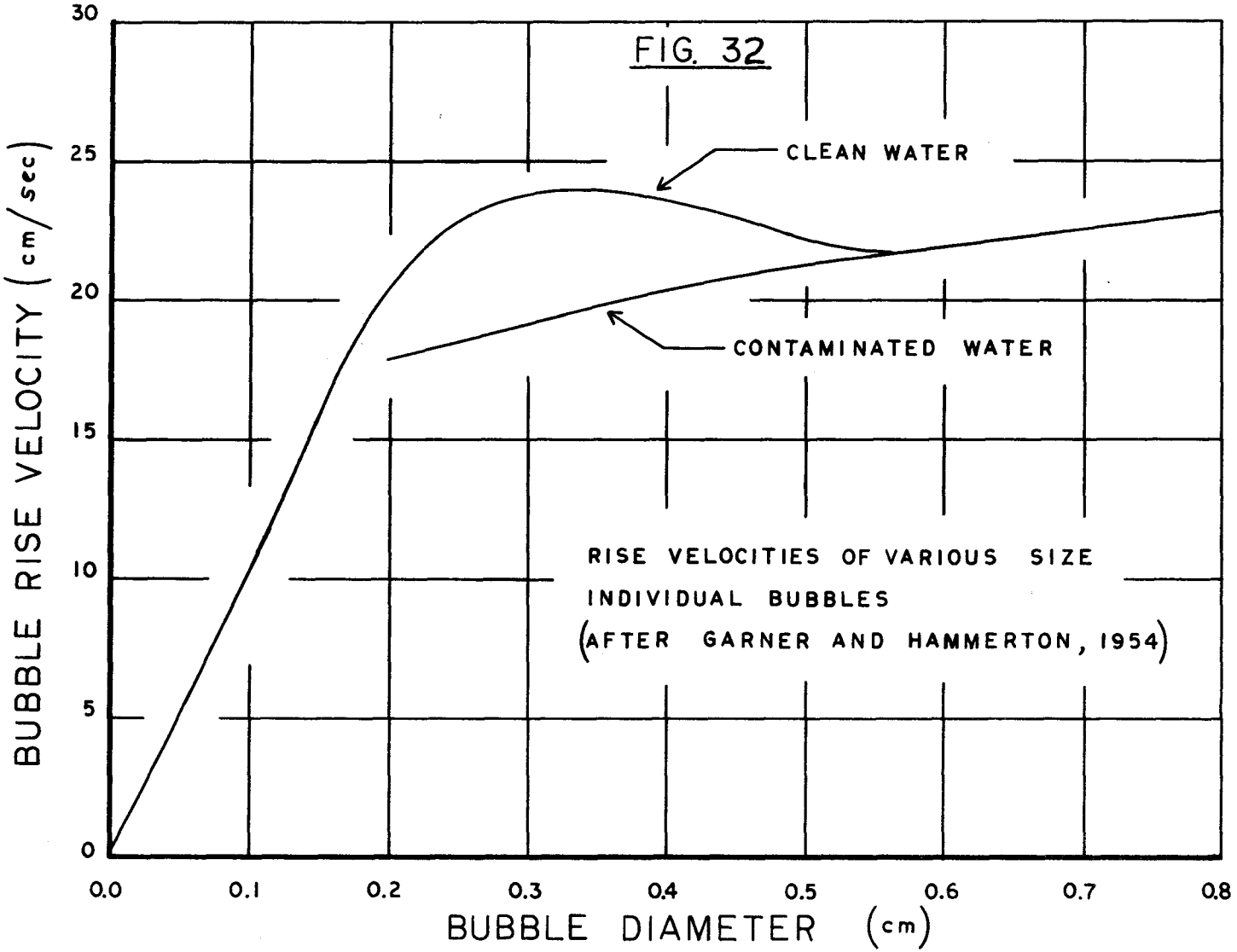
FIG. 32
CLEAN WATER
CONTAMINATED WATER
RISE VELOCITIES OF VARIOUS SIZE INDIVIDUAL BUBBLES
(AFTER GARNER AND HAMMERTON, 1954)
BUBBLE RISE VELOCITY (cm/sec)
BUBBLE DIAMETER (cm)
0
5
10
15
20
25
30
0.0
0.1
0.2
0.3
0.4
0.5
0.6
0.7
0.8

APPENDIX "H"

COMPUTER PROGRAMS USED FOR ANALYSIS

NOMENCLATURE USED FOR COMPUTER PROGRAMS

SYMBOL	
A, AAVG	Intercept on Y-axis for regression fitting.
AKL	Mass transfer coefficient for gas A.
AKLINL	Initial mass transfer coefficient at beginning of run for a circulating bubble of gas A.
AKLFIN	Non-circulating mass transfer coefficient of gas A.
AKL99	Mass transfer coefficient for gas A after 99% of the decay from circulation to non-circulation has transpired.
AM	Mass of gas A in bubble.
AMN2	Mass of nitrogen gas in bubble.
AMO2	Mass of Oxygen gas in bubble.
AMRATE	Rate of decay of mass transfer coefficient of gas A from circulating to non-circulating values.
AMW	Molecular weight of gas A.
AREA	Interfacial Area of bubble.
AV	Volume of gas A in bubble.
BARP	Barometric pressure.
BI	First order coefficient term in parabolic equation $y = a + b_1 x + b_2 x^2$.
B2	Second order coefficient term in parabolic equation $y = a + b_1 x + b_2 x^2$.
BKL	Mass Transfer coefficient for gas B.
BKLINL	Initial mass transfer coefficient at beginning of run for a circulating bubble of gas B.
BKLFIN	Non-circulating mass transfer coefficient of gas B.

SYMBOL	
BKL99	Mass transfer coefficient for gas B after 99% of the decay from circulation to non-circulation has transpired.
BM	Mass of gas B in bubble.
BMRATE	Rate of decay of mass transfer coefficient of gas B from circulating to non-circulating values.
BMW	Molecular weight of gas B.
BUBLM	Total mass of bubble.
BU	Volume of gas B in bubble.
CA	Concentration of gas A dissolved in liquid phase.
CBINIT	Concentration of gas B dissolved in liquid phase.
CO2	Concentration of oxygen in liquid phase.
CN2	Concentration of nitrogen in liquid phase.
CSA	Saturation concentration of gas A.
CSB	Saturation concentration of gas B.
DAM	Incremental change in mass of gas A in bubble.
DAV	Incremental change in volume of gas A in bubble.
DBM	Incremental change in mass of gas B in bubble.
DBV	Incremental change in volume of gas B in bubble.
DECAYT	Time taken for 99% of decay from circulation to non-circulation to occur.
DEGK	Temperature in Degrees Kelvin.
DELA	Incremental change in bubble area.
DELV	Incremental change in bubble volume.
DENOM	Denominator.
DFA	Mass transfer driving force for gas A.

SYMBOL	
DFB	Mass transfer driving force for gas B.
DIAM	Bubble diameter.
DMO2	Incremental change in oxygen mass in bubble.
DMN2	Incremental change in nitrogen mass in bubble.
DT	Increment of time.
DVO2	Incremental change in oxygen volume in bubble.
EX	Abscissa X .
FINMFR	Steady state mass feed rate of gas from micro-pipet.
FINVFR	Steady state volumetric feed rate of gas from micropipet.
HEAD	Static head above bubble.
HGT	Bubble height from teflon tip to top of bubble.
ICOUNT	A control counter used in the program.
J	A control counter used in the program.
NRUN	Run number.
PPA	Dimensionless partial pressure fraction of gas A in bubble.
PPB	Dimensionless partial pressure fraction of gas B in bubble.
PPFN2	Dimensionless partial pressure fraction of nitrogen in bubble.
PPFO2	Dimensionless partial pressure fraction of oxygen in bubble.
RATEV	Volumetric feed rate.
RATEM	Mass feed rate
RATEO2	Volumetric rate of change of oxygen in bubble.

SYMBOL	
R1, R2	Radius of incremental slice of bubble under consideration.
STATHD	Static head above a datum on the apparatus 43.2" above bubble elevation.
SX	$\sum x$
SYX	$\sum xy$
SX2	$\sum x^2$
SX3	$\sum x^3$
SX4	$\sum x^4$
SYX2	$\sum yx^2$
T	Time
TEMP	Temperature in Degrees Centigrade.
TMAX	Length of run.
TOTAV	Cumulative volume of gas A fed to bubble from micropipet.
VEL	Center-line pipe velocity.
VOLUME	Volume of Bubble.
VN2	Volume of nitrogen in bubble.
VO2	Volume of oxygen in bubble.
WYE	Ordinate y.

```
C      BUBBLE AREA AND VOLUME BY METHOD OF CO-ORDINATES USING AN OSCAR
C      INCREMENTAL AREAS OF THE CONVEX SURFACES OF SUCESSIVE FRUSTRUMS
C        OF CONES ARE USED.                                  A. WARREN WILSON.
       DIMENSION  X(800), Y(800)
    88 READ  (5,1)  (X(I), Y(I), I = 1,200,1)
     1 FORMAT (8(2F5.3))
       WRITE (6,99) (X(I), Y(I), I = 1,10)
    99 FORMAT  (1H-,10(2F6.3))
       AREA = 0.0
       VOLUME = 0.0
       J = 0
       DO 3 I = 1,196,2
       H = 0.50 * (X(I + 2) - X(I) + X(I + 3) - X(I + 1))
       R1 = 0.50 * (Y(I + 1) - Y(I))
       R2 = 0.50 * (Y(I + 3) - Y(I + 2))
C      THE FOLLOWING IS A CORRECTION FOR GLASS DISTORTION
       R1 = R1 * 0.7317
       R2 = R2 * 0.7317
       S = SQRT(H * * 2 + (R1 - R2) * * 2)
       DELA = 3.1416 * S * (R1 + R2)
       DELV = 3.1416 * H * (R1 * * 2 + R2 * * 2 + R1 * R2) / 3.0
       AREA = AREA + DELA
       VOLUME = VOLUME + DELV
     3 CONTINUE
       WRITE (6,4) AREA, VOLUME
     4 FORMAT (1H0,14HBUBBLE AREA = ,1PE14.7,/1H0,
      1  16HBUBBLE VOLUME = ,1PE14.7)
       J = J + 1
       IF  (J.GE.9)  GO TO 77
       GO TO 88
    77 STOP
       END
```

```
C      PARABOLIC REGRESSION LINE SPECIFYING Y-INTERCEPT OF THE FORM
C           Y = A + B1 * X + B2 * X * * 2       A. WARREN WILSON.
       DIMENSION  X(500), Y(500)
     1 READ  (5,2)  N, AAVG, (X(I), I = 1,N,1), (Y(I), I = 1,N,1)
     2 FORMAT  (I10, F10.7/ (8F10.6))
       WRITE (6,3)  N, AAVG, (X(I), Y(I), I = 1,N,1)
     3 FORMAT  (1H1,3HN =,I3,5X,13HSPECIFIED A =,F10.7/(2F12.6))
       SX = 0.0
       SYX = 0.0
       SX2 = 0.0
       SX3 = 0.0
       SX4 = 0.0
       SYX2 = 0.0
       DO 4  I = 1,N,1
       SX = SX + X(I)
       SYX = SYX + Y(I) * X(I)
       SX2 = SX2 + X(I) * * 2
       SX3 = SX3 + X(I) * * 3
       SX4 = SX4 + X(I) * * 4
       SYX2 = SYX2 + Y(I) * X(I) * * 2
     4 CONTINUE
       DENOM = SX2 * SX4 - SX3 * * 2
       B1 = (SYX * SX4 - SYX2 * SX3) / DENOM
       B2 = (SYX2 * SX2 - SYX * SX3) / DENOM
       WRITE (6,5)  AAVG, B1, B2
     5 FORMAT  (1H0,3HA =,F12.7/1H0,4HB1 =,F12.7/1H0,4HB2 =,F12.7)
       WRITE (6,6)
     6 FORMAT  (1H-,7X,1HY,15X,1HX)
       EX = 0.130
     7 CONTINUE
       WYE = A + B1 * EX + B2 * EX * * 2
       WRITE (6,8)  WYE, EX
     8 FORMAT  (1H0,(F12.7,5X,F12.7))
       EX = EX + 0.010
       IF (EX.GT.0.220)  GO TO 9
       GO TO 7
     9 CONTINUE
       GO TO 1
    77 STOP
       END
```

```
C     DETERMINING KL RATES FROM STEADY-STATE VOLUMETRIC FEED RATE DATA
C     MASS TRANSFER IN ONE DIRECTION ONLY
C     CONSIDERING WATER VAPOUR PRESSURE EFFECTS
C     VAPOUR PRESSURE OF WATER AT 28.67 DEG. C.  =  29.474 MM. HG.
    1 READ (5,2)  NRUN, HGT, VEL, BARP, STATHD, TEMP, CSA, CA, FINVFR,
     1   AMW
    2 FORMAT (I3,2F10.4/2F10.4/2F10.4/2F10.4/F10.4)
      WRITE (6,3) NRUN, HGT, VEL, BARP, STATHD, TEMP, CSA, CA, FINVFR,
     1   AMW
    3 FORMAT  (1H1,13HRUN NUMBER = ,I3/1H0,16HBUBBLE HEIGHT = ,F10.4,
     1  2HCM/1H0,23HCENTER-LINE VELOCITY = ,F10.4,6HCM/SEC/1H0,22HBAROME
     2TRIC PRESSURE = ,F10.4,5HMM HG/1H0,14HSTATIC HEAD = ,F10.4,
     335HIN. WATER ABOVE TOP HORIZONTAL PIPE/1H0,14HTEMPERATURE = ,F10.4
     4,18HDEGREES CENTIGRADE/1H0,41HSATURATION SOLUBILITY OF DISPERSED G
     5AS = ,F10.4,11HMG/L AT STP/1H0,46HDISPERSED GAS CONCENTRATION IN L
     6IQUID PHASE = ,F10.4,31HMG/L AT EXPERIMENTAL CONDITIONS/1H0,
     736HSTEADY-STATE VOLUMETRIC FEED RATE = ,F10.4,6HCC/MIN/1H0,
     824HDISPERSED GAS MOL WGT = ,F10.4)
      IF (HGT.EQ.0.165)  GO TO 4
      IF (HGT.EQ.0.203)  GO TO 5
    4 CONTINUE
      IF (VEL.EQ.5.0)  GO TO 6
      IF (VEL.EQ.10.0)  GO TO 7
    5 CONTINUE
      IF (VEL.EQ.5.0)  GO TO 8
      IF (VEL.EQ.10.0)  GO TO 9
    6 CONTINUE
      AREA = 0.096
      VOLUME = 0.00345
      GO TO 10
    7 CONTINUE
      AREA = 0.099
      VOLUME = 0.00360
      GO TO 10
    8 CONTINUE
      AREA = 0.130
      VOLUME = 0.00525
      GO TO 10
    9 CONTINUE
      AREA = 0.134
      VOLUME = 0.00550
      GO TO 10
   10 CONTINUE
      WRITE (6,11)  AREA, VOLUME
   11 FORMAT  (1H-,14HBUBBLE AREA = ,F6.3,6H SQ CM/1H0,
     1   16HBUBBLE VOLUME = ,F8.5,6H CU CM)
      DEGK = 273.0 + TEMP
      HEAD = ((STATHD + 43.2) * 25.4 / 13.546) + BARP
      CSA = HEAD * CSA / 760.0
      AV = VOLUME
      AM = (AV * AMW * HEAD * 273.0) / (22.4 * 760.0 * DEGK)
C     THE FOLLOWING CARD CORRECTS FOR WATER VAPOUR CONTENT IN FEED GAS
      FINVFR = FINVFR * (1.0 - (29.474 / HEAD))
      FINMFR = (FINVFR * AMW * HEAD * 273.0) / (22.4 * 760.0 * DEGK)
      WRITE (6,12)  AM, FINMFR
   12 FORMAT  (1H0,31HDISPERSED GAS MASS IN BUBBLE = ,F10.6,2HMG/
     1   1H0,30HSTEADY-STATE MASS FEED RATE = ,F10.6,6HMG/MIN)
      AKL = FINMFR / (AREA * (CSA - CA) * 0.001)
      WRITE (6,13)  AKL
```

```
13 FORMAT  (1H0,32HDISPERSED GAS STEADY-STATE KL = ,F10.4,6HCM/MIN)
   GO TO 1
   END
```

```
C     SIMULATED EXPERIMENTAL RUN
    1 READ (5,2)  NRUN, HGT, VEL, BARP, STATHD, TEMP, CSA, CSB, CA,
     1   AMW, BMW, AKLINL, BKLINL, DECAYT, AKLFIN, BKLFIN, TMAX, DT
    2 FORMAT  (I3, 2F10.4/2F10.4/4F10.4/2F10.4/3F10.4/2F10.4/2F10.4)
      WRITE (6,3)  NRUN, HGT, VEL, BARP, STATHD, TEMP, CSA, CSB, CA,
     1   AMW, BMW
    3 FORMAT  (1H1,13HRUN NUMBER = ,I3/1H0,16HBUBBLE HEIGHT = ,F10.4,
     1  2HCM/1H0,23HCENTER-LINE VELOCITY = ,F10.4,6HCM/SEC/1H0,22HBAROME
     2TRIC PRESSURE = ,F10.4,5HMM HG/1H0,14HSTATIC HEAD = ,F10.4,
     335HIN. WATER ABOVE TOP HORIZONTAL PIPE/1H0,14HTEMPERATURE = ,F10.4
     4,18HDEGREES CENTIGRADE/1H0,41HSATURATION SOLUBILITY OF DISPERSED G
     5AS = ,F10.4,11HMG/L AT STP/1H0,41HSATURATION SOLUBILITY OF DISSOLV
     6ED GAS = ,F10.4,11HMG/L AT STP/1H0,46HDISPERSED GAS CONCENTRATION
     7IN LIQUID PHASE = ,F10.4,31HMG/L AT EXPERIMENTAL CONDITIONS/1H0,
     824HDISPERSED GAS MOL WGT = ,F10.4/1H0,24HDISSOLVED GAS MOL WGT = ,
     9F10.4)
      WRITE (6,301)  AKLINL, BKLINL, DECAYT, AKLFIN, BKLFIN, TMAX, DT
  301 FORMAT  (1H0,27HINITIAL DISPERSED GAS KL = ,F10.4,6HCM/MIN/1H0,
     127HINITIAL DISSOLVED GAS KL = ,F10.4,6HCM/MIN/1H0,72HTIME TAKEN FO
     2R INITIAL KL TO EXPONENTIALLY APPROACH FINAL KL BY 0.990 = ,F10.4,
     33HMIN/1H0,38HFINAL STEADY-STATE DISPERSED GAS KL = ,F10.4,6HCM/MIN
     4/1H0,38HFINAL STEADY-STATE DISSOLVED GAS KL = ,F10.4,6HCM/MIN/
     51H0,16HLENGTH OF RUN = ,F10.4,3HMIN/1H0,24HINTEGRATION INCREMENT =
     6 ,F10.4,3HMIN)
      IF (HGT.EQ.0.165)  GO TO 4
      IF (HGT.EQ.0.203)  GO TO 5
    4 CONTINUE
      IF (VEL.EQ.5.0)  GO TO 6
      IF (VEL.EQ.10.0)  GO TO 7
    5 CONTINUE
      IF (VEL.EQ.5.0)  GO TO 8
      IF (VEL.EQ.10.0)  GO TO 9
    6 CONTINUE
      AREA = 0.096
      VOLUME = 0.00345
      GO TO 10
    7 CONTINUE
      AREA = 0.099
      VOLUME = 0.00360
      GO TO 10
    8 CONTINUE
      AREA = 0.130
      VOLUME = 0.00525
      GO TO 10
    9 CONTINUE
      AREA = 0.134
      VOLUME = 0.00550
      GO TO 10
   10 CONTINUE
      DEGK = 273.0 + TEMP
      CBINIT = ((STATHD * 25.4 / 13.546) + BARP) * CSB / 760.0
      HEAD = ((STATHD + 43.2) * 25.4 / 13.546) + BARP
      CSA = HEAD * CSA / 760.0
      CSB = HEAD * CSB / 760.0
      AKL99 = 0.99 * AKLFIN + 0.01 * AKLINL
      BKL99 = 0.99 * BKLFIN + 0.01 * BKLINL
      AMRATE = ALOG10((AKLINL - AKLFIN) / (AKL99 - AKLFIN)) / DECAYT
      BMRATE = ALOG10((BKLINL - BKLFIN) / (BKL99 - BKLFIN)) / DECAYT
      WRITE (6,11)  AREA, VOLUME, DEGK, CBINIT, HEAD, AMRATE, BMRATE
```

```
11 FORMAT  (1H-,14HBUBBLE AREA = ,F10.5,5HSQ CM/1H0,16HBUBBLE VOLUME
  1= ,F10.5,5HCU CM/1H0,14HTEMPERATURE = ,F10.4,14HDEGREES KELVIN/
  21H0,30HDISSOLVED GAS CONCENTRATION = ,F10.4,31HMG/L AT EXPERIMENTA
  3L CONDITIONS/1H0,14HSTATIC HEAD = ,F10.4,28HMM HG ABOVE BUBBLE ELE
  4VATION/1H0,34HDECAY RATE FOR DISPERSED GAS KL = ,F10.4,5HMIN-1/
  51H0,34HDECAY RATE FOR DISSOLVED GAS KL = ,F10.4,5HMIN-1)
   WRITE (6,12)
12 FORMAT  (1H1,10HTIME (MIN),3X,10HVOLUMETRIC,6X,4HMASS,6X,11HDISP G
  1AS KL, 3X,11HDISS GAS KL,3X,11HVOLUME DISP,3X,12HVOL DISP GAS,3X,
  2 12HVOL DISS GAS/14X,10HFEED  RATE,3X,10HFEED  RATE,5X,8H(CM/MIN),
  36X,8H(CM/MIN),6X,7HGAS FED,7X,9HIN BUBBLE,6X,9HIN BUBBLE/15X,
  48H(CC/MIN),5X,8H(MG/MIN),36X,4H(CC),11X,4H(CC),11X,4H(CC))
   AV = VOLUME
   BV = 0.0
   BUBLM = (AV * AMW * HEAD * 273.0) / (22.4 * 760.0 * DEGK)
   TOTAV = 0.0
   AM = BUBLM
   BM = 0.0
   T = 0.0
13 ICOUNT = 0
14 PPA = AM / BUBLM
   PPB = BM / BUBLM
   DFA = PPA * CSA - CA
   DFB = PPB * CSB - CBINIT
   AKL = AKLFIN + (AKLINL - AKLFIN) * 10.0 * * (-AMRATE * T)
   BKL = BKLFIN + (BKLINL - BKLFIN) * 10.0 * * (-BMRATE * T)
   DAM = AKL * 0.001 * AREA * DFA * DT
   DBM = BKL * 0.001 * AREA * DFB * DT
   DAV = (DAM * 22.4 * 760.0 * DEGK) / (AMW * HEAD * 273.0)
   DBV = (DBM * 22.4 * 760.0 * DEGK) / (BMW * HEAD * 273.0)
   IF (DFB.GE.0.0)  GO TO 15
   IF (DFB.LT.0.0)  GO TO 16
15 DBV = 0.0
16 CONTINUE
   AV = AV + DBV
   BV = BV - DBV
   TOTAV = TOTAV + DAV + DBV
   RATEV = (DAV + DBV) / DT
   RATEM = (DAM + DBM) / DT
   BM = BM - DBM
   AM = (AV * AMW * HEAD * 273.0) / (22.4 * 760.0 * DEGK)
   BUBLM = AM + BM
   IF (T.LT.2.0)  GO TO 17
   IF (T.GE.2.0)  GO TO 18
17 CONTINUE
   IF (ICOUNT.EQ.0)  GO TO 19
   IF (ICOUNT.EQ.250)  GO TO 19
   IF (ICOUNT.EQ.500) GO TO 19
   IF (ICOUNT.EQ.750)  GO TO 19
   GO TO 21
18 CONTINUE
   IF (ICOUNT.EQ.0)  GO TO 19
   IF (ICOUNT.GT.0)  GO TO 21
19 WRITE (6,20)  T, RATEV, RATEM, AKL, BKL, TOTAV, AV, BV
20 FORMAT  (1H0,F8.3,5X,F10.6,5X,F10.6,5X,F7.4,7X,F7.4,6X,F9.6,5X,
  1F9.6,5X,F9.6)
21 CONTINUE
   ICOUNT = ICOUNT + 1
```

```
      T = T + DT
      IF (T.GT.TMAX)  GO TO 22
      IF (ICOUNT.GE.1000)  GO TO 13
      IF (ICOUNT.LT.1000)  GO TO 14
   22 CONTINUE
      GO TO 1
      END
```

```
C     SIMULATION OF MASS TRANSFER PHENOMENA FOR SINGLE AIR BUBBLE
    1 READ (5,2)  DIAM, TMAX, DT, AKL, BKL, CO2, CN2
    2 FORMAT  (7F10.4)
      WRITE (6,3)  DIAM, TMAX, AKL, BKL, CO2, CN2,
    3 FORMAT  (1H1,18HBUBBLE DIAMETER = ,F6.3,2HCM/1HO, 24HBUBBLE RETENT
     1ION TIME = ,F7.3,3HMIN/1HO,18HOXYGEN KL VALUE = ,F7.4,6HCM/MIN/
     21HO,20HNITROGEN KL VALUE = ,F7.4,6HCM/MIN/1HO,
     343HDISSOLVED OXYGEN CONCENTRATION IN LIQUID = ,F8.4,4HMG/L/1HO,
     445HDISSOLVED NITROGEN CONCENTRATION IN LIQUID = ,F8.4,4HMG/L)
      AREA = 3.1416 * (DIAM * * 2)
      VOLUME = 3.1416 * (DIAM * * 3) / 6.0
      T = 0.0
      PPFO2 = 0.20
      PPFN2 = 0.80
      WRITE (6,5)
    5 FORMAT  (1H1,119HOXYGEN VOL   NITROGEN VOL   OXYGEN MASS   NITROGE
     1N MASS   BUBBLE VOL   BUBBLE DIAM       TIME      KLRATE   DISSOLU
     2TION/ 4X, 4H(CC), 10X,4H(CC), 11X,4H(GM), 12X, 4H(GM), 9X, 4H(CC),
     39X, 4H(CM), 10X, 5H(MIN), 5X, 8H(CM/MIN), 2X, 11HRATE OF OXY/
     4110X, 8H(CC/MIN))
    6 CONTINUE
      ICOUNT = 0
    7 CONTINUE
      VO2 = PPFO2 * VOLUME
      VN2 = PPFN2 * VOLUME
      AMO2 = (VO2 * 32.0 * 273.0) / (22.4 * 293.0)
      AMN2 = (VN2 * 28.0 * 273.0) / (22.4 * 293.0)
      DMO2 = -AKL * 0.001 * AREA * (PPFO2 * 43.39 - CO2) * DT
      DMN2 = -BKL * 0.001 * AREA * (PPFN2 * 19.01 - CN2) * DT
      DVO2 = (DMO2 * 22.4 * 293.0) / (32.0 * 273.0)
      RATEO2 = DVO2 / DT
      IF (ICOUNT.EQ.0)  GO TO 8
      IF (ICOUNT.GT.0)  GO TO 10
    8 WRITE (6,9)  VO2, VN2, AMO2, AMN2, VOLUME, DIAM, T, AKL, RATEO2
    9 FORMAT  (1HO, F9.6, 5X, F10.6, 4X, F10.7, 5X, F10.7, 5X, F10.6,
     14X, F8.5, 6X, F9.5, 3X, F7.4, 3X, F10.7)
   10 CONTINUE
      ICOUNT = ICOUNT + 1
      T = T + DT
      AMO2 = AMO2 + DMO2
      AMN2 = AMN2 + DMN2
      VO2 = (AMO2 * 22.4 * 293.0) / (32.0 * 273.0)
      VN2 = (AMN2 * 22.4 * 293.0) / (28.0 * 273.0)
      VOLUME = VO2 + VN2
      PPFO2 = VO2 / VOLUME
      PPFN2 = VN2 / VOLUME
      DIAM = (6.0 / 3.1416 * VOLUME) * * (0.333)
      AREA = 3.1416 * (DIAM * * 2)
      IF (T.GT.TMAX)  GO TO 11
      IF (ICOUNT.GE.250)  GO TO 6
      IF (ICOUNT.LE.250)  GO TO 7
   11 CONTINUE
      GO TO 1
      END
```

RUN NUMBER = 38
BUBBLE HEIGHT = 0.2030CM
CENTER-LINE VELØCITY = 10.0000CM/SEC
BARØMETRIC PRESSURE = 753.7000MM HG
STATIC HEAD = 5.0000IN. WATER ABØVE TØP HØRIZØNTAL PIPE
TEMPERATURE = 28.0000DEGREES CENTIGRADE
SATURATIØN SØLUBILITY ØF DISPERSED GAS = 1327.0000MG/L AT STP
SATURATIØN SØLUBILITY ØF DISSØLVED GAS = 16.7400MG/L AT STP
DISPERSED GAS CØNCENTRATIØN IN LIQUID PHASE = 36.3000MG/L AT EXPERIMENTAL CØNDITIØNS
DISPERSED GAS MØL WGT = 44.0000
DISSØLVED GAS MØL WGT = 28.0000
INITIAL DISPERSED GAS KL = 2.2200CM/MIN
INITIAL DISSØLVED GAS KL = 2.2500CM/MIN
TIME TAKEN FØR INITIAL KL TØ EXPØNENTIALLY APPRØACH FINAL KL BY 0.990 = 0.5000MIN
FINAL STEADY-STATE DISPERSED GAS KL = 0.5370CM/MIN
FINAL STEADY-STATE DISSØLVED GAS KL = 0.4820CM/MIN
LENGTH ØF RUN = 40.0000MIN
INTEGRATIØN INCREMENT = 0.0010MIN

BUBBLE AREA = 0.13400SQ CM
BUBBLE VØLUME = 0.00550CU CM
TEMPERATURE = 301.0000DEGREES KELVIN
DISSØLVED GAS CØNCENTRATIØN = 16.8077MG/L AT EXPERIMENTAL CØNDITIØNS
STATIC HEAD = 844.0794MM HG ABØVE BUBBLE ELEVATIØN
DECAY RATE FØR DISPERSED GAS KL = 4.0000MIN-1
DECAY RATE FØR DISSØLVED GAS KL = 4.0000MIN-1

TIME (MIN)	VOLUMETRIC FEED RATE (CC/MIN)	MASS FEED RATE (MG/MIN)	DISP GAS KL (CM/MIN)	DISS GAS KL (CM/MIN)	VOLUME DISP GAS FED (CC)	VOL DISP GAS IN BUBBLE (CC)	VOL DISS GAS IN BUBBLE (CC)
0.000	0.212097	0.422562	2.2200	2.2500	0.000212	0.005496	0.000004
0.250	0.063279	0.125998	0.7053	0.6588	0.027790	0.004991	0.000509
0.500	0.048174	0.095899	0.5538	0.4997	0.041096	0.004765	0.000735
0.750	0.045532	0.090637	0.5387	0.4838	0.052748	0.004571	0.000929
1.000	0.044104	0.087792	0.5372	0.4822	0.063946	0.004385	0.001115
1.250	0.042801	0.085197	0.5370	0.4820	0.074808	0.004206	0.001294
1.500	0.041519	0.082644	0.5370	0.4820	0.085347	0.004032	0.001468
1.750	0.040250	0.080115	0.5370	0.4820	0.095566	0.003864	0.001636
2.000	0.038993	0.077612	0.5370	0.4820	0.105471	0.003702	0.001798
3.000	0.034128	0.067922	0.5370	0.4820	0.142004	0.003110	0.002390
4.000	0.029588	0.058880	0.5370	0.4820	0.173827	0.002602	0.002898
5.000	0.025448	0.050635	0.5370	0.4820	0.201305	0.002174	0.003326
6.000	0.021757	0.043282	0.5370	0.4820	0.224865	0.001816	0.003684
7.000	0.018533	0.036863	0.5370	0.4820	0.244967	0.001521	0.003979
8.000	0.015773	0.031365	0.5370	0.4820	0.262078	0.001280	0.004219
9.000	0.013449	0.026736	0.5370	0.4820	0.276649	0.001086	0.004414
10.000	0.011521	0.022897	0.5370	0.4820	0.289098	0.000929	0.004570
11.000	0.009943	0.019754	0.5370	0.4820	0.299799	0.000805	0.004695
12.000	0.008664	0.017207	0.5370	0.4820	0.309076	0.000706	0.004794
13.000	0.007638	0.015162	0.5370	0.4820	0.317203	0.000628	0.004872
13.999	0.006819	0.013531	0.5370	0.4820	0.324412	0.000566	0.004933
14.999	0.006170	0.012238	0.5370	0.4820	0.330889	0.000518	0.004981
15.999	0.005657	0.011218	0.5370	0.4820	0.336788	0.000481	0.005019
16.999	0.005255	0.010416	0.5370	0.4820	0.342232	0.000451	0.005048
17.999	0.004939	0.009787	0.5370	0.4820	0.347319	0.000428	0.005071
18.999	0.004692	0.009295	0.5370	0.4820	0.352125	0.000410	0.005089
19.999	0.004499	0.008911	0.5370	0.4820	0.356713	0.000396	0.005103
20.999	0.004349	0.008612	0.5370	0.4820	0.361130	0.000386	0.005114

21.999	0.004232	0.008378	0.5370	0.4820	0.365413	0.000377	0.005122
22.999	0.004141	0.008197	0.5370	0.4820	0.369594	0.000371	0.005129
23.999	0.004070	0.008056	0.5370	0.4820	0.373694	0.000366	0.005134
24.999	0.004015	0.007946	0.5370	0.4820	0.377731	0.000362	0.005138
25.999	0.003972	0.007861	0.5370	0.4820	0.381721	0.000359	0.005141
26.999	0.003939	0.007795	0.5370	0.4820	0.385672	0.000356	0.005143
27.998	0.003913	0.007743	0.5370	0.4820	0.389593	0.000354	0.005145
28.998	0.003893	0.007704	0.5370	0.4820	0.393492	0.000353	0.005146
29.998	0.003877	0.007673	0.5370	0.4820	0.397372	0.000352	0.005147
30.998	0.003865	0.007649	0.5370	0.4820	0.401238	0.000351	0.005148
31.998	0.003856	0.007630	0.5370	0.4820	0.405094	0.000350	0.005149
32.998	0.003849	0.007616	0.5370	0.4820	0.408941	0.000350	0.005149
33.998	0.003843	0.007604	0.5370	0.4820	0.412781	0.000349	0.005150
34.998	0.003839	0.007596	0.5370	0.4820	0.416617	0.000349	0.005150
35.998	0.003835	0.007589	0.5370	0.4820	0.420448	0.000349	0.005150
36.998	0.003833	0.007584	0.5370	0.4820	0.424277	0.000349	0.005150
37.998	0.003831	0.007580	0.5370	0.4820	0.428103	0.000348	0.005150
38.998	0.003829	0.007576	0.5370	0.4820	0.431928	0.000348	0.005150
39.998	0.003828	0.007574	0.5370	0.4820	0.435750	0.000348	0.005150

APPENDIX "I"

DATA, CALCULATIONS, AND RESULTS TABLES

TABLE III

CALCULATIONS OF DIAMETER OF SPHERES OF EQUIVALENT SURFACE AREA

Bubble Height (cm)	Pipe Center-Line Velocity (cm/sec.)	Actual Bubble Area (cm^2)	Actual Bubble Area Divided by 3.1416 (cm^2)	$\sqrt{\frac{\text{Actual Area}}{3.1416}}$ Dia. of a Sphere of Equivalent Surface Area (cm)
0.165	5.0	0.096	0.0305	0.174
0.165	10.0	0.099	0.315	0.1775
0.203	5.0	0.130	0.414	0.203
0.203	10.0	0.134	0.426	0.206

TABLE IV

CALCULATIONS OF AVERAGE k_L VALUES FOR THE CO_2- DEGASIFIED WATER RUNS

Run Number	Reynolds Number	Temperature (^oC)	Static Head at Bubble (mm Hg)	CO_2 Conc'n in liquid (mg/l)	Pipe Centre-line Velocity (cm/sec.)	Bubble Height (cm)	Avg of $\frac{dV}{dt}$ beyond t = 4 min (cc/min)	k_L Value (cm/min) for each Run	k_L Value (cm/min) Avg'd over Repeated Series
64	246	29.0	834.0	45.8	10.0	0.203	0.056	0.595	
65	246	30.0	837.7	30.3	10.0	0.203	0.056	0.602	
66	246	29.5	837.5	31.7	10.0	0.203	0.053	0.564	0.587
67	121	30.5	840.8	132.0	5.0	0.203	0.038	0.461	
68	121	29.0	840.5	135.1	5.0	0.203	0.035	0.409	
69	121	27.5	840.9	49.9	5.0	0.203	0.308	0.401	0.424
70	212	28.0	840.5	56.9	10.0	0.165	0.040	0.564	
71	212	28.0	839.9	63.9	10.0	0.165	0.038	0.525	
72	212	29.0	839.5	57.4	10.0	0.165	0.043	0.637	0.575
73	104	28.5	839.5	61.1	5.0	0.165	0.029	0.429	
74	104	28.0	841.0	42.8	5.0	0.165	0.031	0.447	
75	104	27.0	840.9	51.7	5.0	0.165	0.028	0.396	0.424

TABLE V

CALCULATIONS FOR CO_2 - SULFITE DATA

Run Number	Pipe Center line Velocity (cm/sec.)	Equivalent Bubble Diameter (cm)	Steady State k_L Value (cm/min)	Average Steady State k_L (cm/min)	Reynolds Number $\left(\frac{d V_\infty}{\nu}\right)$	Sherwood Number $\left(\frac{k_L d}{D}\right)$	Peclet Number $\left(\frac{dV_\infty}{D}\right)$	$(Re)^{1/2} (Sc)^{1/3}$
64	10.0	0.206	0.5735					
65	10.0	0.206	0.5809	0.566	246	88.3	9.37×10^4	113.8
66	10.0	0.206	0.5437					
67	5.0	0.203	0.4451					
68	5.0	0.203	0.3950	0.409	121	62.8	4.61×10^4	79.7
69	5.0	0.203	0.3869					
70	10.0	0.1775	0.5445					
71	10.0	0.1775	0.5062	0.555	212	74.6	8.06×10^4	105.8
72	10.0	0.1775	0.6151					
73	5.0	0.174	0.4139					
74	5.0	0.174	0.4309	0.409	104	53.9	3.95×10^4	73.9
75	5.0	0.174	0.3816					

The Boussinesq relationship ($Sh = 1.13\ Pe^{1/2}$) was used to calculate the circulating k_L values at the beginning of a run for all gases used.

The following equations obtained from Griffith (1960) were used to determine the non-circulating k_L values which were rapidly approached after each run commenced:

for carbon dioxide	$Sh = 2.0 + 0.72\ Re^{1/2}\ Sc^{1/3}$
for nitrogen	$Sh = 2.0 + 0.63\ Re^{1/2}\ Sc^{1/3}$
for oxygen	$Sh = 2.0 + 0.58\ Re^{1/2}\ Sc^{1/3}$

TABLE VI

k_L VALUES USED IN FITTING THE EXPERIMENTAL DATA

Run Number	Velocity (cm/min)	Equivalent Bubble Dia. (cm)	Carbon Dioxide k_L (cm/min)		Nitrogen k_L (cm/min)		Oxygen k_L (cm/min)	
			Circulating	Non-Circ.	Circulating	Non-Circ.	Circulating	Non-Circ.
38	10.0	0.206	2.22	0.537	2.25	0.482	-	-
41	5.0	0.203	1.58	0.386	1.61	0.347	-	-
45	10.0	0.1775	2.38	0.590	2.42	0.525	-	-
48	5.0	0.174	1.71	0.418	1.74	0.378	-	-
52	10.0	0.206	2.22	0.537	-	-	2.43	0.494
56	5.0	0.203	1.58	0.386	-	-	1.74	0.356
57	10.0	0.1775	2.38	0.590	-	-	2.61	0.536
61	5.0	0.174	1.71	0.418	-	-	1.87	0.387

TABLE VII

SURFACTANT DETERMINATIONS

Run Number	Aliquot of Sample Used (ml)	Spectrophotometer Percent Transmittancy	Milligrams ABS	Apparent Concentration of ABS as ABS (mg/l)	Average Apparent Concentration of ABS as ABS (mg/l)
76	50.0	36.0	0.078	1.56	
76	50.0	33.2	0.083	1.66	
76	50.0	40.0	0.070	1.40	
76	50.0	37.2	0.075	1.50	1.53
79	15.0	29.3	0.094	6.27	
79	15.0	26.7	0.102	6.80	
79	15.0	31.9	0.089	5.93	
79	15.0	27.9	0.097	6.47	6.37
78	20.0	21.0	0.122	6.10	
78	20.0	14.1	0.163	8.15	
78	20.0	14.6	0.158	7.90	
78	20.0	15.5	0.152	7.60	7.44

TABLE VIII

EXPERIMENTAL CONDITIONS FOR THE SURFACTANT RUNS

Run Number	Center-line Velocity (cm/sec.)	Bubble Height (cm)	ABS Concentration (mg/l)	Temperature (^oC)	Static Head (mm/Hg)	CO_2 Concentration (mg/l)
39	10.0	0.203	0.00	27.0	844.6	65.6
77	10.0	0.203	1.53	27.0	832.2	57.3
79	10.0	0.203	6.37	27.5	824.2	33.3
78	10.0	0.203	7.44	27.5	824.5	68.8

To calculate the mass feed rate $\left(\frac{dm}{dt}\right)$ from the volumetric feed rate $\left(\frac{dV}{dt}\right)$, the following relationship was used:

$$\left(\frac{dm}{dt}\right) = \left(\frac{dV}{dt}\right) \cdot \left(\frac{273.0}{\text{Temp.}}\right) \cdot \left(\frac{\text{Static Head}}{760.0}\right) \cdot \left(\frac{\text{Molecular Weight}}{22.4}\right)$$

where the temperature is in degrees Kelvin and the static head is in mm Hg.

The following relationships exist for the experimental conditions in this study:

for run #39 - $\frac{dm}{dt} = \frac{dV}{dt} \times 1.985$

for run #77 - $\frac{dm}{dt} = \frac{dV}{dt} \times 1.959$

for run #79 - $\frac{dm}{dt} = \frac{dV}{dt} \times 1.938$

for run #78 - $\frac{dm}{dt} = \frac{dV}{dt} \times 1.938$

TABLE IX

$\frac{dm}{dt}$ CALCULATIONS FOR VARIOUS SURFACTANT LEVELS

Time (minutes)	Run Number	Volumetric Feed Rate (cc/min)	Mass Feed Rate (mg/min)
0.25	39	0.054	0.107
0.75	77	0.047	0.0925
1.25	79	0.050	0.0968
1.75	78	0.040	0.0775
2.25	39	0.037	0.0734
2.75	77	0.035	0.0689
3.25	79	0.032	0.0620
3.75	78	0.032	0.0620
4.25	39	0.027	0.0536
4.75	77	0.026	0.0512
5.25	79	0.027	0.0523
5.75	78	0.022	0.0426
6.25	39	0.021	0.0417
6.75	77	0.020	0.0342
7.25	79	0.019	0.0368
7.75	78	0.017	0.0329
8.25	39	0.017	0.0337
8.75	77	0.015	0.0295
9.25	79	0.014	0.0271
9.75	78	0.014	0.0271
10.25	39	0.012	0.0238

TABLE IX (CONT'D)

Time (minutes)	Run Number	Volumetric Feed Rate (cc/min)	Mass Feed Rate (mg/min)
10.75	77	0.011	0.0217
11.25	79	0.011	0.0213
11.75	78	0.011	0.0213
12.25	39	0.0092	0.0183
12.75	77	0.0100	0.0196
13.25	79	0.0090	0.0174
13.75	78	0.0100	0.0194
14.25	39	0.0080	0.0159
14.75	77	0.0090	0.0177
15.25	79	0.0072	0.0140
15.75	78	0.0070	0.0136
16.25	39	0.0070	0.0139
16.75	77	0.0072	0.0142
17.25	79	0.0062	0.0120
17.75	78	0.0068	0.0132
18.25	39	0.0062	0.0123
18.75	77	0.0064	0.0126
19.25	79	0.0052	0.0101
19.75	78	0.0066	0.0128
20.25	39	0.0048	0.0095
20.75	77	0.0054	0.0106

TABLE IX (CONT'D)

Time (minutes)	Run Number	Volumetric Feed Rate (cc/min)	Mass Feed Rate (mg/min)
21.25	79	0.0050	0.0097
21.75	78	0.0064	0.0124
22.25	39	0.0044	0.0087
22.75	77	0.0050	0.0098
23.25	79	0.0052	0.0101
23.75	78	0.0062	0.0120
24.25	39	0.0054	0.0107
24.75	77	0.0044	0.0097
25.25	79	0.0048	0.0093
25.75	78	0.0050	0.0097
26.25	39	0.0032	0.0064
26.75	77	0.0052	0.0102
27.25	79	0.0038	0.0074
27.75	78	0.0048	0.0093
28.25	39	0.0026	0.0052
28.75	77	0.0042	0.0083
29.25	79	0.0046	0.0089
29.75	78	0.0058	0.0112
30.25	39	0.0030	0.0060
30.75	77	0.0038	0.0075
31.25	79	0.0042	0.0081

TABLE IX (CONT'D)

Time (minutes)	Run Number	Volumetric Feed Rate (cc/min)	Mass Feed Rate (mg/min)
31.75	78	0.0046	0.0089
32.25	39	0.0028	0.0056
32.75	77	0.0040	0.0079
33.25	79	0.0036	0.0070
33.75	78	0.0048	0.0093
34.25	39	0.0030	0.0060
34.75	77	0.0046	0.0091
35.25	79	0.0040	0.0078
35.75	78	0.0038	0.0074
36.25	39	0.0042	0.0083
36.75	77	0.0036	0.0071
37.25	79	0.0034	0.0066
37.75	78	0.0044	0.0085

APPENDIX "J"

NOMENCLATURE

NOMENCLATURE

Term	Meaning
A	Area, or as a subscript, gas A.
a	Interfacial surface area per unit volume of aeration tank, or an empirical constant, or as a subscript, gas A.
ABS	Alkyl Benzene Sulfonate.
B	A constant characteristic of an aeration system, or as a subscript, gas B.
b	An empirical constant.
c	Concentration of solute gas.
C_i	Interfacial concentration of solute gas.
C_L	Concentration of solute gas in the bulk of the liquid phase.
C_s	Saturation solubility.
D	Diffusivity.
D_G	Diffusivity in the gaseous phase.
D_L	Diffusivity in the liquid phase.
d	Diameter.
f	Fanning friction factor.
G	As a subscript, the gaseous phase.
g	Gravitational constant.
h	Height of an aerator.
i	As a subscript, interface.
K	Ratio of proportionality between terminal velocity of a rigid sphere and that of an equivalent fluid sphere.

NOMENCLATURE (CONT'D)

Term	Meaning
k_G	Mass transfer coefficient for the gaseous film.
k_L	Mass transfer coefficient for the liquid film.
k_La	Overall mass transfer coefficient for the liquid film.
L	Liquid film thickness, or as a subscript, the liquid phase.
m	Mass of solute gas.
MW	Molecular Weight.
(1-m)	An exponent used in characterizing an aerator.
N	Number of bubbles produced per unit time.
(1-n)	An exponent used in characterizing an aerator.
P	Pressure.
P_i	Partial pressure of solute gas at the interface.
P_G	Partial pressure of solute gas in the bulk of the gaseous phase.
Pe	Peclet number.
Q	Water flow rate.
q	Air flow rate.
r	Radius, or, rate of surface renewal.
$\bar{r}$	Critical radius.
Re	Reynolds number
Sc	Schmidt number
Sh	Sherwood number
T	Temperature

NOMENCLATURE (CONT'D)

Term	Meaning
t	Time.
t_e	Time of exposure of liquid eddy at the interface.
V	Volume.
V_{max}	Maximum flow velocity in pipe (normally the center-line velocity).
$V_{Q/A}$	Average flow velocity in pipe.
V_t	Terminal velcoity
V_∞	Rise rate of Bubble.
W	Width.
W'	Apparent width.
y	Distance perpendicular to the interface.
Y_G	Gaseous film thickness.
Y_L	Liquid film thickness.
α	Ratio of k_La for waste to k_La for tap water.
π	3.1416.
P_1, P_2	Density of dispersed and continuous phases respectively.
μ_1, μ_2	Viscosity of dispersed and continuous phases respectively.
ν	Kinematic viscosity.
σ	Surface tension.